Johannes Gutenberg-Universität Mainz

DISSERTATION

Identification and Functional Characterization of Potential Biomarkers in Cisplatin Resistance Through Bioinformatic Analyses

Ayşegül Varol

Mainz, November 2025

License Information

„Identification and Functional Characterization of Potential Biomarkers in Cisplatin Resistance Through Bioinformatic Analyses “

Kumulative Dissertation

zur Erlangung des Grades

„Doktorin der Naturwissenschaften“

im Promotionsfach Pharmazie

am Fachbereich Chemie, Pharmazie,

Geographie und Geowissenschaften der

Johannes Gutenberg-Universität in Mainz

vorgelegt von Ayşegül Varol

geboren am 04.06.1990 in Turkey

Mainz, November 2025

Betreuer:

Uni.-Prof. Dr. Thomas Efferth

Gutachter der Arbeit:

Uni.-Prof. Dr. Peter Langguth

Uni.-Prof. Dr. Thomas Efferth

Tag der mündlichen Prüfung:

27.11.2025

Prüfungskommission:

Uni.-Prof. Dr. Peter Langguth (Vorsitzende)

Uni.-Prof. Dr. Thomas Efferth

Junior-Prof. Dr. Marie Winz

Frau Dr. Rümeysa Yücer (Protokoll)

D77 (Dissertation Universität Mainz)

Publications

Original articles as the first author

1) ***Ayşegül Varol,** Serap Sezen, Dilhan Evcimen, Atefeh Zarepour, Gönül Ulus, Ali Zarrabi, Icon,Gamal Badr, Sevgi Durna Daştan, Asya Gülistan Orbayoğlu, Zeliha Selamoğlu, Mehmet Varol, Cellular targets and molecular activity mechanisms of bee venom in cancer: recent trends and developments**.** Toxin Reviews, 2022. **41**(4): p. 1382-1395. DOI:10.1080/15569543.2021.2024576.

2) ***Ayşegül Varol,** Sabine M. Klauck, Françoise Dantzer, Thomas Efferth, Enhancing cisplatin drug sensitivity through PARP3 inhibition: The influence on PDGF and G-coupled signal pathways in cancer. Chemico-Biological Interactions, 2024: p. 111094. DOI: 10.1016/j.cbi.2024.111094.

3) ***Ayşegül Varol,** Joelle C. Boulos, Chunmei Jin, Sabine M. Klauck, Anatoly Zhitkovich, Thomas Efferth, (2024). The Inhibition of MSH6 Augments the Antineoplastic Efficacy of Cisplatin in Non-Small Cell Lung Cancer as Autophagy Modulator. Chemico-biological interactions, 2024. **402**: p. 111193. DOI: 10.1016/j.cbi.2024.111193.

4) ***Ayşegül Varol,** Sabine M. Klauck, Susan P. Lees-Miller, Thomas Efferth, (2025), Comprehensive transcriptomic analysis in wild-type and ATM knockout lung cancer cells: Influence of cisplatin on oxidative stress-induced senescence. Chemico-Biological Interactions, 2025: p. 111563. DOI: 10.1016/j.cbi.2025.111563.

Original articles as co-author

1) Vaishali Aggarwal, Hardeep Singh Tuli, **Ayşegül Varol**, Falak Thakral, Mukerrem Betul Yerer, Katrin Sak,Mehmet Varol, Aklank Jain, Md. Asaduzzaman Khan and Gautam Sethi, Role of Reactive Oxygen Species in Cancer Progression: Molecular Mechanisms and Recent Advancements. Biomolecules. Biomolecules, 2019. **9**(11): p. 735. DOI: 10.3390/biom9110735.
2) Min Zhou, **Ayşegül Varol**, Thomas Efferth. Multi-omics approaches to improve malaria therapy. Pharmacological Research. Pharmacological Research, 2021. **167**: p. 105570. DOI: 10.1016/j.phrs.2021.105570.
3) Iman Zare, Shahrzad Zirak, Hassan Kiadeh, **Ayşegül Varol,** Tuğba Ören Varol, Mehmet Varol, Serap Sezen, Atefeh Zarepour, Ebrahim Mostafavi, Shima Zahed

Nasab, Amid Rahi, Arezoo Khosravi, Ali Zarrabi, Glycosylated nanoplatforms: From glycosylation strategies to implications and opportunities for cancer theranostics. Journal of Controlled Release, 2024. 371: p. 158-178. DOI: 10.1016/j.jconrel.2024.05.032.

Conference papers

1- EACR-Sponsored 3rd Anticancer Agent Development Congress, Volume:3, Page: 65. Izmir, TURKEY, 2015. **Varol, A**., Koparal, A.T., Varol, M., Candan, M., Tay, T., Türk, A., A natural small-molecule alectoronic acid inhibits angiogenesis and suppresses proliferation of various cancer cells.

2- 5th International Congress of Molecular Medicine, Volume:5, Page: 58. Izmir, TURKEY, 2015. **Varol, A.,** Candan, M., Tay, T., Türk, A., Koparal, A.T., Varol, M., Anti-cancer and anti-angiogenic activities of a lichen-derived substance: α-collatolic acid.

3- 3rd International BAU-Drug design Congress, Volume: 3, Page: 194. Istanbul, TURKEY, 2015. Varol, M., Elmalı, D., Salih, B., **Varol, A**., Koparal, A.T., Novel across adjacent ring formed metallophthalocyanines-mediated photodynamic therapy inhibits the proliferation of human lung adenocarcinoma A549 cells and human keratinocytes HaCaT cells.

4- 4th International Congress of the Molecular Biology Association of Turkey, Volume: 4, Page: 133. Ankara, TURKEY, 2015. **Varol, A.,** Elmalı, D., Varol, M., Koparal, A.T., Salih, B., Investigation of new sandwich-type metallophthalocyanines-mediated photodynamic therapy.

5- ISACS19: Challenges in Organic Chemistry, Volume:19, Page: P05. Irvine, USA, 2016. Candan, M., **Varol, A**., Karabacak, R.T., Koparal, A.T., Varol, M., Tay, T., Alteration of anti-proliferative activity of vulpinic acid in novel colloidal system vulpinic acid treated poly (vinyl benzyl chloride).

6- 28. Ulusal Kimya Kongresi (Uluslararası Katılımlı), S-E1-001, Mersin, Türkiye, 2016. Elmalı, D., **Varol, A**., Koparal, A.T., Varol, M., Salih, B., Facile synthesis of unprecedented heteronuclear phthalocyanine ring and its evaluation in photodynamic therapy.

7- 41st FEBS Congress "Molecular and Systems Biology for a Better Life", Volume:283, Page: 344. Aydın, Turkey, 2016. Tay, T., **Varol, A**., Koparal, A.T., Varol, M., Candan, M., Investigation of some lichen-derived substances' cosmetic potential for skin protection against ultraviolet B.

8- 41st FEBS Congress "Molecular and Systems Biology for a Better Life", Volume:283, Page: 344. Aydın, Turkey, 2016. Candan, M., **Varol, A**., Koparal, A.T., Varol, M., Tay, T., Blockage of ultraviolet B-induced damage in human keratinocytes by a lichen compound norstictic acid.

9- 41st FEBS Congress "Molecular and Systems Biology for a Better Life", Volume:283, Page: 413. Aydın, Turkey, 2016. Varol, A., Elmalı, D., Varol, M., Salih, B., Koparal, A.T., Across adjacent ring formed titanium phthalocyanine-mediated photodynamic therapy alters and degrades filamentous actin cytoskeleton and internal membranes,

10- 6th European Association of Chemical and Materials Societies (EuCheMs) International Congress, Seville, Spain, 2016. Varol, A., Elmalı, D., Koparal, A.T., Varol, M., Salih, B., Internal membranes and actin cytoskeleton alteration by zinc phthalocyanine-mediated photodynamic therapy on human lung carcinoma and keratinocyte cells

Contribution to articles included in the dissertation

1. Title: Enhancing cisplatin drug sensitivity through PARP3 inhibition: The influence on PDGF and G-coupled signal pathways in cancer

Authorship contribution: Ayşegül Varol: Writing – review & editing, Writing – original draft, Validation, Software, Methodology, Investigation, Data curation, Conceptualization. Sabine M. Klauck: Writing – review & editing, Software, Methodology, Investigation, Data curation, Conceptualization. Françoise Dantzer: Methodology, Investigation, Conceptualization. Thomas Efferth: Writing – review & editing, Supervision, Project administration, Conceptualization.

2. Title: Inhibition of MSH6 augments the antineoplastic efficacy of cisplatin in non-small cell lung cancer as autophagy modulator

Authorship contribution: Ayşegül Varol: Writing – review & editing, Writing – original draft, Methodology, Investigation, Data curation, Conceptualization. Joelle C. Boulos: Methodology. Chunmei Jin: Methodology. Sabine M. Klauck: Writing – review & editing, Software, Methodology, Investigation, Data curation, Conceptualization. Anatoly Zhitkovich: Methodology, Investigation. Thomas Efferth: Writing – review & editing, Supervision, Project administration, Conceptualization.

3. Title: Comprehensive transcriptomic analysis in wild-type and ATM knockout lung cancer cells: Influence of cisplatin on oxidative stress-induced senescence

Authorship contribution: Ayşegül Varol: Writing – review & editing, Writing – original draft, Methodology, Investigation, Data curation, Conceptualization. Sabine M. Klauck: Writing – review & editing, Software, Methodology, Investigation, Data curation, Conceptualization. Susan P. Lees-Miller: Methodology, Investigation. Thomas Efferth: Writing – review & editing, Supervision, Project administration, Conceptualization

Erklärung

Hiermit erkläre ich an Eides statt, dass ich diese Arbeit selbständig verfasst und keine anderen als die angegebenen Quellen und Hilfsmittel verwendet habe.

27.11.2025 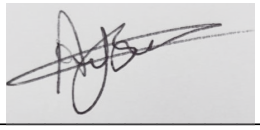

Ort, Datum Unterschrift

Acknowledgments

First and foremost, I would like to express my deepest gratitude to my esteemed supervisor, Prof. Dr. Thomas Efferth, for providing me the opportunity to pursue my Ph.D. within his prestigious research group. His strong scientific expertise and outstanding academic achievements in cancer research have been a constant source of inspiration, guiding me in carrying out various anti-cancer research projects. His invaluable mentorship, continuous support, and patience have played a crucial role in helping me overcome challenges throughout this journey.

I am also grateful to the Ministry of National Education of the Republic of Turkey for their financial and moral support during my studies and life in Germany. This scholarship has enabled me to realize my dream of pursuing a Ph.D. Moreover, it has provided not only financial assistance but also significant psychological support; for this, I sincerely thank my expert psychological counselor, Seçkin Çalışkan, for their guidance throughout this process.

I wish to express my deepest respect and gratitude to the great leader Mustafa Kemal Atatürk, who laid the foundation for women to pursue scientific careers as equal and strong individuals, and who continues to inspire and encourage us.

I am grateful to Prof. Dr. Thomas Efferth, Prof. Dr. Peter Langguth, and Junior-Prof Dr. Marie-Luise Winz for serving on my dissertation committee, and to Dr. Rümeysa Yücer for her role as secretary during the oral examination.

I would also like to express my heartfelt gratitude to my elder brother, Assoc. Prof. Dr. Mehmet Varol, who has guided me throughout my educational journey and served as a constant role model. I am deeply thankful to my mother, Döne Varol, for always listening with patience and dedicating her time and effort to support me. I would also like to sincerely thank my brother's wife, Assoc. Prof. Dr. Tuğba Ören Varol, and their son, Hazar Mete Varol, for their continuous support and encouragement. I dedicate this work to my late father, Allaattin Varol, with deep respect.

Finally, I am sincerely grateful to my friends, whom I consider family, for their constant support during difficult times: Dr. Assia Drif, Dr. Min Zhou, Dr. Nasim Shahhamzehei, Dr. Rümeysa Yücer, Dr. Mona Dawood, Dr. Joelle Boulos, Shila Prajapati, Ejlal Omer, Xiao Lei, Chunmei Jin, Faranak Bahramimehr, and the other members of the AK Efferth Group.

Abstract

Platinum-based chemotherapies, particularly cisplatin, are often limited by the emergence of drug resistance, driven not only by genetic alterations in DNA repair pathways but also by clinical factors such as patient age, race, gender, metastasis status, and tumor stage. To address these challenges, we performed integrative bioinformatics and experimental analyses across more than 7,500 tumors spanning 23 cancer types, aiming to identify key genetic determinants of chemoresistance.

Through comprehensive mutation profiling and overall survival analyses of genes involved in base excision repair (BER), mismatch repair (MMR), and double-strand break (DSB) repair pathways, we identified *PARP3*, *MSH6* and *ATM* as candidate predictive biomarkers. Functional studies using CRISPR/Cas9- and shRNA-mediated gene knockdown revealed that silencing these genes significantly increased cisplatin sensitivity in cancer cell lines.

Mechanistic investigations further showed that *PARP3* loss disrupted PDGF and G protein-coupled receptor (GPCRs) signalling pathways, enhancing drug efficacy. *MSH6* depletion shifted the balance of autophagy from pro-survival to pro-death, sensitizing cells to cisplatin. In parallel, *ATM* knockout induced oxidative stress-mediated senescence via suppression of NRF2 signaling.

Collectively, our findings identify *MSH6*, *ATM*, and *PARP3* as promising therapeutic targets for overcoming chemoresistance. The discovery of their associations with previously uncharacterized signalling pathways underscores their clinical and biological relevance. By integrating mutational landscapes with functional vulnerabilities, this study provides a conceptual framework for the development of personalized combination therapies tailored to the molecular profile of individual tumors, ultimately offering innovative strategies to enhance treatment efficacy in oncology.

Zusammenfassung

Platinbasierte Chemotherapien, insbesondere Cisplatin, sind häufig durch das Auftreten von Arzneimittelresistenzen begrenzt, die nicht nur durch genetische Veränderungen in DNA-Reparaturwegen, sondern auch durch klinische Faktoren wie Alter, ethnische Zugehörigkeit, Geschlecht, Metastasierungsstatus und Tumorstadium der Patienten bedingt sind. Um diesen Herausforderungen zu begegnen, führten wir integrative Bioinformatik- und experimentelle Analysen an über 7.500 Tumoren aus 23 Krebsarten durch, mit dem Ziel, zentrale genetische Determinanten der Chemoresistenz zu identifizieren.

Durch umfassende Mutations- und Überlebensanalysen von Genen, die an der Basenexzisionsreparatur (BER), der Mismatch-Reparatur (MMR) und der Reparatur von Doppelstrangbrüchen (DSB) beteiligt sind, identifizierten wir *PARP3*, *MSH6* und *ATM* als potenzielle prädiktive Biomarker. Funktionelle Studien unter Verwendung von CRISPR/Cas9- und shRNA-vermitteltem Gen-Silencing zeigten, dass die Stilllegung dieser Gene die Cisplatin-Empfindlichkeit in Krebszelllinien signifikant erhöhte.

Mechanistische Untersuchungen zeigten zudem, dass der Verlust von PARP3 die PDGF- und G-Protein-gekoppelten Rezeptor-(GPCRs)Signalwege störte und so die Wirksamkeit des Medikaments erhöhte. Der Verlust von MSH6 verschob das Gleichgewicht der Autophagie von pro-survival zu pro-death und sensibilisierte die Zellen für Cisplatin. Parallel dazu induzierte der ATM-Knockout eine durch oxidativen Stress vermittelte zelluläre Seneszenz durch Unterdrückung der NRF2-Signalübertragung.

Insgesamt identifizieren unsere Ergebnisse PARP3, MSH6 und ATM als vielversprechende therapeutische Zielstrukturen zur Überwindung von Chemoresistenz. Die Entdeckung ihrer Verbindungen zu bisher unbekannten Signalwegen unterstreicht ihre klinische und biologische Relevanz. Durch die Integration von Mutationslandschaften mit funktionellen Schwachstellen bietet diese Studie ein konzeptuelles Rahmenwerk für die Entwicklung personalisierter Kombinationstherapien, die auf das molekulare Profil individueller Tumoren zugeschnitten sind – mit dem Ziel, innovative Strategien zur Verbesserung der Behandlungseffektivität in der Onkologie zu entwickeln.

Table of contents

1.Introduction

1.1. Cancer

Cancer is defined as the uncontrolled proliferation of abnormal cells with the potential to invade surrounding tissues. Despite significant advances in cancer therapeutics over the past few decades, cancer remains a major clinical challenge for many patients [1]. Fatal relapses can occur years or even decades following the initial treatment process, often appearing as a metastatic disease — the leading cause of cancer-related mortality [1-3].

With over 100 known types, cancers can be broadly classified into six major histological categories: carcinoma, sarcoma, leukaemia, lymphoma, myeloma, and mixed forms [4]. Originating from normal tissues, malignant cells acquire the capacity to disseminate through the bloodstream and lymphatic system to distant organs. Each day, human cells are exposed to thousands of DNA lesions. The primary etiology of cancer results from genetic mutations or alterations that impair the normal regulation of cell proliferation and division. These mutations may occur spontaneously or be inherited through germline transmission.

To preserve genome integrity, cells have developed a series of sophisticated and intricate signalling networks that enable the repair of DNA lesions or the elimination of damaged cells [5]. In general, DNA damage response (DDR) encompasses several key mechanisms: (a) the repair of DNA lesions and the restoration of DNA duplex integrity; (b) the activation of DNA damage checkpoints, which halt cell cycle progression to facilitate repair and prevent the propagation of damaged or incompletely replicated chromosomes; (c) the transcriptional response, which modulates gene expression profiles in a manner that may support cellular adaptation and survival; and (d) apoptosis, a programmed cell death pathway that eliminates cells with extensive damage or severe regulatory dysfunction [6, 7]. However, the onset of cancer remains a seemingly inevitable consequence in many individuals despite the presence of evolutionarily conserved mechanisms designed to maintain genomic fidelity and cellular homeostasis. Understanding the molecular underpinnings of tumorigenesis opens way to the identification of key signalling pathways and cellular processes that are hijacked by cancer cells. In particular, identifying driver mutations and revealing their roles in tumors represents key areas of focus in cancer genome research.

Tumorigenesis is now accepted as a multistep evolutionary process resulting from alterations of genetic and epigenetic mechanisms. Hanahan and Weinberg proposed a seminal framework outlining ten hallmarks that underlie cancer development: (1) sustaining proliferative

signalling, (2) evading growth suppressors, (3) resisting immune destruction, (4) enabling replicative immortality, (5) promoting tumor-associated inflammation, (6) activating invasion and metastasis, (7) inducing angiogenesis, (8) genome instability and mutation, (9) resisting cell death, and (10) deregulating cellular energetics [8, 9]. Understanding these interconnected hallmarks remains a focal point to modern anticancer research.

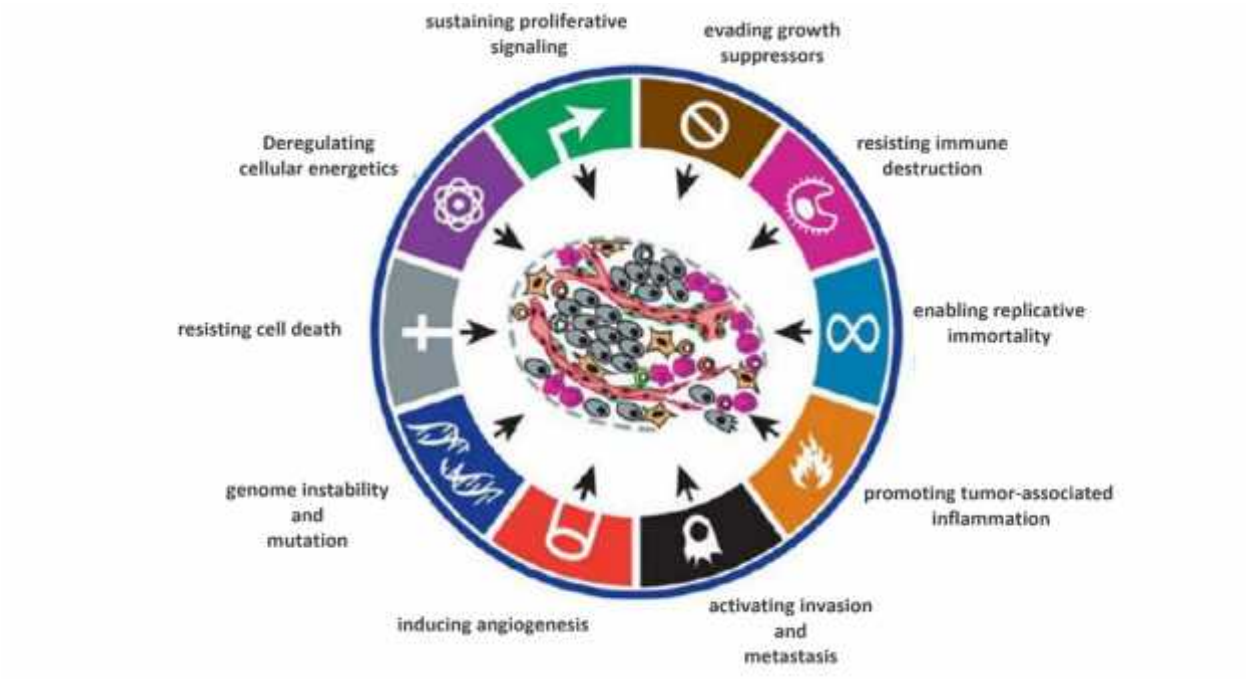

Figure 1: The hallmarks of cancer. The ten physiologic changes acquired by malignant cells for tumor development. [9] (With permission from Elsevier; Copyright 2011.)

1.2. Cancer treatment

Since its approval over six decades ago, conventional chemotherapy has remained a foundational component of cancer treatment strategies [10]. It continues to be one of the most commonly used therapies, used either alone or in combination with radiotherapy [11]. In current clinical practice, a multimodal approach — including surgical resection, radiation therapy, pharmacological agents, and other supportive therapies — is employed to cure cancer or prevent disease progression [12].

In recent years, significant therapeutic approaches have emerged such as stem cell therapy, immunotherapy, radiomics, nanoparticle-based systems, targeted therapies, ablation techniques, natural antioxidants, hormonal therapy, and gene therapy-based strategies [11].

Modern oncological research continues non-stop to develop safe, precise, and effective cancer nanomedicines.

Stem cell therapy is a promising strategy for regenerating and repairing damaged with the capacity to target both primary tumors and metastatic lesions. Immunotherapy — including monoclonal antibodies, immune checkpoint inhibitors, cancer vaccines, and adoptive cell transfer — has emerged as a transformative approach in oncology. This offers significantly improved clinical outcomes [13].

Radiotherapy induces DNA damage in malignant cells, leading to cell death [14]. Similarly, nanoparticles open the way to novel diagnostic and therapeutic opportunities, particularly through targeted drug delivery systems. This enhances treatment efficacy while reducing systemic toxicity.

Targeted therapies have enabled high specificity by selectively inhibiting molecular pathways involved in tumor growth and metastasis, thereby minimizing harm to normal tissues. Ablative techniques — such as thermal and cryogenic ablation — offer minimally invasive options to eradicate tumor masses without requiring open surgery.

Natural antioxidants contribute to cancer prevention and treatment by neutralizing free radicals and mitigating oxidative stress. Hormonal therapy remains an effective and comparatively low-toxicity intervention, particularly in hormone-responsive cancers such as breast and prostate malignancies [15]. Although its effectiveness is greatest in these tumors, some other tumor forms have also shown minimal hormonal reactivity.

Gene therapy has also emerged as a promising domain in cancer treatment, encompassing a variety of strategies such as prodrug-activating suicide genes, anti-angiogenic gene delivery, oncolytic virotherapy, immune-modulating gene constructs, correction or compensation of genetic mutations, regulation of apoptotic and metastatic signalling pathways, antisense oligonucleotides, and RNA interference (RNAi)-based techniques [16]. The central aim of gene therapy is to deliver and express therapeutic genes in target tissues to restore or enhance physiological functions or to inhibit pathological processes. Several of these experimental approaches have reached in various stages of clinical evaluation.

Ultimately, the choice of treatment modality depends on factors such as cancer type, stage of progression, and therapeutic intent [13].

1.2.1 Classical chemotherapy

The advancement of cytotoxic chemotherapy has fundamentally changed the cancer treatment paradigms [17]. In the early 20th century, German chemist Paul Ehrlich pioneered the use of chemotherapy for infectious diseases and, through animal studies, discovered its potential in cancer treatment [18]. His work opened door to improving modern chemotherapeutic approaches against various cancers [19].

Chemotherapeutic agents can be employed via oral, intramuscular, or intravenous routes to achieve systemic therapeutic concentrations. However, these drugs lack tumor specificity, targeting both rapidly dividing malignant cells and normal proliferative tissues such as hair follicles, gastrointestinal epithelium, and bone marrow stem cells. This non-selective action leads to significant adverse effects and damage to healthy tissues [20]. Chemotherapy agents can be categorized under various classes:

1) Antimetabolites:

Antimetabolites, the most extensively utilized class of anticancer agents dates back to the mid-20th century [21]. They began with folate analogs such as aminopterin and methotrexate [19]. As the earliest designed chemotherapeutic drugs, antimetabolites specifically target nucleic acid synthesis by interfering with RNA and DNA production, positioning them as the first generation of targeted cancer therapies.

2) Alkylating agents:

Alkylating agents have been preferred in cancer therapy for more than sixty years. These compounds display their effects by directly interacting with DNA, forming cross-links at the N-7 position of guanine residues [22]. Their effects include DNA strand breaks, faulty base pairing, disruption of cell division, and ultimately, cell death [23]. However, their clinical effectiveness results in systemic toxicity and the development of drug resistance.

3) Mitotic spindle inhibitors:

Cancer cells proliferate and metastasize through relentless mitotic divisions. Microtubules are elongated polymers composed of tubulin monomers. Their role is in chromosome segregation during cell division by facilitating their separation [24, 25]. Regarding mitotic inhibitors, the majority of clinically utilized agents bind to tubulin, the fundamental component of microtubules and disrupting mitotic spindles [26]. Among the most well-known mitotic spindle inhibitors are the *Vinca* alkaloids (*e.g.*, vinblastine, vincristine) and the taxane group (*e.g.*,

paclitaxel, docetaxel) [25]. However, these drugs have notable adverse effects *in vivo*, which restrict their therapeutic potential.

4) Anthracyclines:

Since their discovery in the early 1960s, anthracyclines have become a cornerstone of anticancer chemotherapy [27]. The earliest members of this class, daunorubicin and doxorubicin, were derived from pigment-producing *Streptomyces* species [27, 28]. The mechanism underlying anthracycline-induced cardiotoxicity is considered multifactorial [29]. They were previously attributed primarily to reactive oxygen species (ROS)-mediated DNA damage, [30]. However, their main side effects of anthracyclines include acute myelosuppression, cumulative dose-related cardiotoxicity, mucositis, nausea, vomiting, alopecia, and radiation recall reactions [27].

5) Antihormones:

Hormonal activity is recognized as a critical determinant in the pathogenesis of numerous highly prevalent cancers worldwide, such as endometrial, breast, and ovarian neoplasms in women, and prostate cancer in men [31]. Hormones have an influence carcinogenesis by modulating cellular proliferation dynamics [32].

1.2.2 Targeted therapy

Targeted therapy represents a therapeutic strategy that employs pharmacological agents or other biologically active substances to selectively inhibit specific enzymes, growth factor receptors, and intracellular signalling pathways implicated in the proliferation, survival, and metastasis of cancer cells [33]. Due to its specificity and individualized approach, this modality is frequently accepted as “precision medicine” or “personalized medicine.” The targeted therapeutic approaches include: (1) small molecule inhibitors, (2) therapeutic monoclonal antibodies, (3) cancer-specific vaccines, and (4) gene therapy.

1) Small molecule drugs

A fundamental limitation of chemotherapy results from its non-selective mechanism of action, which fails to differentiate between malignant and healthy cells, thereby leading to substantial systemic toxicity and adverse side effects [34]. In response to these challenges, modern science has increasingly shifted from traditional cytotoxic agents to small targeted cancer therapies [35]. Small molecules aim to achieve therapeutic efficacy with minimal toxicity by selectively targeting specific molecular markers unique to cancer cells. To date, some of the most well-

known examples of small-molecule targeted anti-cancer agents include kinase inhibitors, such as receptor tyrosine kinase inhibitors (targeting ALK, c-Met, EGFR, FLT3, VEGFR/FGFR/PDGFR, TRK), non-receptor tyrosine kinase inhibitors (targeting Bcr-Abl1, BTK, JNK), and serine/threonine kinase inhibitors (targeting BRAF/MEK/ERK, CDK, PI3K/AKT/mTOR), as well as epigenetic inhibitors (targeting EZH2, HDAC, IDH1/2), BCL-2 inhibitors, Hedgehog pathway inhibitors, proteasome inhibitors, and PARP inhibitors [34].

2) Monoclonal antibodies

Monoclonal antibodies are designed to inhibit a specific antigen expressed on the surface of cancer cells [36]. This antigen may also be present in the surrounding tumor microenvironment or adjacent tissues [37]. Among the most commonly used monoclonal antibodies in oncology are trastuzumab, which targets the HER2 receptor in HER2-positive breast cancer, and rituximab, which binds to the CD20 antigen in non-Hodgkin lymphoma [38, 39].

3) Cancer vaccines

The primary objective of therapeutic cancer vaccines is to promote tumor regression, eliminate minimal residual disease, generate durable antitumor immune memory, and minimize nonspecific or deleterious immune responses, such as Gardasil-9® and Bacillus Calmette-Guérin [40]. Nevertheless, the immunosuppressive and immunoresistant properties induced by tumors present considerable obstacles to the successful attainment of these outcomes.

4) Gene therapy

Gene therapy involves the introduction of genetic material, such as RNA or DNA, into a host organism via a delivery vector designed to facilitate the transfer of exogenous genetic sequences [41]. This genetic material can be administered directly into the target tissue or organ (*in vivo* gene therapy) or used to genetically modify autologous cells *ex vivo*. Gene therapy has used to restore normal gene function by supplying a functional copy of the defective gene, enhancing the expression of therapeutic genes, or inhibiting the activity of pathogenic genes [42, 43]. At present, four structurally distinct classes of gene-editing nuclease enzymes have been developed: meganucleases, zinc finger nucleases (ZFNs), transcription activator-like effector nucleases (TALENs), and CRISPR-associated (Cas) nucleases [41].

The CRISPR/Cas9 system represents one of most efficient genome-editing platforms. Currently, It has been applied across diverse fields of biomedical and molecular research [44]. The CRISPR/Cas9 system originated as an adaptive immune strategy in bacteria and archaea,

having naturally evolved to counteract phage invasions and impede horizontal gene transfer *via* plasmids [45]. The CRISPR/Cas9 system has been widely utilized for several targets including genome engineering, the targeted activation or repression of gene expression [46]. Cas9 endonuclease is guided by a single-guide RNA (sgRNA) to introduce site-specific double-strand breaks in DNA [47]. These breaks are subsequently repaired by cellular mechanisms such as non-homologous end joining (NHEJ) or homology-directed repair (HDR), leading to gene disruption or precise sequence modifications. This technology has been employed a wide range of biomedical fields, including combating oncogenic viral infections, developing anticancer therapeutics, advancing oncolytic virotherapy, and enhancing cancer immunotherapy [47]. In particular, the CRISPR-Cas9 system is a promising strategy due to its high efficiency and relative simplicity, particularly in validating drug targets, identifying genes associated with drug resistance, and discovering novel therapeutic targets.

1.3. The role of cisplatin in cancer treatment

Cisplatin has been utilized in the treatment of various human malignancies, particularly bladder, head and neck, lung, ovarian, and testicular cancers [48]. Cisplatin exerts its effects by binding to bases within the DNA. It binds to the N-7 positions of purine bases, notably adenine and guanine [49]. This binding results in the formation of both intrastrand and interstrand DNA crosslinks, impairing the normal structure and function of DNA. Consequently, essential cellular processes such as replication and transcription are hindered [50]. Then, cisplatin prevents cell proliferation and trigger apoptotic cell death [51].

Despite its clinical efficacy, cisplatin treatment has major challenges, particularly due to the development of drug resistance and the occurrence of severe side effects [52]. These adverse effects include acute kidney injury, gastrointestinal disorders, hemorrhage, and a diminished immune response, commonly observed in a substantial proportion of cancer patients [53]. Patients treated with cisplatin in a long-term period, cisplatin significantly leads to the accumulation of mutations. Mutations can impair its interaction with DNA, leading to dysregulated gene expression and subsequent aberrant protein production. This triggers to appear the primary mechanisms underlying cisplatin resistance.

Resistance to cisplatin arises from both intrinsic and acquired cellular mechanisms [54]. Principal factors are known as decreased drug uptake, increased efflux, and enhanced inactivation by sulfhydryl-containing molecules such as glutathione, as well as elevated DNA repair activity [55]. The alterations in oncogene expression and disruptions in apoptotic

signalling pathways result in resistance development [55]. Enhanced excision of DNA adducts through repair pathways or increased lesion bypass further contribute to resistance, while dysregulation of apoptosis-regulating signalling proteins modulates cellular sensitivity to the drug [54]. Advancing the understanding of these resistance mechanisms opens way to identifying novel therapeutic targets, thereby offering opportunities to enhance cisplatin's clinical efficacy in cancer treatment.

1.4 Overview of DNA repair mechanisms

1.4.1 Reversion repair

Reversion repair includes three distinct DNA repair mechanisms. These are single-step repair by MGMT, DNA-damage reversal by AlkB homologues, and photoreactivation, respectively.

The single-step repair mechanism occurs through O^6-methylguanine-DNA methyltransferase (MGMT). It functions in cellular defense against alkylating agents [56]. MGMT is specifically responsible for repairing O^6-alkylation lesions in DNA through a direct alkyl transfer reaction [57]. *O*^{6}-methylguanine–DNA methyltransferase plays a role in the execution of the reaction [58]. This repair mechanism involves the transfer of an alkyl group from the O^6 position of guanine to a cysteine residue in the catalytic pocket of MGMT, thereby restoring genomic integrity. This mechanism leads to the irreversible inactivation of the enzyme [58, 59]. Each O^6-alkylated guanine base requires one MGMT molecule for repair [60].

AlkB homologues function in the direct reversal of DNA alkylation damage [61]. AlkB repairs alkylated DNA bases by removing methyl groups from 1-methyladenine (1-meA) and 3-methylcytosine (3-meC) through oxidative demethylation, restoring them to normal adenine and cytosine [62]. This mechanism prevents mutagenesis caused by alkylating agents. In humans, several AlkB homologues (*e.g.*, ALKBH2, ALKBH3) participate in both DNA and RNA repair processes [57].

In the evolutionary changes of photoreactivation, photolyase recognizes UV-induced DNA lesions in a light-independent manner; however, the enzymatic repair process occurs in visible light and proceeds via a light-dependent photoreactivation mechanism [57].

1.4.2 Base excision repair (BER)

Living organisms have different excision repair pathways as defense mechanisms against DNA damage arising spontaneously within cells [63]. DNA integrity in the cell is affected every day by damaging agents of endogenous and exogenous origin including UV light, ionizing

radiation, and oxidative stress [64]. Among them, reactive oxygen species (ROS)-induced damage is particularly significant [65]. In particular, ROS are generated by the electron transport chain in mitochondria, or onizing radiation and UV irradiation[66]. The rate of oxidative DNA damage in living cells is not clear, but oxidation reactions collectively account for the main sources of DNA damage. Base oxidation typically occurs at specific reactive sites, leading to the formation of mutagenic 8-hydroxyguanine and ring-opened forms of purines (formamidopyrimidines) [67]. Most ROS-induced oxidized base lesions give rise to point and sometimes more complex mutations [65]. Single nucleotide polymorphisms (SNPs), revealed at quite high frequency (1 in 300 bp) in mammalian genomes, are likely produced from such spontaneous mutations [65]. Spontaneous mutations in oncogenes and tumor suppressor genes contribute significantly to sporadic cancers, though environmental and lifestyle factors are also important. [68].

DNA repair mechanisms is to ensure genomic integrity against the constant threat resulting from these damaging agents [69]. DNA damage leads to a temporary arrest of cell-cycle progression which results in the action of DNA repair mechanisms prior to replication [70]. The type of DNA damage is a major factor indetermining the pathway performing therepair process [71]. Base excision repair pathway (BER) is a main mechanism thatcorrects the plethora of oxidative damages deaminations, alkylations, and abasic single base damage including apurinic/apyrimidinic (AP) sites [72]. If the existing lesions do not correct through DNA repair mechanism, they can influence normal cellular processes by the inhibition of replication, transcription, and result in chromosome rearrangements, instability, cell death, aging, and diseases including cancer [73, 74].

BER is a highly preserved mechanism from bacteria to humans and also responsive for removing the tens of thousands of DNA damages occurred daily in each of human cell [75]. BER is probably the most frequently used mechanism to correct DNA lesions in nature [63]. The loss of BER function result in drastic consequences including hypermutation and increased cancer risk in human [75]. Although BER plays role to repair of a majority of cellular DNA damages, the exact mechanism of BER in prevention of disease remains under investigation [65]. However, in the general mechanism of BER is accepted in the five steps including (i) base removal; (ii) incision of the resulting abasic site; (iii) processing of the generated termini at the strand break; (iv) DNA synthesis, and (v) ligation [76]. In the nucleus, the process is known as the mainly active in the G1 phase of the cell cycle [77]. The several multienzyme and multistep process play a role to keep the cellular genome through BER mechanism [78]. The key enzymes in this process is supposed to highly preserved during evolution [63]. Firstly, Thomas Lindahl

found in 1974 that enzymatic activity has a role of deamination cytosine [79]. This was a considerable progress to understand of DNA glycosylases that played a pioneer role and BER mechanism [71]. The enzyme discovered, uracil DNA glycosylase has been paid a way to discover a new type of enzyme that released the damaged base [6].

The first step of BER is initiated by damaged specific DNA glycosylases [6]. Obviously, DNA glycosylases have an essential role to protect the long-term integrity of genome [80]. DNA glycosylases evolved to correct the many different forms of chemical damage occurring to DNA bases [80]. They recognize and remove the damaged base to organize the regular DNA structure with high accuracy [71, 80]. DNA glycosylases are relatively small protein that perform activity without metal ions or other co-factors [81]. Totally 11 DNA glycosylases have been identified to extract alkylated bases, deaminated bases, oxidized bases, and mismatched bases among others [80, 82]. DNA glycosylases are responsible for cleaving the N-glycosylic bond between the target base and deoxyribose [70]. They catalyse N-glycosidic bond hydrolysis to remove damaged base [83].

In BER, DNA glycosylases fall into two major classes because of the different catalytic mechanism [84]. Monofunctional DNA glycosylases cleave the glycosidic bind using water as a nucleophile that result in apurinic and apyrimidic (AP) sites [71]. However, bifunctional DNA glycosylases use amine nucleophile of protein to attack C1´ instead of water [84]. Monofunctional glycosylases is responsive for only catalyse base excision, whereas bifunctional glycosylases made a lyase activity by cleaving the backbone immediately 3` to the AP site as well as glycosylases [85]. After lyase activity, bifunctional glycosylases form a Schiff-base intermediate, and subsequently cleave the DNA backbone 3´ to the lesion [80]. To sum up, the monofunctional glycosylases exhibit glycosylase activity, bifunctional glycosylases have glycosylase/β-lyases activities [83]. UNG, SMUG1, MBD4, TDG, MYH, MPG are accepted as monofuntional DNA glycosylases, although OGG1, NTHL1, NEIL1, NEIL2, NEIL3 belong to the bifuntional DNA glycosylase subgroub (Table 1) [80].

In the monofuntional glycosylases, uracil-N glycosylase (UNG) is responsible for removing uracil from the genomic DNA [86]. Also, UNG interact with the replication protein (RPA) and proliferation cell nuclear antigen (PCNA) to co-localize for replication foci during S phase [87]. Single-strand-specific monofunctional uracil DNA glycosylase 1 (SMUG1) excise uracil and certain oxidized bases during DNA repair [88]. Thymine DNA glycosylase (TDG) has a capability of excising thymine from guanine thymine mismatches [89]. Also, it plays a major role in the repair of thymine residues arising from deamination of 5-methylcytisone (5-meC) [71]. Moreover, it regulates gene transcription [89]. The 3-methyl-purine glycosylase (MPG)

responsive for excising a range of alkylated bases from DNA [80]. Mismatch specific thymine glycosylase MBD4 is a member of the methyl-CpG-binding protein family that contains a methyl CpG-binding domain (MBD) and a C-terminal glycosylase domain [85]. MBD4 excises thymines from G:T mispairs [90]. MutY homolog DNA glycosylase (MYH) is an enzyme excising adenine from A:G mispairs that was first detected in *E.coli* [91].

In the bifunctional glycosylases, 8-OxoG DNA glycosylase 1 (OGG1) repair the damaged base by oxidation by N-glycosylase and β-lyase activities [92]. Oxidative stress cause 8-oxoG opposite C in DNA that relatively abundant, but the lesion is removed by OGG1[6]. OGG1 is among the best studied of a large group of glycosylases repaired the damaged DNA bases [92]. Polymorphisms in the human *OGG1* gene impairing the 8-oxoG incision activity were related to non-small cell lung cancer and an increased risk of childhood acute lymphoblastic leukemia [93, 94]. Apart from OGG1, there are four human DNA bifunctional glycosylases to recognize oxidized pyrimidines and formamidopyrimidines [75]. The endonuclease III-like protein 1 encoded by NTHL1 and NEIL1/2/3 (endonuclease VIII-like glycosylase 1-2-3) is involved in BER to recognizes and removes mainly oxidized pyrimidines and ring-opened purines [95].

Table 1: Classification of DNA glycosylases based on substrate specificity and enzymatic function.

Enzyme		Name	Monofunctional/bifunctional glycosylase	Physiological substrates
	UNG	Uracil-N glycosylase	M	U, 5-FU, ss and dsDNA
	SMUG1	Single-strand-specific monofunctional uracil DNA glycosylase 1	M	U, 5-hmU, 5-FU, ss and dsDNA
Pyrimidine derivates in mismatches	MBD4	Methyl-binding domain glycosylase 4	M	T, U, 5-FU, εC, opposite G, dsDNA
	TDG	Thymine DNA glycosylase	M	T, U, 5-FU, εC, 5-hmU, 5-fC, 5-caC; opposite G, dsDNA
Oxidative base damage	OGG1	8-OxoG DNA glycosylase 1	B	8–oxoG, FaPy, opposite C, dsDNA
	MYH	MutY homolog DNA glycosylase	M	A opposite 8–oxoG, C or G, 2–hA opposite G, dsDNA
Alkylated purines	MPG	Methylpurine glycosylase	M	3–meA, 7-meG, 3- meG, hypoxanthine, εA, ss and dsDNA
Oxidized, ring-fragmented or –saturated pyrimidines	NTHL1	Endonuclease III-like 1	B	Tg, FaPyG, 5-hC, 5-hU, dsDNA
	NEIL1	Endonuclease VIII-like glycosylase 1	B	Tg, FaPyG, FaPyA, 8-oxoG, 5–hU, 5– hC, ss and dsDNA
	NEIL2	Endonuclease VIII-like glycosylase 2	B	Similar to NTHL1 and NEIL1
	NEIL3	Endonuclease VIII-like glycosylase 3	B	FaPyG, FaPyA, prefers ssDNA

U, uracil; A, adenine; T, thymine; , C, cytosine, G, guanine; ss single stranded; ds, double stranded; 5–hm, 5–hydroxymethyl; 5-FU, 5- fluorouracil; ε, etheno; 5-fC, 5-formylcytosine; 5-caC, 5-carboxylcytosine; 8–oxoG, 8–oxo-7,8-dihydroguanine; Tg, thymine glycol; FaPy, 2,6-diamino-4-hydroxy-5-N-methylformamidopyrimidine; me, methyl; h, hydroxyl [80, 95].

The activities of DNA glycosylases remove damaged bases and leave AP sites, the intermediate product of BER, which is a substrate for AP endonucleases [78, 95]. AP sites can be mutagenic and cytotoxic which pose to a major threat to cell survival [96]. According to some results,

10,000 AP sites per day are generated in mammalian cells, mainly due to purine loss [97]. To cope with the large number of mutagenic and cytotoxic abasic lesions in DNA, organisms have a multifunctional enzyme, named AP-endonucleases [96]. AP-endonucleases (APEs) incise into DNA at 5´ of an AP site endonucleolytically, resulting in a single-stranded nick in the DNA strand with a 3'-OH terminus and 5'-deoxyribose phosphate structure [97]. Human basic AP endonuclease 1 (APE1), a member of a large family of nucleases, is important for mammalian cells [97, 98]. APE1 is responsible for both an AP endonuclease activity and a redox function required for activation of several transcription factors [95]. Additionally, APE2 is a second APE family member with only weak AP endonuclease activity human [99]. APE2 is different from APE1 at the N- and C- terminal ends, but it has many of the essential active site residues [96]. APE2 has 3´ phosphodiesterase activity and a 3´-5´ exonuclease activity that helps remove mismatched nucleotides from the 3´ end of the nick [75]. In mammalian cells, AP-endonucleases facilitates binding of Polβ to DNA and stimulates the deoxyribose phosphodiesterase activity of Polβ *in vitro* [96].

After AP-endonuclease activity, the BER pathway is followed by at least two BER sub-pathways: 'short-patch' BER (SP-BER) and 'long-patch' BER (LP-BER) [100]. The two sub-pathways that involve different subsets of enzymes result in the replacement of one nucleotide (short-patch BER) or two and more nucleotides (long-patch BER) [101]. Additionally, the oxidized and reduced abasic sugar governs the selection between the sort- and long-patch BER modes, because modified sugar is a barrier for DNA polymerase β (Polß) activity [102, 103]. In the short patch BER pathway, with the unmodified deoxyribose phosphate (dRP) group, pol β distracts the 5‘- dRP through lyase activity [104]. Pol β, one of the four known nuclear DNA polymerases, is composed of a single polypeptide (39 to 45 k D in vertebrates) that highly conserved among higher eukaryotes [104]. In the BER pathway, polβ has two key activities: DNA polymerase and dRP lyase activities [75]. Thus, It fills small gaps and nicks in DNA [104]. Subsequently, DNA ligase III-XRCC1 complex completes the sealing of the nicked strand [105]. XRRC1 is known as X-ray repair cross complementing protein 1 that acts as a scaffolding protein in coordinating base excision repair and also single strand break repair [66]. At this point, XRCC1 has been shown to be linked to a number of BER proteins [75]. XRCC1 has the capability to mediate the assembly of large multiprotein DNA repair complexes as well as facilitating the requirement of DNA repair protein to sites of DNA lesions [66]. In particular, it is essential for the stability of DNA ligase III [106].

In the long patch BER pathway, the oxidized and reduced abasic sugar is required for cleavage activity. If the sugar group is oxidized or reduced, it is not removed by the pol β dRB lyase

activity and the nick cannot be sealed by DNA ligase [103]. In order to remove modified sugar, long-path BER is initiated [75]. To sum up, main differences of LP-BER from SP-BER are the removal of the incised abasic residue (5´dRp) [101]. The flap structure-specific endonucleases (FEN1) cleaves the 5'-dRp residue to create strand displacement synthesis [107]. The strand displacement synthesis occurs by polβ as well as polδ and polε [67]. The role of the polymerases participating in the long patch BER pathway is still not understood, but polß plays a vital role in the initiation of strand displacement synthesis [101]. Obviously, polβ relies on cleavage by FEN 1 to remove barriers and accomplish long patch BER [103]. FEN1 stimulates polβ-mediated DNA synthesis on the long patch BER pathway [102]. Additionally, FEN1 is an important family of enzymes enzyme involved in Okazaki fragment processing [108]. In this process, proliferating cell nuclear antigen (PCNA) activates flap endonucleases I releasing the oligonucleotide (2- to 11-nucleotide) containing the dRP moiety [67]. Obviously, PCNA plays a role as a molecular adaptor in base excision repair, because its role is not only to combine the damage-scanning by uracil DNA-*N*-glycosylase (UNG2) and adenine DNA glycosylase (MYH) with the DNA replication, but also to recruit polδ/polε, FEN1, and DNA ligase 1 in the process of repair [109].

Additionally, Rad9a, Hus1 and Rad1 (the 9-1-1 complex) acts as mediators of DNA repair like PCNA. The 9-1-1 complex displays structural and functional similarity with PCNA [110]. The 9-1-1 complex plays an important role in recognizing base lesion and to recruit appropriate proteins to repair sites [102]. The 9-1-1 complex interacts with five independent enzyme participated in BER, namely APE1, FEN1, MYH, Polß and DNA ligase 1 [102, 111]. In particular, 9-1-1 enables the strand displacement activities of polβ by FEN1 to flap cleavage before ligation to repair base lesion [102]. In the last step, DNA ligase I and III complete LP-BER [57]. In the long patch BER, DNA ligase I is associated with PCNA and Polβ [57, 112]. Recently, it has been shown that DNA ligase I, rather than DNA ligase III, may play important roles as the nuclear DNA ligase both in the short patch BER and long patch BER, but DNA ligase III is important in mitochondria [95]. Thus, the base repair is completed in the LP-BER.

1.4.3 Mismatch repair (MMR)

Mismatch repair (MMR), an evolutionarily conserved pathway, functions to maintain genomic stability [113, 114]. As a key mutation-avoidance system, MMR corrects base-base mismatches and insertion-deletion loops that arise during DNA replication and recombination [115, 116]. Thus, it ensures the faithful transmission of genetic information in dividing cells. MMR proteins prevent their propagation by excising the erroneous strand and resynthesizing it using the

parental strand as a template [113, 115]. In addition to correcting replication errors, MMR enables to cellular responses to certain types of DNA damage. While it does not directly repair all DNA lesions, MMR mediates cell cycle arrest or apoptosis in response to methylated bases, oxidative lesions, and other genotoxic stressors [117].

Beyond its canonical repair function, MMR plays an important role in initiating biological processes such as cell cycle arrest and apoptosis in response to genotoxic stress [118]. These processes are tightly regulated by a complex network of MMR proteins (Table 2) [116], which also contribute to the cellular response to environmental stressors like chemical carcinogens and UV radiation [118]. Additionally, the role of MMR includes the suppression of recombination between divergent DNA sequences, influencing immune system development, and involvement in meiotic processes [119].

In multicellular organisms, DNA repair is often followed by the elimination of irreparably damaged cells via apoptosis, necrosis, mitotic catastrophe, or senescence [114]. MMR-mediated signalling can activate cell cycle arrest or programmed cell death in response to specific types of DNA damage [118]. Loss of MMR function impairs these apoptotic responses, allowing damaged cells to persist and acquire a selective growth advantage for the multi-step carcinogenesis process [120]. Although the precise molecular mechanisms are unclear, MMR may directly alter apoptotic signals through both p53-dependent and p53-independent pathways [121, 122]. The tumor suppressor protein p53 triggers apoptosis if MutSα and MutLα are functional [123, 124].

MMR deficiency not only facilitates carcinogenesis but also contributes to resistance against DNA-damaging agents such as alkylating compounds, certain chemotherapeutic drugs, and UV radiation [125]. Particularly, MMR-deficient cells display resistance to detecting DNA damage and initiating apoptosis [126].

MMR deficiency leads to the accumulation of mutations in mono- and dinucleotide repeats due to unrepaired insertion/deletion loops [127]. This genomic instability underlies hereditary nonpolyposis colorectal cancer (HNPCC), also known as Lynch syndrome [116, 128]. Germline mutations in any of the five core MMR genes—*MSH2*, *MLH1*, *MSH6*, *PMS2*, and *PMS1*—account for 1–5% of all colorectal cancer cases [129]. Two distinct forms of genomic instability commonly observed in colorectal cancer are microsatellite instability (MSI) and chromosomal instability (CIN) [130]. The eukaryotic genome contains numerous short tandem repeats (STRs) motifs in DNA. They make up approximately 3% of the human genome [131].

Loss of MMR leads to high rates of mutation in these microsatellite regions, a phenomenon known as microsatellite instability (MSI) [132]. Conversely, chromosomal instability (CIN), which involves the gain or loss of whole chromosomes or chromosomal fragments, is also linked to characteristic mutation accumulation and defective repair pathways [133, 134].

MMR proteins are encoded by two conserved gene families: *MutS* (*MSH2, MSH3, MSH6*) and *MutL* (*MLH1, MLH3, PMS1, PMS2*) [135]. MMR consists in three primary steps: mismatch recognition, excision of the error-containing strand, and DNA resynthesis [136]. Recognition is mediated by two heterodimeric MutS complexes: MutSα (MSH2–MSH6) and MutSβ (MSH2–MSH3), which bind to different types of mismatches [137-139]. MutSα predominantly recognizes single base mismatches and small insertion-deletion loops (1–2 nucleotides), whereas MutSβ detects larger insertions or deletions (2–10 nucleotides) more effectively [139-141].

Table 2: The role of proteins involved in mismatch repair.

Mismatch repair component (*Homo sapiens*)	**Molecular function**
MutSα (MSH2-MSH6) MutSβ (MSH2-MSH3)	Recognition of DNA mismatches and insertion/deletion [116]
MutLα (MLH1-PMS2) MutLβ (MLH1-PMS1) MutLγ (MLH1-MLH3)	Primarily, MutLα plays a core role to strand incision [128]. Molecular matchmaker; endonuclease activity, termination of excision by leading to nicks in discontinued strands [116]
PCNA	Initiates repair process, supporting DNA re-synthesis [116], activates nick-directed excision [142]
RPA 1-3	Promoting to DNA resynthesis, acts as stimulator for EXO1 activity [139]
EXO1	5′-3′ dsDNA exonuclease, completes the excision step [128]
RFC	Loading of PCNA [119]
Pol delta	Completing repair synthesis [119]
Ligase 1	Sealing nicks after DNA resynthesis [120]

At the initial stage of the mismatch repair (MMR) process, ATP hydrolysis activates of MutS proteins [143]. The ATPase activity of MutS mediates to the proofreading function, mismatch recognition, and coordination of downstream repair events [144]. Based on various

biochemical, structural, and genetic studies, there are wo primary models to explain the ATP-dependent movement of MutS along DNA [128].

The first model, known as the “sliding clamp model”, suggests that MutS initially binds to the mismatched DNA in an ADP-bound state, which then undergoes a rapid exchange of ADP for ATP [128, 145]. This ATP binding induces a conformational change in MutS, transforming it into a sliding clamp structure that diffuses away from the mismatch in an ATP hydrolysis-independent manner [120, 129]. In this context, sliding is not essential for recruiting MutL but is required for the eventual removal of the mismatch [146]. The ATP-activated MutS sliding clamp further activates the MutL homodimer [141].

The second model, referred to as the “translocation model”. In this proposes, ATP hydrolysis provides the energy necessary for MutS to translocate along the DNA [128, 145]. In this model, MutS moves away from the mismatch site in an ATP-dependent manner, potentially facilitating communication with other repair components [125].

In eukaryotic cells, MutL introduces a nick in the newly synthesized DNA strand. This establishes an entry or terminate site for the excision process. The MutL family forms three distinct heterodimers with specific functions: MutLα (MLH1–PMS2), MutLβ (MLH1–PMS1), and MutLγ (MLH1–MLH3) [147, 148]. Among them, MutLα is the most significant complex involved in DNA mismatch repair in human cells [149]. While all three heterodimers share structural and functional similarities, they differ in their recruitment mechanisms, substrate specificity, and strand-nicking activity [148]. Moreover, these complexes are also involved in meiotic recombination and the proper segregation of homologous chromosomes during meiosis [148].

The MutS–MutL complex facilitates strand discrimination during repair, although the precise mechanism of strand selection in eukaryotes remains unclear [119]. However, it has been hypothesized that pre-existing nicks and gaps in the daughter strand serve as signals to differentiate it from the parental strand [150]. Biochemical evidence suggests that proliferating cell nuclear antigen (PCNA) is a key factor in strand discrimination, particularly on the leading strand [128, 137].

PCNA interacts with multiple MMR proteins to coordinate the repair process as well as play an important role in DNA synthesis and excision [139, 151]. Eukaryotic MutS homologs contain five conserved domains and an N-terminal PCNA-interacting motif that facilitates this interaction [120]. Although the exact function of the PCNA–MutS/MutL interaction remains

to be fully elucidated, PCNA enhances the binding specificity of MutSα to mismatched DNA and stimulates repair activity [152-154]. In this context, replication factor C (RFC) is responsible for loading PCNA onto DNA at the site of a nick [119, 155].

Ultimately, the coordinated interaction among MutLα, PCNA, RFC, and the DNA substrate enables strand discrimination and the initiation of repair over a distance from the mismatch site [150]. MutLα becomes activated in the presence of MutSα, RFC, PCNA, and ATP [156]. Upon activation, MutLα introduces nicks in the nascent strand both proximal and distal to the mismatch site [119]. These nicks serve as initiation points for excision.

During the excision step, exonuclease 1 (EXO1) degrades the discontinuous strand in the 5′ to 3′ direction from a nick, creating a single-stranded DNA gap [128, 141]. The eukaryotic single-stranded DNA-binding protein RPA (Replication Protein A) enhances EXO1 activity in a MutSα-dependent manner but only while the mismatch persists [154, 157]. Once the mismatch is removed, RPA stimulation ceases [141]. EXO1 activity is also supported by MSH2 and MLH1 [125].

In the final phase of MMR, the resulting gap is filled in by DNA polymerase δ and possibly polymerase ε, which synthesize the correct DNA sequence [119, 158]. The remaining nick is subsequently sealed by DNA ligase, and the repair process is completed [125].

1.4.4 Nucleotide excision repair

Nucleotide excision repair (NER) is a highly versatile and sophisticated DNA repair pathway by which damaged bases are removed from the genome [159]. In eukaryotic DNA repair mechanisms, each pathway corrects a different subset of DNA lesions [160]. NER is responsible for removing the deleterious effects of a multitude of DNA lesions resulting from environmental sources including mainly the shortwave UV component of sunlight [161]. The main lesions removed by NER are known as bulky adducts, such as cyclobutane pyrimidine dimers (CPDs) and photoproducts (6-4PPs) by induced ultraviolet (UV) radiation; intrastrand cross-link, large chemical adducts result from aflatoxin, benzo(α)pyrene and other genotoxic agents [57, 162]. In addition, ionizing irradiation, electrophilic agents, some drugs, and chemically active endogenous metabolites including reactive oxygen and nitrogen species lead to bulky covalent adducts [163]. In human cells, the NER machinery consists of more than 20 proteins [159, 164]. Mutations in genes encoding transcription factors or factors involved in NER can cause various clinical symptoms [165]. Deficiencies of NER are a major cause to extremely skin cancer-prone inherited disorders, *e.g.*, Xeroderma pigmentosum (XP),

Cockayne´s syndrome (CS), and trichothiodystrophy(TTD) [166, 167]. These disorders are characterized by a common increased sensitivity of UV irritation, multi-system immunological and neurological symptoms [163].

NER is responsible for a wide variety of DNA helix distorting lesions through a *cut-and-patch* mechanism [168]. NER is completed through highly coordinated actions of multiple proteins [169]. The process includes: detection of the DNA lesions, incision in the damaged strand, and then removal of the oligonucleotide containing the lesion [170]. In eukaryotic organisms, 24-32 nt single strand oligonucleotides are removed from a damaged strand [163]. The following process includes the resynthesize of the missing nucleotide sequence in the gapped heteroduplex using the intact complementary strand as template and ligation [170]. NER can be classified in two sub-pathways: global genome NER (GGR) responsible for the repair of lesions over the entire genome and transcription-coupled NER (TCR) to repair transcription-blocking lesions present in transcribed DNA strands [161].

TCR removes lesions from the transcribed stand of expressed genes [168]. In particular, Cockayne´s syndrome, a rare autosomal recessive disorder, is associated with defective TCR [167, 171]. Cells from CS patients show a reduced recovery of DNA and RNA synthesis after exposure to UV, but GGR is unaffected [167]. The cellular abnormalities observed are directly connected to a specific defect in TCR [172]. CS patients exhibit several clinical symptoms including cachectic dwarfism, severe neurological manifestations including microcephaly and cognitive deficits, pigmentary retinopathy, cataracts, sensorineural deafness, and feeding difficulties which cause death by 12 years of age on average [173]. In general, CS patients have the symptoms of skeletal abnormalities such as bird-like face, dental caries, kyphosis of the spinal cord, and osteoporosis in older patients [174]. CS individuals show photosensitivity of the skin, but have no predisposition to sunlight-induced skin cancer in comparison to XP patients [167]. In addition, trichothiodystrophy is an autosomal recessive diseases resulting from gene mutations involved in NER [175, 176]. The genetic disorder known as “transcriptional syndrome” was reported by Price in 1980 [177]. Trichothiodystrophy symptoms exhibits characteristic sulphur-deficient, brittle hair and scaling of the skin [176]. Marked photosensitivity, ichtyosis, neurological and skeletal degeneration as well as growth and mental retardation are also known as mainly possible clinical symptoms [178]. TTD results from mutations in the gene encoding the subunit of transcription and DNA repair factor TFIIH, mainly *XPD* and *XPB* genes (*XPD* is known as *ERCC*; *XPB* is known as *ERCC3*) [179, 180]. Transcription factor TFIIH is one of the best-studied basal transcription complexes because of

their importance in the biological process involved in the transcription of mainly all mRNA-coding genes as well as DNA repair [181]. TFIIH plays an essential role during transcription, including nuclear receptors, tissue-specific transcription factors, chromatin remodelling complex and RNA [181]. Apart from its role in transcription, TFIIH is required for cell cycle control [182]. For this reason, mutations in TFIIH subunits result in many forms of cancer and disease syndromes because of the consequent of deficiencies in transcription and DNA repair [183].

Xeroderma pigmentosum is one of the disorders resulting from mutations in XPB and XPD [182]. Additionally, looking at the molecular mechanism of XP, the disease is not only the result of XPB and XPD mutations alone, but also of seven other nucleotide excision repair complementation group enzymes [184]. Patients with XP have inherited germline mutations in the *XPA, XPB/ERCC3, XPC, XPD/ERCC2, XPE/DDB2, XPF/ERCC4,* and *XPG/ERCC5* genes or in the trans-lesion synthesis gene, PolE [185, 186]. Xeroderma pigmentosum was first described by Moritz Kaposi [187]. Faulty repair of ultraviolet DNA damages causes extreme sensitivity to UV light, resulting in sunburn , pigment changes in the skin, and a greatly elevated incidence of skin cancer [182, 188]. If the individuals are not protected from sunlight, the symptoms including pigmentation, skin aging, and multiple skin cancers are dramatically increasing [188]. In addition to these clinical symptoms, neurological defect in XP cases may be observed, including diminished deep-tendon reflexes, sensorineural deafness, peripheral neuropathy, walking difficulties and progressive mental deterioration [189]. The reason underlying these condition is primary neuronal degradation with loss neurons [174].

TCR is a strongly conserved repair sub-pathway identified in several organism including bacteria, yeast, and mammals [168]. TCR determines the damaged lesion through its ability to sense the blocking of transcript elongation [162]. The process is requirement to the TCR specific CSA protein (Cockayne syndrome proteins A; also known as ERCC8) and CSB (Cockayne syndrome proteins B; also known as ERCC6) and the UV-stimulated scaffold protein A (UVSSA) protein [190]. At this point, RNA pol II stalls at the DNA lesion and is supposed to start the signal for other factors participating in TCR, but the exact nature of TCR is still unclear [164]. Arrested RNA Pol II is phosphorylated on the site of carboxy-terminal domain and then polyubiquitylated by a process involving CSA and CSB [189]. Two different perspectives have been advocated. One indicates that ubiquitination of RNA Pol II results in degradation, which activates genes accessible for repair and lead to the resumption of transcription [165, 189]. This increases the possibility that RNA Pol II is removed from the

lesion sites so that repair processes can take place [165].The other perspective advocates that blocked RNA Pol II is not necessary degraded to facilitate repair, and the ubiquitylation is not important for TCR [189].

CSA and CSB are important factors in the further process [162]. Mainly, CSB and CSA enable efficient repair only during the elongation stages of RNA pol II transcription [164]. Also, the UV-stimulated scaffold protein A (UVSSA) allows RNA Pol II-blocking lesions to be rapidly removed from the transcribed strand of active genes [191]. Moreover, UVSSA enables the stabilization of CSB and protects CSB from UV-induced degradation [192]. XAB2 is another factor in TCR, contributing to the process by interacting with CSA and CSB as well as RNA Pol II [193].

In the next step, DNA damage recognition is performed for both TCR and GGR. The damage verification is mediated by TFIIH, xeroderma pigmentosum complementation group A (XPA) and replication protein A (RPA) [168]. The transcription factor (TFIIH) provides local DNA unwinding by the helicase activities of the XPD and XPB subunits [164]. TFIIH consisting of nine different proteins (XPB, XPD, GTF2H1, GTF2H2, GTF2H3, GTF2H4, CDK7, CCNH and MNAT1) is recruited to the site of DNA damage [57]. TFIIH contributes to the mechanism that distinguishes damaged strands from undamaged strands [189]. Then, ERCC1-XPF and XPG are structure-specific endonucleases enabling the incisions at the 5´and 3´ ends of the damage subsequently [194]. In the final step of TCR, the single strand gap is filled by DNA polymerase δ and its cofactor PCNA (proliferating cell nuclear antigen) and RFC [168]. The RFC complex is composed of five different subunits and confers ATP-dependent PCNA loading onto DNA near the 3´-end of a gap flanking DNA fragment [163]. Subsequently, DNA ligase carries out the ligation of the 5´ end of a newly synthesized patch to the original sequence [161]. DNA ligase III-XRCC1 is sealed in both dividing and non-dividing cells, although DNA polymerase ε and DNA ligase 1 play a role in dividing cells in addition to DNA polymerase δ and DNA ligase III-XRCC1 [168].

On the other hand, GGR removes lesions throughout the genome [176]. In contrast to TCR, global genome NER is initiated by XPC-RAD23B and UV-DDB (DDB1-DDB2 containing E3 ubiquitin ligase complex) [168]. XPC-RAD23B plays a role as the main early damage detector [189]. The XPC protein is the first NER protein to localize to the site of lesion [195]. RAD23B includes ubiquitin-associated domains, thought to be connected with the ubiquitin/proteasome protein degradation pathway and is necessary for stabilizing XPC [196]. The rate of repair for GGR varies according to the lesion types because of differences in affinities of the damage

sensor XPC-RAD23B [161]. For example, 6-4PPs is processed much faster than CPDs to be removed [161]. The process is facilitated by XPE in the recognition process, which is involved in two protein subunits, the damaged DNA binding protein (DDB) and p48 [196]. Also, DDB is composed of two subunits (DDB1 and DDB2) associated with XPE [197]. The damaged DNA binding protein complex is responsible for the recruitment of XPC at the damage sites, and also promotes remodelling of chromatin structures [198]. In the damage recognition process, TFIIH, XPG, XPA, and replication protein (RPA) are recruited to the lesion that result in the local unwinding of DNA double helix [199]. Full opening of the DNA helix around the lesion is linked to the presence of ATP and TFIIH complex [200].

RPA is a heterodimeric complex that is responsible for NER, replication, and recombination [201]. RPA facilitates DNA unwinding by coupling with TFIIH [174]. XPA has many interactions with other NER proteins, including the replication protein A (RPA), the TFIIH complex, and the ERCC1/XPF endonuclease [174]. The following process resembles with TCR. Two structure specific endonucleases, the XPF-ERCC1 complex and XPG, cause single strand breaks at the 5´ and 3´ sides of the lesion, leading the excision of the oligonucleotide including the injured bases [199, 202]. In GGR, the DNA repair is completed by gap filling and ligation [168].

1.4.5 DNA double-strand breaks

Double-strand breaks (DSB) result from genotoxic chemicals, ionizing radiations, collapsed replication forks, and other endogenous DNA breaks [203]. DSBs are the most dangerous form of DNA damage [204]. Unrepaired DSBs can probably result in gene deletion, chromosome loss, and other chromosomal aberrations, which may lead to cell death by apoptosis or initiate carcinogenesis [205]. The broken DNA backbone may prevent the distribution of equal genetic information to daughter cells [206]. Therefore, eukaryotic organisms have evolved highly advanced systems during evolution of life to repair DSBs [207]. Human cells possess two major mechanisms to repair DSBs, *i.e.*, non-homologous end joining and homologous recombination [208].

Non-homologous end joining (NHEJ) is a major pathway of DSB repair that contributes to cell survival following exposure of mammalian cells to agents that cause DSBs [208, 209]. Also, it is known as error-prone mechanism because it can lead to small insertions and deletions [206]. NHEJ is evolutionarily conserved in eukaryotes, and simplified versions are also found in some prokaryotes [209]. NHEJ occurs particularly in the G1 phase of the cell cycle to maintain

mammalian cells [210]. Initially, the core component to complete NHEJ is Ku complex (initially recognizes the DNA break), protein kinase DNA-PKcs activates repair proteins in NHEJ), potential DNA-end processing enzymes (for example, Artemis), and the XRCC4-ligase IV complex (which re-ligates the broken DNA ends) [211]. The general mechanism is composed of four steps, including (1) recognition of DSBs, (2) the formation of a molecular bridge that brings the two DNA ends back together, (3) a processing procedure that modifies non-matching and/or damaged DNA ends into compatible ends and finally (4) re-ligation of the broken DNA molecule [212].

In NHEJ, the DNA-dependent protein kinase (DNA-PK) is an important player, which is composed of catalytic subunit (DNA-PKcs) and the DNA-end binding component, Ku [210]. The Ku heterodimer consists of the Ku70 and Ku80 subunits [213]. The Ku heterodimer recognizes and binds to DSBs [204]. This maintains the stability of DNA ends by protecting them from non-specific processing, which prevents chromosomal aberrations and genomic instability [204]. Additionally, the Ku heterodimer creates a scaffold for the assembly of other NHEJ enzymes and forms a complex with DNA-PKcs [212]. Also, DNA-PK acts as a DNA damage recognition factor [208]. The complex bridges the DNA ends and activates other components of the end joining pathway [214]. Ku activates the serine/threonine kinase activity of DNA-PKcs to bind the DNA around the break [205].

Non-complementary DNA ends are required for the further processing involving nucleolysis and polymerization before the final ligation step. If the nucleases remove several nucleotides from single-stranded overhangs at the DSB ends termini, DNA polymerases fill in nucleotide gaps [215]. Finally, the ligase IV/XRCC4 complex catalyses the ligation of the processed DNA ends in the presence of XLF [212]. XLF is required for the activity of DNA ligase IV towards mismatched and non-cohesive DNA ends [204].

Homologous recombination (HR) is a main pathway for the accurate repair of DSBs. Its function involves the genome stability, telomere maintenance, and the preservation of genetic integrity [216]. Unlike the error-prone NHEJ, HR needs to a homologous DNA template to repair DNA damage. The process begins with recognition and resection of DNA ends by the MRN complex (Mre11-Rad50-Nbs1), which activates ATM kinase [217, 218]. Resection generates 3′ single-stranded DNA (ssDNA), which is stabilized by replication protein A (RPA) [219]. BRCA2 facilitates the replacement of RPA with RAD51, enabling strand invasion and homologous pairing [220] [221]. RAD51 and its paralogs (RAD51B/C/D, XRCC2, XRCC3) mediate D-loop formation and strand exchange [222, 223].

As a next step, there are two alternatives of HJ, *i.e.*, DSB repair (DSBR) and synthesis-dependent strand annealing (SDSA) [224]. In DSBR, it is established base pairs by DNA polymerase [224]. Second end is captured and Holiday junction is occurred [203]. Then, the resolution of Holiday junction enables the repair of breaks [224]. It may produce crossover or non-crossover products [203]. In the SDSA pathway, unwound and freed ssDNA anneal with complementary strands associating with DSBs [203]. Subsequently, gap filling and ligation complete the repair.

1.4. The relevance of Parp3 as a target for cancer resistance

In the DNA repair machinery, one of the major processes in response to DNA damage is poly(ADP-ribosyl)ation, a post-translational modification catalyzed by poly(ADP-ribose) polymerases (PARPs) [225, 226]. PARylation includes the formation of ADP-ribose polymers using nicotinamide mononucleotide (NMN) and ATP as substrates [227]. PARPs transfer ADP-ribose units either to target proteins (heteromodification), such as Glu, Lys, or Asp residues, or to themselves (automodification), which results in linear or branched poly(ADP-ribose) chains [228].

The PARP enzyme family comprises 18 members involved in various cellular processes, including DNA repair, chromatin remodelling, and transcriptional regulation [229]. Among them, PARP1, PARP2, and PARP3 are directly activated in response to DNA strand breaks, and function in the DNA damage response [228].

PARP3, originally identified via expressed sequence tag (EST) library screening using the catalytic domain of PARP1, displays distinct expression patterns compared to the ubiquitously expressed PARP1 and PARP2 [230, 231]. Despite these differences, PARP3 has a conserved catalytic glutamate residue and structural similarity in its catalytic domain with PARP1 and PARP2 [232, 233]. PARP3 initiates mono-ADP-ribosylation by transferring the first ADP-ribose unit, which can subsequently be elongated by PARP1/PARP2 to form poly(ADP-ribose) chains [234]. This activity stimulates PARP1 automodification and enhances its enzymatic function [235].

PARP3 plays a critical role in NHEJ, particularly in cooperation with APLF and PARP1 [233]. In addition, PARP3 is involved in regulating fundamental cellular processes such as genomic stability, transcription, cell differentiation, metabolism, and cell death [236].

Its role in chromosomal rearrangements, repair of programmed and stress-induced DSBs, and TGFβ-induced epithelial-to-mesenchymal transition (EMT) has also been identified [236, 237]. Moreover, the inhibition of PARP3 has shown therapeutic potential, particularly in limiting mTORC2-mediated tumor progression [238]. All findings highlight its influence as a novel anticancer target. However, its interactions with diverse signalling pathways remain poorly understood and require further investigation.

Although PARP3 overexpression is not related to centrosome duplication or amplification, it has been associated with disruption of the G1/S phase transition in the cell cycle [239]. Notably, PARP3 depletion makes cells vulnerable to anticancer agents. For instance, lentiviral shRNA-mediated knockdown of PARP3 in glioblastoma models results in reduced cell proliferation and suppressed tumor growth in xenograft mouse models [240]. Furthermore, PARP3 silencing enhances the radiosensitivity of glioblastoma cells when combined with radiotherapy [240]. Nevertheless, even though the findings suggest a promising therapeutic potential, the precise molecular mechanisms underlying this enhanced sensitivity remain to be fully elucidated.

1.5.The relevance of MSH6 as a target to overcome cancer drug resistance

The MutS homolog 6 (*MSH6*) gene is a core component of the DNA mismatch repair (MMR) machinery in mammalian cells [241, 242]. From a general perspective, the role of *MSH6* gene includes (1) the recognition and (2) correction of base-base mismatches and (3) the repair of small insertion-deletion loops [241, 242]. Disruptions in *MSH6* impair DNA repair capacity, which leads to the accumulation of mutations that contribute to the process of carcinogenesis [243].

Findings by Edelmann and colleagues demonstrated the role of mutations within the *MSH6* gene responsible in tumorigenesis [244]. These alterations have been observed not only in hereditary cancer predisposition syndromes — such as Lynch syndrome — but also in certain sporadic tumors that do not exhibit microsatellite instability [244]. Furthermore, mutations in the *MSH6* gene have been associated with the development of resistance to anticancer therapeutics [121, 245]. According to Yang et al., the *MSH6* T1219D missense mutation disrupts mismatch repair activity but preserves the capacity to initiate apoptosis in response to DNA-damaging agents [246]. However, the relationship between the mutations in MSH6 and other cell death pathways such as autophagy and ferroptosis is unclear.

Resistance to DNA-damaging chemotherapeutics, particularly cisplatin, has been increasingly linked to dysfunction of MMR components such as MSH6. MSH6-deficient cells show

increased resistance to cisplatin. To date, reduced expression of MSH6 has been correlated with prolonged survival of osteosarcoma cells, which indicates its potential role in chemoresistance. Notably, MSH6 inhibition in combination with cisplatin treatment hinders the proliferation of human osteosarcoma cells [243].

1.6.The relevance of ATM as a target to overcome cancer drug resistance

Understanding the relevance of ATM as a target in overcoming cancer drug resistance is a crucial step for improving novel drug cancer agents. ATM is a serine/threonine protein kinase belonging to the phosphatidylinositol 3-kinase-related kinase (PIKK) family [247]. ATM mediates multiple cellular signalling networks activated in response to DNA DSBs [248]. DSBs can originate endogenously, such as from the collapse of stalled replication forks, or exogenously, for instance through exposure to ionizing radiation (IR) [249]. ATM is a major player in the initiation of the G1/S cell cycle checkpoint, acting to halt cell cycle progression and thereby preventing the replication of damaged DNA during S-phase entry [247]. Additionally, ATM regulates key pathways including metabolism and responses to hypoxia and oxidative stress to maintain cellular homeostasis [250].

To date, ATM has been frequently mutated in a broad range of human cancers including lung, colorectal, breast and haematopoietic cancers [247]. Ataxia telangiectasia is the most well-known disorder caused by mutations in the *ATM* gene [251]. ATM-deficient cells show hypersensitivity to DNA damage, suggesting the potential of ATM as a therapeutic target in cancer therapy. Several ATM inhibitors have been identified with potential properties, including caffeine, wortmannin, CP466722, KU-55933, and its optimized analogue KU-60019 [247]. Caffeine and wortmannin work in the lab, but they are not useful for patients due to low specificity and high toxicity [252]. More selective inhibitors such as CP466722, KU-55933, and its optimized analogue KU-60019 have improved potency and specificity toward ATM. However these compounds sensitize cancer cells with minimal effects on normal cells, these compounds sensitize cancer cells, particularly those with p53 deficiencies, to ionising radiation [247].

Beyond KU-55933, second-generation ATM inhibitors such as KU-60019 and KU-59403 have been introduced with enhanced pharmacological properties. KU-60019 exhibited potent radiosensitising activity *in vivo*, notably in glioma models harbouring p53 mutations. However, its therapeutic applicability remains a challenge due to suboptimal bioavailability. In contrast,

KU-59403 dissolved better and spread more in the body, which strongly supports treatment when given with drugs that target topoisomerase [253].

The identification of novel ATM inhibitors is not only useful in targeted cancer therapies but also presents a compelling approach to enhance therapeutic efficacy by overcoming cisplatin resistance via combination regimens. In the present Ph.D. thesis, we demonstrate that downregulation of ATM expression sensitizes non-small cell lung cancer (NSCLC) cells to cisplatin treatment through the activation of Erk, Akt, and MAPK signalling pathways. Moreover, accumulating evidence underscores a significant link between the emergence of chemoresistance and the EMT process [254].

2. Objectives of the thesis

Cisplatin is a cornerstone of classical chemotherapy. Cisplatin has been widely used in the treatment of various cancer cases, including non-small cell lung cancer (NSCLC), ovarian, bladder, and head and neck cancers. Despite its initial efficacy, drug resistance emerges in patients treated with cisplatin and significantly limiting its therapeutic potential and contributing to cancer relapse.

The mechanisms underlying cisplatin resistance have been vastly studied over the past decades. Cisplatin resistance occurs through multiple mechanisms, including (a) increased DNA repair capacity, (b) reduced intracellular accumulation, (c) inhibition of cell death pathways, (d) activation of pro-survival signalling pathways, (e) diminished intracellular detoxification and (f) phenotypic alterations such as epithelial mesenchymal transition (EMT). The complexity of these mechanisms has driven efforts to better understand the molecular processes of resistance in different cancer types.

Recent efforts to overcome cisplatin resistance have increasingly focused on identifying reliable biomarkers capable of predicting treatment response. Identified biomarkers according to patient status and distinct cancer cases contribute to the improvement of personalized therapeutic strategies. However, the current literature often includes inconsistent or contradictory findings, largely due to limited patient samples and the lack of advanced computational methodologies. To avoid conflicting data, this Ph.D. thesis adopts an integrated approach to predict the most promising biomarkers. The overarching objective is to identify predictive biomarkers associated with cisplatin resistance according to altered gene expression profiles and mutation frequency. Further, our aim is to elucidate signalling pathways associated with biomarkers, thereby enabling the development of more effective combination therapy strategies.

PARP3 (Poly[ADP-ribose] polymerase 3**)** is a member of the PARP enzyme family involved in DNA repair processes. While the role of PARP3 in DNA repair is increasingly understood, its interactions with oncogenic signalling pathways remain insufficiently characterized. In this study, PARP3 was selected as a focal point based on its relevance, identified through integrated bioinformatic analysis — including the evaluation of 27 base excision repair (BER) genes across 23 cancer types and mutation hotspot mapping. The specific objectives related to PARP3 are to: (1) elucidate the effects of PARP3 inhibition on key oncogenic signalling pathways by using IPA analyses. The second objective is to: (2) determine whether targeting PARP3 can

sensitize cancer cells to cisplatin treatment. This line of investigation aims to contribute to the design of precision-based combination therapies through PARP3 inhibition.

MSH6 is necessary for the DNA mismatch repair (MMR) system. This study explores the role of MSH6 in modulating the response to cisplatin in NSCLC. Additionally, the relationship between MMR and autophagy signaling requires further investigation. The mechanisms underlying the dual roles of autophagy in promoting cell survival and inducing cell death remain a subject of debate, particularly in the context of its association with MMR. The specific objectives are to: (1) determine whether suppression of MSH6 enhances the antitumor efficacy of cisplatin by influencing autophagy-related pathways; and (2) uncover novel interactions between the mismatch repair mechanism and autophagy signalling.

Ataxia-Telangiectasia Mutated (ATM) is a serine/threonine protein kinase involved in the DNA damage response. However, the precise role of ATM mutations in modulating cisplatin sensitivity remains unclear. Following comprehensive bioinformatics analyses, ATM was selected to investigate its role. Our aim is to conduct a transcriptomic comparison between wild-type and ATM-knockout lung cancer cells to elucidate the molecular effects on oxidative stress-induced senescence upon cisplatin exposure. Specifically, the objectives are to: (1) identify genes related to oxidative stress-induced senescence pathways and (2) determine the function of ATM in response to cisplatin sensitivity by using gene editing methods. The goal is to reveal potential combination therapies that could enhance therapeutic efficacy in cisplatin-resistant cancers.

3. Results and discussion

3.1. Enhancing cisplatin drug sensitivity through PARP3 inhibition: The influence on PDGF and G-coupled signal pathways in cancer

Considering the heterogeneity of cancer, we examined the m-RNA expression profiles of 27 base excision repair (BER) genes across five clinical parameters: age, gender, race, metastasis stage, and tumor stage. In the Kaplan–Meier survival analyses, high expression levels of 15 BER genes were significantly associated with reduced overall survival. Among them, *PARP3*, *NEIL3*, and *TDG* demonstrated consistent negative correlations with survival across three independent clinical variables (race, gender, and metastasis stage), identifying them as strong prognostic candidates. In contrast, the remaining BER genes showed associations in fewer than three parameters.

As a result of mutation mapping, *PARP3* showed the highest frequency of missense, nonsense, and frameshift mutations in coding regions, compared to *NEIL3* and *TDG*. These mutations were found in PARP3's functional domains, potentially affecting its interaction with DNA repair proteins related to drug response.

From computational analyses to wet-lab experiments, PARP3-knockout (*PARP3*$^{-/-}$) MDA-MB231 breast cancer cells were generated via CRISPR/Cas9 gene editing. Cell viability assays demonstrated that PARP3-deficient cells exhibited significantly enhanced sensitivity to cisplatin, carboplatin, and doxorubicin compared to wild-type cells ($p < 0.01$).

Comparative transcriptomic analysis using Ingenuity Pathway Analysis (IPA) identified key signalling alterations related to *PARP3* deficiency. In *PARP3*$^{+/+}$ cells, cisplatin treatment maintained strong activation of pro-survival pathways, particularly the PDGF and GPCR signalling cascades, with z-scores of 2.4 and 2.236, respectively. Additional activation of downstream networks such as oxytocin, apelin endothelial, and mTOR signalling was also observed, likely as a result of upstream PDGF/GPCR activation — implying the involvement of these pathways in cisplatin resistance mechanisms.

Conversely, in *PARP3*$^{-/-}$ cells treated with cisplatin, the activity of the PDGF and GPCR pathways was markedly suppressed. In addition, downregulation of EIF2 and protein kinase A signalling indicated impaired cellular stress adaptation and proliferation. These transcriptomic findings were further validated through qPCR. As a result, decreased expression of PDGF- and GPCR-associated genes was observed in PARP3-deficient cells.

Functionally, the combined effect of PARP3 gene silencing and cisplatin exposure resulted in reduced proliferation, and decreased cell survival in MDA-MB231 cells as well as increased DNA damage. These results suggest that targeting PARP3 may sensitize cancer cells to cisplatin. This offers a potential therapeutic strategy to be applied in combinational therapy.

Further reading: Appendix I

Enhancing cisplatin drug sensitivity through PARP3 inhibition: The influence on PDGF and G-coupled signal pathways in cancer

Ayşegül Varol, Sabine M. Klauck, Françoise Dantzer, Thomas Efferth

3.2 Inhibition of MSH6 augments the antineoplastic efficacy of cisplatin in non-small cell lung cancer as autophagy modulator

To determine the distribution of MMR gene mutations, mutational data across 23 cancer types were obtained via c-Bioportal. Among the eight MMR genes, *MSH3* and *MSH6* displayed the highest mutation frequencies at specific hotspot regions. Based on survival analysis, *MSH6* and EXO1 were notably associated with poor prognosis in various cancer cases..

Comprehensive bioinformatic analyses were conducted, preparing m-RNA expression data considered to five parameters: age, race, gender, tumor stage, and metastasis status. MMR gene expression patterns varied significantly depending on cancer type and patient characteristics, emphasizing the need for personalized approaches. Among all MMR genes, *MSH6* and *EXO1* ranked first due to their influence on patient survival. High *EXO1* expression correlated with poor survival across all subgroups, while elevated *MSH6* expression was significantly associated with reduced survival, particularly with respect to age, race, and gender. When we considered both mutation analysis and survival analysis together, our focus turned to selecting MSH6 for further investigation, particularly in lung cancer.

To understand the role of *MSH6* in drug sensitivity, cytotoxicity assays were performed using cisplatin, carboplatin, and gemcitabine on $MSH6^{+/+}$ and $MSH6^{-/-}$ H460 cells. After 72 hours, $MSH6^{-/-}$ cells exhibited increased drug sensitivity compared to wild-type cells. The cisplatin IC_{50} value decreased from 12.3 ± 0.3 µM in $MSH6^{+/+}$ H460 to 4.4 ± 0.5 µM $MSH6^{-/-}$ H460.

Microarray hybridization was conducted to elucidate pathway mechanisms underlying altered drug response due to *MSH6* inhibition. Ingenuity Pathway Analysis (IPA) revealed distinct pathway alterations between the two cell lines following cisplatin treatment. In the canonical pathway of *MSH6*$^{+/+}$ cells, mTOR pathway inhibition was observed, promoting autophagy, particularly via microautophagy. Particularly, pathway analyses clearly displayed activation and inactivation of autophagy following altered gene expression involved in the mTOR pathway. We compared two canonical pathways according to positive z-score. As a result of comparative analysis, downregulation of NRF2-mediated oxidative stress, HIF1α, PI3K/AKT, and PKA signalling was also seen in the wild type H460 cancer cell line. Conversely, *MSH6*$^{-/-}$ cells exhibited increased activation of oxidative stress-induced senescence, MYC-mediated apoptosis, and indications of ferroptosis in the cisplatin exposure. Notably, BAX was upregulated and BCL-2 expression altered, suggesting enhanced apoptotic signalling. These gene expression patterns were confirmed via q-PCR.

Further, we selected autophagy-related genes to verify altered autophagy activation (*PTEN, MAP1LC3B, RPTOR*, and *PIK3R1*) in the inhibition of MSH6. As a result of q-PCR experiment, *PTEN* and *MAP1LC3B* were significantly downregulated in *MSH6*$^{-/-}$ cells, while *RPTOR* and *PIK3R1* were upregulated, suggesting downregulated autophagic activity upon *MSH6* loss.

Additionally, western blot analysis confirmed these findings at the protein level, demonstrating reduced expression of PTEN and LC3B-I/II, and increased RPTOR expression in *MSH6*$^{-/-}$ cells following cisplatin treatment, indicating the loss of pro-survival role in autophagy signaling.

We obtained similar ROS levels between both cell lines, even under lower cisplatin concentrations in *MSH6*$^{-/-}$ cells. These similar ROS levels in both cell lines may result from altered NRF2-pathway responses, implying modified oxidative stress regulation in the absence of *MSH6*.

Finally, flow cytometry and comet assay revealed that *MSH6*$^{-/-}$ cells exhibited a more pronounced S-phase arrest and higher DNA damage following cisplatin exposure, indicating increased drug sensitivity and impaired DNA repair mechanisms.

Further reading: Appendix II

Inhibition of MSH6 augments the antineoplastic efficacy of cisplatin in non-small cell lung cancer as autophagy modulator

Ayşegül Varol, Joelle C. Boulos, Chunmei Jin, Sabine M. Klauck, Anatoly Zhitkovich Thomas Efferth

3.3 Comprehensive transcriptomic analysis in wild-type and ATM knockout lung cancer cells: Influence of cisplatin on oxidative stress-induced senescence

The main reason underlying cisplatin resistance results from increased mutations in DNA damage response genes, particularly ATM. Targeting the disruption of signaling pathways caused by the accumulation of mutations is a logical step toward overcoming resistance challenges. To identify promising predictive biomarkers, mutation hotspot regions across the functional domains of 23 DSB repair genes were analyzed, considering the number of missense, nonsense, and frameshift mutations. Among these, ATM displayed the highest mutation frequency, particularly within the PI3_ PI4 kinase domain. We observed the highest number of ATM mutations in various cancer cases, but lung cancer was selected to further investigation.

The m-RNA expression analysis showed that high *ATM* expression was significantly associated with poor survival in breast cancer patients. In lung cancer, elevated expression levels of *DCLRE1B, RAD54B, XRCC6,* and *XRCC3* were correlated with poor prognosis.

In the drug sensitivity assays, $ATM^{-/-}$ A549 cells exhibited altered responses to cisplatin, carboplatin, and 5-fluorouracil, as reflected by significantly lower IC_{50} values compared to $ATM^{+/+}$ cells. Obviously, the IC_{50} values for cisplatin decrease from 9.91 ± 2.5 μM in the wild-type cells to 3.36 ± 1.31 μM in the $ATM^{-/-}$ A549 cells.

According to Ingenuity Pathway Analysis (IPA), *ATM* inhibition in A549 cells led to broad transcriptomic changes, including suppression of proliferation-associated pathways such as mTOR, EIF2, NOTCH4, and WNT/β-catenin. Additionally, *ATM* loss was clearly correlated with increased activation of oxidative stress-induced senescence. Additionally, ATM enhanced activation of alternative cell death pathways — such as necroptosis, ferroptosis, and senescence—under cisplatin treatment, even at lower doses.

Through qPCR, we confirmed the upregulation of key senescence-associated genes, including *CDKN2A*, *IL8*, and *IL6*, in ATM-deficient cells after cisplatin exposure. This was further supported by β-galactosidase staining, which demonstrated increased senescence levels.

Flow cytometric analysis showed a shift from S-phase to enhanced G2/M arrest in $ATM^{-/-}$ cells, which is in consistent with findings reported in the literature. These results accompanied by increased necrosis and reduced apoptosis. Moreover, ROS levels were significantly increased in $ATM^{-/-}$ A549 cancer cells, even at low cisplatin concentrations. In the comet assay, $ATM^{-/-}$ A549 cells were more susceptible to cisplatin-induced DNA damage compared to wild-type controls.

As a result of that, loss of *ATM* increases sensitivity to oxidative stress and shifts the cellular response to cisplatin from apoptosis toward non-apoptotic cell death mechanisms. These findings support the development of combination therapies targeting multiple cell death pathways.

Further reading: Appendix III

Comprehensive transcriptomic analysis in wild-type and ATM knockout lung cancer cells: Influence of cisplatin on oxidative

Ayşegül Varol, Sabine M. Klauck, Susan P. Lees-Miller, Thomas Efferth

4. Published articles

4.1. Enhancing cisplatin drug sensitivity through PARP3 inhibition: The influence on PDGF and G-coupled signal pathways in cancer

Contribution Statement

The study investigates the role of PARP3 inhibition in enhancing the sensitivity of cancer cells to cisplatin through modulation of the PDGF and G-protein-coupled receptor (GPCR) signaling pathways.

My main contribution to this publication includes the conceptualization of the research, bioinformatics and experimental analyses, and data interpretation concerning the relationship between PARP3 silencing and cisplatin sensitivity. The findings demonstrated that PARP3 inhibition induces a synthetic lethal interaction with PDGF and GPCR pathways, suggesting PARP3 as a promising therapeutic target for overcoming cisplatin resistance.

This article was written under the supervision of Prof. Dr. Thomas Efferth at the Department of Pharmaceutical Biology, Johannes Gutenberg University Mainz.

Authorship Contribution

Ayşegül Varol: Writing – review & editing; Writing – original draft; Validation; Software; Methodology; Investigation; Data curation; Conceptualization. **Sabine M. Klauck:** Writing – review & editing; Software; Methodology; Investigation; Data curation; Conceptualization. **Françoise Dantzer:** Methodology; Investigation; Conceptualization. **Thomas Efferth:** Writing – review & editing; Supervision; Project administration; Conceptualization.

Publication Information

Title: *Enhancing cisplatin drug sensitivity through PARP3 inhibition: The influence on PDGF and G-coupled signal pathways in cancer* **(DOI:** https://doi.org/10.1016/j.cbi.2024.111094)

Journal: *Chemico-Biological Interactions*

Volume: 398

Article Number: 111094

Year: 2024

Chemico-Biological Interactions 398 (2024) 111094

Contents lists available at ScienceDirect

Chemico-Biological Interactions

journal homepage: www.elsevier.com/locate/chembioint

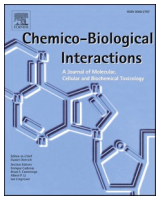

Research paper

Enhancing cisplatin drug sensitivity through PARP3 inhibition: The influence on PDGF and G-coupled signal pathways in cancer

Ayşegül Varol [a], Sabine M. Klauck [b], Françoise Dantzer [c], Thomas Efferth [a,*]

[a] Department of Pharmaceutical Biology, Institute of Pharmaceutical and Biomedical Sciences, Johannes Gutenberg University-Mainz, 55128, Mainz, Germany
[b] Division of Cancer Genome Research, German Cancer Research Center (DKFZ) Heidelberg, National Center for Tumor Diseases (NCT), NCT Heidelberg, a Partnership between DKFZ and University Hospital Heidelberg, 69120, Heidelberg, Germany
[c] Poly(ADP-ribosyl)ation and Genome Integrity, Laboratoire d'Excellence Medalis, UMR7242, Centre Nationale de la Recherche Scientifique/Université de Strasbourg, Institut de Recherche de l'Ecole de Biotechnologie de Strasbourg, 300 bld. S. Brant, CS10413, 67412, Illkirch, France

ARTICLE INFO

Keywords:
Chemotherapy
Drug resistance
Prognostic factors
Signal transduction
Survival analysis
Transcriptomics

ABSTRACT

Drug resistance poses a significant challenge in cancer treatment despite the clinical efficacy of cisplatin. Identifying and targeting biomarkers open new ways to improve therapeutic outcomes. In this study, comprehensive bioinformatic analyses were employed, including a comparative analysis of multiple datasets, to evaluate overall survival and mutation hotspots in 27 base excision repair (BER) genes of more than 7,500 tumors across 23 cancer types.

By using various parameters influencing patient survival, revealing that the overexpression of 15 distinct BER genes, particularly *PARP3*, *NEIL3*, and *TDG*, consistently correlated with poorer survival across multiple factors such as race, gender, and metastasis. Single nucleotide polymorphism (SNP) analyses within protein-coding regions highlighted the potential deleterious effects of mutations on protein structure and function. The investigation of mutation hotspots in BER proteins identified PARP3 due to its high mutation frequency.

Moving from bioinformatics to wet lab experiments, cytotoxic experiments demonstrated that the absence of PARP3 by CRISPR/Cas9-mediated knockdown in MDA-MB-231 breast cancer cells increased drug activity towards cisplatin, carboplatin, and doxorubicin. Pathway analyses indicated the impact of PARP3 absence on the platelet-derived growth factor (PDGF) and G-coupled signal pathways on cisplatin exposure.

PDGF, a critical regulator of various cellular functions, was downregulated in the absence of PARP3, suggesting a role in cancer progression. Moreover, the influence of PARP3 knockdown on G protein-coupled receptors (GPCRs) affects their function in the presence of cisplatin.

In conclusion, the study demonstrated a synthetic lethal interaction between GPCRs, PDGF signaling pathways, and PARP3 gene silencing. PARP3 emerged as a promising target.

1. Introduction

Cellular integrity is under constant threat from exogenous chemicals, physical agents, and endogenous reactive metabolites, leading to the formation of DNA lesions that are toxic and mutagenic [1]. These lesions primarily occur during normal DNA metabolic processes, replication, recombination, and repair. If left unrepaired, they can result in mutations, contributing to age-related diseases and cancer development [2]. To counteract this, cells possess sophisticated defence systems encompassing DNA repair processes, resilience to damage, regulatory checkpoints, and pathways that ultimately govern cellular survival or demise [3,4].

Resistance to cisplatin, a commonly used chemotherapeutic drug, mainly occurs due to increased DNA repair mechanisms, reduced intracellular drug accumulation, and enhanced drug inactivation [5]. To date, a multitude of key biomarkers have been identified that exhibit associations with cisplatin resistance in oncology, as well as poor prognosis and diminished survival outcomes [5]. However, the existing body of literature is characterized by conflicting data, primarily attributable to insufficient and inadequate analyses [5]. Therefore, a comprehensive approach that integrates biomarker expression profiling and polymorphism screening is necessary to accurately determine a patient's resistance status.

Safeguarding against mutagenesis and upholding genome stability relies significantly on the indispensable function of DNA repair

* Corresponding author.
E-mail address: efferth@uni-mainz.de (T. Efferth).

https://doi.org/10.1016/j.cbi.2024.111094
Received 16 February 2024; Received in revised form 7 May 2024; Accepted 31 May 2024
Available online 1 June 2024

Abbreviations

BER	base excision repair
EMT	epithelial-mesenchymal transition
ERK	extracellular signal-regulated kinase
GPCRs	G-protein coupled receptors
IPA	Ingenuity Pathway Analysis software
MAPK	mitogen-activated protein kinase
NF-κB	nuclear factor kappa B-cells
PARP3	poly (ADP-ribose) polymerase 3
PDGF	platelet-derived growth factor
PI3K/Akt	phosphatidylinositol 3 kinase
qPCR	quantitative polymerase chain reaction
ROS	reactive oxygen species
SNP	single nucleotide polymorphisms
TCGA	The Cancer Genome Atlas

mechanisms [3,6]. Among these mechanisms, base excision repair (BER) rectifies minor base alterations induced by oxidation, deamination, and alkylation [7]. BER involves a series of steps, including the removal of base damage, cleavage of the phosphodiester backbone, removal of the sugar-phosphate moiety, and repair completion through short or long patch pathways, depending on the lesion size [8–10]. Although key biomarkers associated with BER proteins have been identified in relation to cisplatin resistance, the exact involvement of BER in drug resistance remains not entirely elucidated [11].

Poly(ADP-ribose) polymerase 3 (PARP3) is a protein intricately involved in BER and has been linked to diverse biological processes, including genome integrity, transcriptional regulation, differentiation, cell metabolism, and cell death [12,13]. PARP3 functions as an activator of PARylation, enhancing PARP1 activity and auto-modification [12, 14]. Its role in transcriptional regulation, chromosomal rearrangements, programmed and stress-induced double-strand break repair, and TGFβ-induced epithelial-mesenchymal transition (EMT) has been established [13,15]. Furthermore, the inhibition of PARP3 function has exhibited potential in curtailing tumor malignancy triggered by mTORC2 signaling, making it a compelling candidate for therapeutic intervention in cancer [16]. However, the exact significance of directing therapeutic efforts towards PARP3 in cancer treatment strategies is yet to be fully understood.

The objective of this study was to investigate alterations in the expression of 27 BER proteins across 23 different cancer types in cancer patients. The study considered parameters such as age, race, gender, metastasis stage, tumor stage, and mutation profile. The primary aim was to predict the most likely target affecting cancer survival and uncover the underlying biological mechanisms. Computational bioinformatics analysis was employed to interpret the genomic data and predict the association between genetic variations and cancer.

Ultimately, the study focused on *PARP3* due to its high expression levels, which correlated with poor survival rates among patients with different parameters, including white race, male gender, and M0 metastasis stage. Furthermore, the association between *PARP3* inhibition and sensitivity to the anticancer drug cisplatin was investigated. The findings demonstrated that inactivating *PARP3* heightened the sensitivity of cancer cells to cisplatin by modulating the G-coupled protein and platelet-derived growth factor (PDGF) signaling pathway. PDGF plays a critical role in various cellular processes, encompassing cell proliferation, transformation, migration, invasion, apoptosis, angiogenesis, and metastasis [17]. Therefore, suppressing PDGF acts as a central regulator of signaling pathways relevant to cancer survival, such as the PI3K/AKT, mTOR, NF-κB, ERK, MAPK, and Notch pathways [17–19]. Targeting the PDGFD receptor signaling pathway is a crucial step in the treatment of cancer patients [20]. Additionally, G-coupled proteins mediate diverse signaling pathways initiated by ligand binding [21]. Identifying selective components that regulate G-protein coupled receptors (GPCRs) may offer novel and effective treatment strategies against cancer [22]. In sum, in this study we endorse the inhibition of *PARP3* to boost the effectiveness of cancer drug therapies by suppressing tumor-promoting actions mediated by GPCRs and PDGF.

2. Material and methods

2.1. Survival analysis

To assess the survival curves associated with the expression of 27 BER genes at the mRNA level, we utilized the Cancer Genome Atlas (TCGA) dataset obtained from cBioportal (https://www.cbioportal.org; accessed between 2020 and 2021) as our primary data source. The TCGA dataset provided comprehensive information on 23 different cancer types, encompassing the expression levels of BER genes, as well as five key parameters: age, race, gender, metastasis, and tumor stage [23]. Subsequently, we conducted Kaplan-Meier survival analyses on each BER gene within the afore-mentioned context.

To determine the statistical significance, we employed the "log-rank" test statistics. By applying this statistical test, we identified survival curves that exhibited noteworthy differences. Specifically, we considered survival curves with a p-value below 0.05 as statistically significant. Subsequently, we compared all the survival curves obtained and focused on the BER gene that demonstrated the highest prevalence in influencing poor patient survival across the five parameters mentioned above.

2.2. Mutation hotspot analysis

To identify mutation hotspots within the coding region of 27 BER proteins, we conducted a comprehensive analysis of mutations across 7,528 patients representing 23 different cancer types [23]. Initially, we employed UniProt, a widely recognized resource for protein information (UniProt, 2023), to determine all the domain sites associated with these proteins. Subsequently, we obtained mutation data from cBioPortal, a valuable platform for exploring cancer genomics data (cBioPortal, 2023) for the years 2020–2021 [23,24]. By examining the mutation profiles of the 27 BER proteins, we identified hotspot sites based on the total number of mutations, irrespective of mutation type. These mutations were categorized as missense, nonsense, or frameshift mutations, allowing us to gain insights into the prevalence and distribution of genetic alterations within this set of proteins. Additionally, we showed the total mutation rate of selected top genes (*PARP3*, *NEIL3*, and *TDG*) in cancer cases.

2.3. Knockout of PARP3 using CRISPR/nCas9-mediated genome editing

Gene knockout of *PARP3* was conducted as previously described [16]. Briefly, cellular transfections into MDA-MB-231 breast cancer cells were carried out with two plasmids, each expressing a pair of guide RNAs (gRNAs) to perform gene knockout experiments. The first plasmid contained gRNAs targeting exon 2 of *PARP3* and co-expressed nCas9-EGFP, while the second plasmid contained gRNAs targeting exon 5 of *PARP3* and co-expressed nCas9-mCherry. Additionally, these plasmids harbored selection cassettes for neomycin or hygromycin resistance, corresponding to the respective gRNA sets. Following transfection, a flow cytometric sorting approach was employed to isolate cells exhibiting co-expression of EGFP and mCherry signals. Subsequently, these cells were cultured for a period of three days in growth media supplemented with hygromycin (350 μg/mL) and G418 (500 μg/mL). Following the selection process, individual colonies were manually picked, expanded, and subjected to genotyping via PCR using primers located upstream of exon 2 and downstream of exon 5 (as mentioned in Ref. [16] before). Subsequently, the PCR products were subjected to sequencing, and the absence of *PARP3* protein in the resulting *PARP3*$^{-/-}$

Table 1
Selected primers for qPCR experiments.

Gene Symbol	Forward Primer	Reverse Primer
PDGFD	CGCCAACCTCAGGCGAGAT	AGAGTGAAGCCGCCATGTCA
MAP2K4	TCCCAATCCTACAGGAGTTCAA	CCAGTGTTGTTCAGGGGAGA
GNB1L	TAGGAGCAGGCGTTCCCGA	CAAACTGGGGGTCTGGAGGT
GPR107	GATGGCGGCCCTTCCTTTCA	ACAACAGCCCAGCCTTCGAT
GPR89A	TCCCAGCAGATAACCTTGCCTC	GCGCATGAAGAAAAGCCACC
GAPDH	TTCGACAGTCAGCCGCATCT	CCGACCTTCACCTTCCCCAT

MDA-MB-231 cells was confirmed through Western blot analysis [16].

2.4. Cytotoxicity assay

The cytotoxicity was assessed employing the resazurin reduction assay, a well-established methodology [25]. This assay facilitates the determination of viable cells based on the reduction of resazurin to resorufin. The impact of carboplatin (ranging from 0.001 μM to 300 μM), as well as doxorubicin and cisplatin (ranging from 0.003 μM to 100 μM) on *PARP3*$^{+/+}$ MDA-MB-231 and *PARP3*$^{-/-}$ MDA-MB-231 cancer cell lines was investigated. The cells were seeded onto 96-well plates. Once they attained approximately 70 %–80 % confluence, the cells were exposed to the specified compounds for a duration of 72 h. Subsequently, the cells were subjected to an additional 4 h incubation period with 20 μL/well of resazurin (Sigma-Aldrich, Germany) diluted in double-distilled water (ddH_2O). The resultant outcomes were recorded using the fluorescence wavelength of 544 nm and an emission wavelength of 590 nm, employing the infinite M2000 ProTM plate reader (Tecan, Germany). The concentrations at which 50 % inhibition occurred (IC_{50}) were calculated using nonlinear regression analysis, utilizing Microsoft Excel.

2.5. Microarray-based expression profiling for predicting canonical pathways

To ascertain the canonical pathway affected by PARP3$^{-/-}$ MDA-MB-231 cells, we conducted microarray hybridization expression analyses. Both the MDA-MB-231 PARP3$^{+/+}$ and PARP3$^{-/-}$ cell lines were subjected to treatment with cisplatin concentrations of 1.6 μM and 0.7 μM, respectively, for a duration of 24 h. Subsequently, total RNA was extracted using the InviTrap® Spin Universal RNA Mini Kit (Invitek Molecular, Berlin, Germany). Following this, complementary DNA (cDNA) was synthesized, labeled, and subjected to hybridization on Affymetrix GeneChips® employing the human Clariom S™ assay (Affymetrix, Santa Clara, CA, USA) at the Genomics and Proteomics Core Facility of the German Cancer Research Center (DKFZ, Heidelberg,

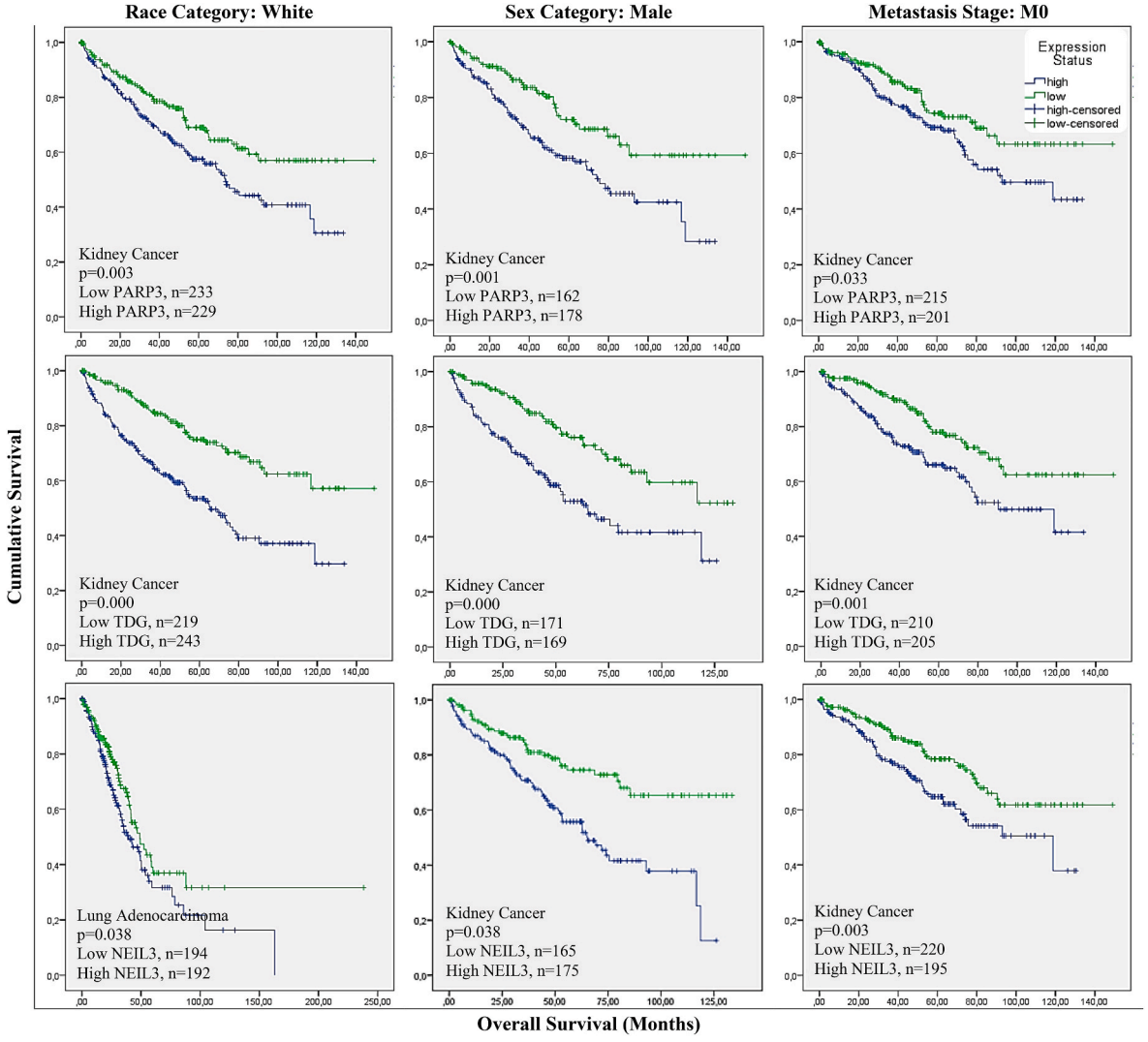

Fig. 1. The association of *PARP3, TDG* and *NEIL3* expression with overall survival of patients (Kaplan-Meier analysis) in kidney renal clear carcinoma and lung adenocarcinoma.

Table 2
The mutational hotspot sites and the mutation frequency of 27 base excision repair genes.

Gene	Missense	Nonsense	Frameshift	Hotspot domain	Total mutation number
LIG3	17	4	2	DNA ligase N terminus (261–435)	23
TDP1	25	1	1	Tyrosyl-DNA phosphodiesterase (163–582)	27
TDP2	16	2	4	Endonuclease/exonuclease/phosphatase family (117–351)	22
SMUG1	15	3	1	Uracil DNA glycosylase (71–262)	19
HUS1	15	2	2	HUS1 (1–280)	19
RAD9A	14	–	4	Rad9 (13–265)	18
PARP1	18	–	–	PARP polymerase catalytic (788–1014)	18
PARP3	16	1	–	PARP catalytic (313–533)	17
APEX1	13	1	3	Endonuclease/exonuclease/phosphatase (65–309)	17
NEIL1	9	2	6	Formamidopyrimidine-DNA glycosylase N-terminal domain (2–123)	17
TDG	15	1	–	Uracil DNA glycosylase (139–300)	16
LIG1	15	1	–	DNA ligase N terminus (287–465)	16
MPG	14	1	1	Methylpurine-DNA glycosylase (139–300)	16
UNG	13	1	1	Uracil DNA glycosylase (139–300)	15
RAD1	12	2	1	Rad1 (16–257)	15
NEIL3	9	–	5	GRF zinc finger (506–548) (552–595)	14
MUTYH	12	–	1	Nudix hydrolase (364–495)	13
PARP2	10	1	2	PARP catalytic (356–583)	13
NEIL2	11	–	1	Formamidopyrimidine-DNA glycosylase N-terminal domain (2–180)	12
NUDT1	7	2	1	Nudix hydrolase (45–168)	10
XRCC1	8	1	1	BRCT1 (315–403)	10
NTHL1	9	–	1	HhH-GPD (135–271)	10
PCNA	7	1	–	PCNA C terminal (127–254)	8
PNKP	7	1	–	Polynucleotide kinase 3 phosphatase (166–328)	8
OGG1	7	–	–	8-oxoguanine DNA glycosylase (25–141)	7
FEN1	6	–	1	I-domain (122–253)	7
MBD4	4	1	–	Methyl-CpG binding domain (80–149)	5

Germany). The affected genes were then observed utilizing Chipster software (version 3.16.3) (accessed on 21 June 2020), whereby their variable expression and significance were evaluated based on the empirical Bayes *t*-test ($p < 0.05$).

To demonstrate the canonical pathway affected by *PARP3* inhibition, we employed Ingenuity Pathway Analysis software (IPA; Ingenuity Systems, Redwood City, CA, USA), utilizing the content version 51963813, released on 01/01/2023. IPA facilitated the assessment of changes in canonical pathways between the $PARP3^{+/+}$ and $PARP3^{-/-}$ MDA-MB-231 cancer cell lines following cisplatin exposure. To compare the effects of cisplatin exposure on $PARP3^{+/+}$ and $PARP3^{-/-}$ MDA-MB-231 cells, gene heatmaps and canonical pathway analyses were conducted, employing activation z-scores and *p*-values as metrics.

2.6. Quantitative real-time qPCR for validating relative gene expression

After identifying the canonical pathway associated with the absence of *PARP3*, we proceeded to validate the microarray findings through the utilization of qPCR technique. Primers were designed using the Primer BLAST online tool (https://www.ncbi.nlm.nih.gov/tools/primer-blast/) (accessed in 2023) and procured from Eurofins Genomics (Ebersberg, Germany). The selected primers are presented in Table 1 for selected signaling pathway and Supplementary Table S2. Subsequently, qPCR was performed on the selected genes. Briefly, the MDA-MB-231 wild-type and MDA-MB-231 *PARP3* knockout cancer cells were treated with cisplatin concentrations equivalent to their respective IC_{50} values, specifically 1.6 μM and 0.7 μM, for a duration of 24 h. Total RNA extraction was carried out using the InviTrap® Spin Universal RNA Mini Kit (Invitek Molecular, Berlin, Germany). The conversion from mRNA to cDNA was accomplished utilizing the LunaScript® RT SuperMix Kit cDNA Synthesis Kit (New England Bio Labs, Darmstadt, Germany). Subsequently, gene amplification was performed using the EvaGreen master mix (5 × Hot Start Taq EvaGreen® qPCR Mix (no ROX); Axon Labortechnik, Kaiserslautern, Germany) according to the manufacturer's instructions.

Real-time PCR was conducted on a CFX384TM instrument (Bio-Rad, Munich, Germany) using a 38-well plate and employing 40 cycles. The run conditions consisted of three steps: an initial denaturation phase at 95 °C for 15 s, followed by a gradient annealing step ranging from 62 °C to 47 °C for 30 s, and finally, an elongation step at 72 °C for 1 min. To determine the fold-change in gene expression, the comparative Cq ($2^{-\Delta\Delta Cq}$) method was employed [26].

2.7. Single cell gel electrophoresis (comet assay)

The comet assay was conducted utilizing the Oxiselect™ Comet Assay Kit (3-Well Slides) sourced from Cell Biolabs/Biocat in Heidelberg, Germany. Initially, $PARP3^{+/+}$ and $PARP3^{-/-}$ MDA-MB-231 cells were seeded at a density of 1×10^6 cells per well in 6-well plates. Subsequently, these cells were subjected to treatment with cisplatin concentrations corresponding to their respective IC_{50} values, specifically 1.6 μM and 0.7 μM, over a period of 24 h. Additionally, H_2O_2 at a concentration of 50 μM was applied as a positive control for a duration of 15 h.

Following treatment, the cells were collected, subjected to centrifugation at 3000×*g* for 10 min, and then reconstituted in PBS. Subsequently, cell suspensions at a concentration of 1×10^5 cells/mL were blended with molten agarose at 37 °C at a ratio of 1:6. The resulting mixtures were then evenly spread onto comet slides and allowed to incubate in darkness at 4 °C for 30 min. The slides were subsequently immersed in a pre-chilled lysis buffer (comprising of 14.6 g NaCl, 20 mL EDTA solution, and 10 × lysis solution at pH 10.0) for a duration of 1 h at 4 °C in darkness. Post-lysis, the slides were withdrawn from the lysis buffer and immersed in a pre-chilled alkaline electrophoresis solution buffer (consisting of 12 g NaOH, 2 mL EDTA solution, and 1000 mL distilled water) for 40 min at 4 °C in darkness. The slides were then placed into an electrophoresis chamber filled with the afore-mentioned alkaline electrophoresis solution buffer, and electrophoresis was conducted at 20 V for 20 min. Subsequently, the slides underwent two washes with prechilled distilled water, each for 5 min. Following the washes, the slides were immersed in cold ethanol (70 %) for 5 min, after which they were allowed to air-dry. Upon complete desiccation, 100 μL of Vista Green DNA dye, diluted at a ratio of 1:10,000 in TE buffer (comprising of 10 mM Tris and 1 mM EDTA at pH 7.5), was added to each slide and permitted to incubate for 15 min at room temperature. Subsequently, 50 comets from each treatment group were randomly

Table 3
The prevalence of genetic modifications in *PARP3, TDG*, and *NEIL3* across specific cancer types investigated by The Cancer Genome Atlas (TCGA) was examined using the cBioPortal database to analyze the distribution of gene alterations.

Cancer type	Total number of cases	Cases with altered genes (%)		
		PARP3	*TDG*	*NEIL3*
Breast invasive cancer	963	9 (0.9)	5 (0.5)	18 (1.9)
Glioblastoma multiforma	273	1 (0.4)	3 (1.1)	2 (0.7)
Colorectal adenocarcinoma	220	1 (0.5)	2 (0.9)	8 (4)
Esophageal carcinoma	184	6 (3)	3 (1.6)	9 (5)
Stomach adenocarcinoma	441	13 (2.9)	9 (2)	20 (5)
Head and neck squamous cell carcinoma	504	6 (1.2)	3 (0.6)	17 (3)
Kidney renal clear cell carcinoma	448	52 (12)	1 (0.2)	1 (0.2)
Liver hepatocellular carcinoma	366	4 (1.1)	7 (1.9)	12 (3)
Lung adenocarcinoma	230	1 (0.6)	3 (1.7)	12 (7)
Pancreatic adenocarcinoma	149	–	2 (1.3)	2 (1.3)
Prostate adenocarcinoma	492	5 (1)	8 (1.6)	8 (1.6)
Skin cutaneous melanoma	287	4 (1.4)	5 (1.7)	8 (2.8)
Thyroid carcinoma	399	–	–	1 (0.3)
Ovarian cancer	311	4 (1.3)	7 (2.3)	17 (5)
Uterine corpus endometrial carcinoma	56	–	–	1 (1.8)
Bladder urothelial carcinoma	127	5 (4)	2 (1.6)	5 (4)
Cervical cancer	191	4 (2.1)	–	6 (3)
Sarcoma	243	5 (2.1)	5 (2.1)	7 (2.9)
Testicular	149	1 (0.7)	–	1 (0.7)
Thymoma	123	–	–	1 (0.8)
Pediatric acut lymphoid leukemia	95	–	–	5(%5)
Pediatric neuroblastoma	1089	–	–	1(% 0.1)

selected and subjected to analysis via OpenComet, a software tool integrated within Image J, developed by the National Institutes of Health. Tail DNA% was employed as the parameter for quantifying DNA damage [27].

3. Results

3.1. Survival analysis

First and foremost, we have identified the target gene that is most frequently associated with poor survival across five parameters in 23 different cancer types. In order to identify the target gene specifically related to survival, we thoroughly examined the results obtained from the five parameters age, race, gender, metastasis stage, and tumor stage. Our scrutiny involved an in-depth analysis of survival curves derived from the expression patterns of 27 genes involved in the BER pathway. Notably, statistically significant survival curves were discerned for 15 genes within the BER pathway. Furthermore, it is noteworthy that no statistically significant survival curves were observed in relation to age and tumor stage, as elucidated in Fig. 1, Supplementary Table S1, and Supplementary Fig. S1.

Subsequently, we conducted a comparative analysis to determine the most commonly observed protein in terms of survival curves across different categories. Based on the survival curves, we revealed that high expression levels of *PARP3*, *TDG*, and *NEIL3* had a significant impact on cancer survival. This impact was particularly notable in three distinct categories: race, gender, and metastasis stage. In contrast, the remaining BER gene expressions were observed in fewer than three categories.

Specifically, in kidney renal clear carcinoma cancer, the high expression of *PARP3* and *TDG* was associated with decreased overall patient survival in the white race, male patient group and M0 metastasis stage. Furthermore, high expression of *NEIL3* resulted in poor survival among the white race in both lung adenocarcinoma and kidney cancers, as well as in the male patient group and M0 metastasis stage and in kidney cancer types (Fig. 1).

3.2. Determination of mutation hotspots

For identification of most probable predictive target, our investigation primarily concentrated on missense, nonsense, and frameshift mutations, aiming to determine mutation hotspot sites based on the existing mutation data across 23 different cancer types. Initially, we exhaustively examined all domain sites associated with the 27 BER genes and subsequently identified the hotspots exhibiting the highest mutation frequencies. These mutation hotspot domain sites across the 27 BER genes are visually represented in Table 2. Additionally, total mutation rates of selected genes in the different cancer types are shown in Table 3. Considering the outcomes of our survival analyses, we prioritized the gene with the highest mutation frequency. Consequently, we conducted further analyses specifically focusing on *PARP3* to gain a comprehensive understanding of its impact on cancer survival. The rationale behind this choice is rooted in the fact that *PARP3* exhibited the highest mutation frequency among the selected three genes, as observed through the consequences of the survival analyses. The mutation profiles of *PARP3, TDG*, and *NEIL3* are shown in Table 3 and Fig. 2.

3.3. Cytotoxicity assay

The cytotoxicity assay to assess cell viability was conducted using cisplatin, carboplatin, and doxorubicin, and a comparison was made between the $PARP3^{+/+}$ MDA-MB-231 cell line and the $PARP^{-/-}$ MDA-MB-231 cells. The *PARP3* knockout MDA-MB-231 cells exhibited diminished growth compared to the wild-type cells in response to the three drugs after 72 h. Interestingly, the absence of *PARP3* appeared to enhance the efficacy of cisplatin, carboplatin, and doxorubicin.

Specifically, the $PARP3^{-/-}$ MDA-MB-231 cells demonstrated a 50 % inhibition of cell viability (IC_{50}) at a cisplatin concentration of $0.7 \pm < 0.01$ μM, a carboplatin concentration of 2.2 ± 0.7 μM, and a doxorubicin concentration of $0.2 \pm < 0.01$ μM. In contrast, $PARP3^{+/+}$ MDA-MB-231 cell exhibited a IC_{50} value at a cisplatin concentration of 1.6 ± 0.15 μM, a carboplatin concentration of 8 ± 0.57 μM, and a doxorubicin concentration of 0.4 ± 0.03 μM (Fig. 3). These findings indicate that the $PARP3^{-/-}$ MDA-MB-231 cell line was sensitized to the cytotoxic effects of cisplatin, carboplatin, and doxorubicin, leading to a significant reduction in cell viability.

3.4. Microarray-based mRNA expression profiling for predicting canonical pathways

Upon identification of the most probable target genes based on the overall survival analyses and mutation profiles in 23 types of cancer, we proceeded to perform a microarray analysis with the objective of examining the consequences of *PARP3* inhibition as a target for cancer drug therapy. Subsequently, we compared two groups, namely the $PARP3^{+/+}$ and $PARP3^{-/-}$ MDA-MB-231 cell lines, following exposure to cisplatin, in order to unveil the mechanisms associated with *PARP3* through comparative analysis using Ingenuity Pathway Analysis (IPA). The data obtained revealed a significant impact of *PARP3* inhibition on signal pathways implicated in cancer cell survival.

The data derived from this analysis divulged that the inhibition of

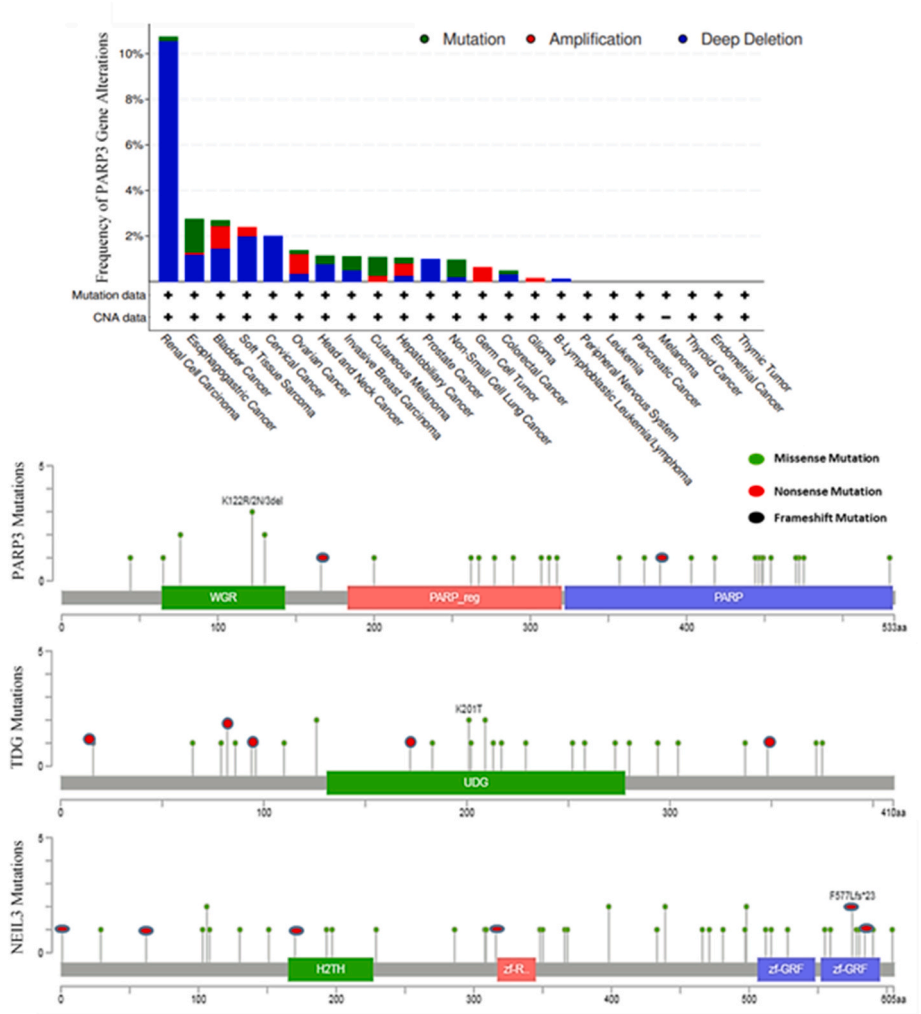

Fig. 2. Frequency of *PARP3* gene modifications in the specified cancer cases, alongside the distribution of mutation profiles associated with *PARP3*, *TDG*, and *NEIL3*.

PARP3 exerts a significant impact on signal pathways that decrease the survival of cancer cells. Specifically, in the *PARP3*$^{+/+}$ MDA-MB-231 cell line, following exposure to cisplatin, signal pathways closely associated with cellular growth and proliferation remained active, as depicted in Fig. 4. Notably, upon scrutinizing the canonical pathway of *PARP3*$^{+/+}$ MDA-MB-231, PDGF and GPCRs emerged as the most prominently active signaling cascades. Remarkably, both PDGF and GPCRs pathways exhibited highly positive z-scores, registering at 2.4 and 2.236, respectively. Consequently, we directed our focus towards these two crucial signal pathways.

However, it is worth noting that these afore-mentioned pathways (*i.e.*, GPCR and PDGF) did not exhibit activation in the *PARP3*$^{-/-}$ MDA-MB-231 cell line following exposure to cisplatin. Instead, the absence of *PARP3* led to a decrease in the activation of EIF2 and protein kinase A signaling. On the other side, upon examining the canonical pathways, we observed the activation of the oxytocin signal, the apelin endothelial signal, and the m-TOR signal pathway due to the influence of the GPCR and PDGF pathways in the *PARP3*$^{+/+}$ MDA-MB-231 cell lines.

3.5. Quantitative real-time qPCR for validating relative gene expression

To validate the findings from the microarray analyses, quantitative polymerase chain reaction (qPCR) experiments were performed. Pathway analysis was conducted to investigate whether the absence of *PARP3* in the context of cisplatin treatment impacted the PDGF and GPCR canonical pathways. For this analysis, we selected specific genes, namely *PDGFD*, *MAP2K4, GNB1L, GP107*, and *GPR89A* which are known to be involved in the PDGF and GPCR signaling pathways. The selected primers demonstrated a downregulation of gene expression in the presence of *PARP3* inhibition in the cell line exposed to cisplatin. Conversely, the expression of all genes investigated were upregulated in the *PARP3*$^{+/+}$ MDA-MB-231 cell line following cisplatin treatment (Fig. 5C). This finding was consistent with the results obtained from the microarray analyses (Fig. 5A), reinforcing the concordance between the two experimental approaches.

3.6. Single cell gel electrophoresis (comet assay)

In order to evaluate DNA damage in MDA-MB-231 cell lines devoid of *PARP3*, we utilized the alkaline comet assay as a means of detection. Our investigation revealed a noteworthy elevation in DNA damage within the *PARP3*$^{-/-}$ MDA-MB-231 cell line if exposed to a cisplatin concentration of 0.7 μM. Conversely, under the application of a higher cisplatin concentration (1.6 μM) in the wild-type cell line, the percentage of comets decreased and, therefore, less DNA damage was observed (Fig. 6). This discernible discrepancy suggests that the lack of *PARP3* renders the cells more susceptible to lower concentrations of cisplatin.

4. Discussion

Drug resistance represents a pervasive phenomenon encountered in cancer treatment, particularly in the context of platinum-based drugs

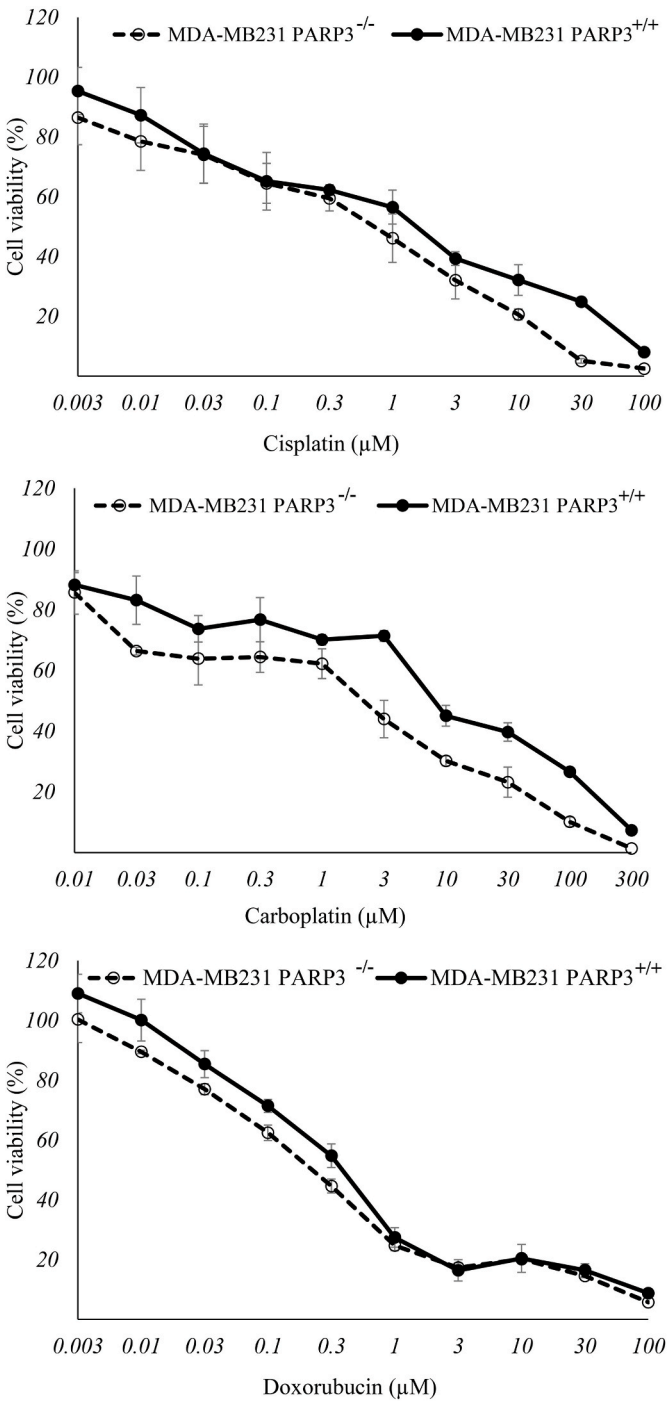

Fig. 3. Growth inhibition of *PARP3*$^{+/+}$ and *PARP3*$^{-/-}$ MDA-MB-231 cell lines for cisplatin, carboplatin, and doxorubicin by using the resazurin reduction assay.

such as cisplatin [5,28]. The primary factor underlying the development of cisplatin resistance lies in the compromised cellular uptake of the drug, the perturbation of DNA repair mechanisms, diminished cell death signaling, and augmented drug inactivation [29,30]. Despite cisplatin's substantial clinical efficacy across various cancer types, the emergence of drug resistance continues to impede patient survival and therapeutic efficacy [30]. Evidently, the identification and targeting of key molecular pathways associated with drug resistance hold significant promise in enhancing drug activity and improving clinical outcomes for patients [5]. The accurate prediction of appropriate biomarkers can be facilitated through the utilization of comprehensive bioinformatics analysis. Consequently, we employed a comparative analysis of multiple datasets in this study. By evaluating the overall survival and identifying mutation hotspots in 27 BER genes across 23 cancer types, encompassing a cohort of 7,528 patient samples, we successfully identified the most probable predictive targets.

Overall survival is known as a parameter denoting the duration between a patient's entry into a clinical trial and their demise from any cause [31,32]. Analyzing the overall survival times allows the assessment of treatment outcomes [33,34], cancer-specific biomarkers [35], as well as biological or other interventions within the realm of oncological clinical trials [36]. Patient survival is influenced by various factors, including age, race, gender, and lifestyle choices [37]. Identifying the factors that contribute to increased overall survival time is crucial for expediting the development of novel and efficacious therapies. Moreover, considering multiple factors not only helps prevent conflicting data but also aids in identifying the most probable target associated with overall survival. Undoubtedly, employing novel multiple data models is imperative for selecting a target linked to patients' survival [38]. In the present study, we compared five parameters to identify the most likely target impacting patient survival. Ultimately, we observed that the overexpression of 15 distinct BER genes under various parameters led to poorer survival outcomes (provided as Supplementary File). *PARP3*, *NEIL3*, and *TDG* emerged as the most compelling targets, as the high expression of all three BER genes was consistently associated with poorer survival across three out of the five parameters assessed, which encompassed race, gender, and metastasis stage.

Up to now, high expression of *PARP3*, *NEIL3* and *TDG* have been found to be related to poor prognostic outcomes [39–41]. Especially, the high expression of genes involved in DNA repair were directly correlated with increasing drug sensitivity and cancer progression [42]. Thus, the inhibition of DNA repair is accepted as means to increase anticancer agents' sensitivity [43]. In contrast, the downregulation of these genes are likely to exhibit a reduced DNA repair activity, leading to the accumulation of mutations [44]. Obviously, mutated genes may lead to the loss of the nuclear expression of the corresponding proteins. However, there are numerous other factors affecting protein expression, including the level of transcription, splicing, the stability of mRNA, posttranslational modifications, and epigenetic factors [45].

In addition to the analysis of survival curves, we conducted a comparative analysis in terms of single nucleotide polymorphisms (SNPs). SNPs occurring within protein-coding regions have garnered significant attention within the scientific community, despite the fact that these regions account for only approximately 2 % of the total human genome [46]. The rationale behind this attention stems from the potential deleterious effects resulting from mutations within protein cores, which can lead to protein misfolding or alterations in protein translation [47]. Furthermore, these mutations can impact gene expression levels in two distinct ways: by modifying gene dosage through changes in the number of gene copies, or by affecting gene regulation [48]. Generally, missense mutations have the potential to influence protein expression levels, hinder protein function, or directly impact drug-binding affinities, while nonsense mutations result in the truncation of proteins [46,48]. In addition to missense and nonsense mutations, frameshift mutations pose a greater likelihood of causing more severe phenotypic effects. This is due to their propensity to cause extensive alterations in the nucleotide sequence, resulting in either silent mutations or conservative changes in protein products [49]. It is evident that point mutations lead to structural modifications in proteins, which can potentially impact gene network interactions. These alterations may include changes in binding affinity towards natural partners, as well as impairment in interactions with ligands and/or inhibitors [46]. The presence of such point mutations can disrupt protein function, leading to the development of drug resistance. Therefore, evaluating the mutation status offers valuable insights into the correlation between resistance and structural alterations in proteins, shedding light on the underlying mechanisms. Following the identification of the most

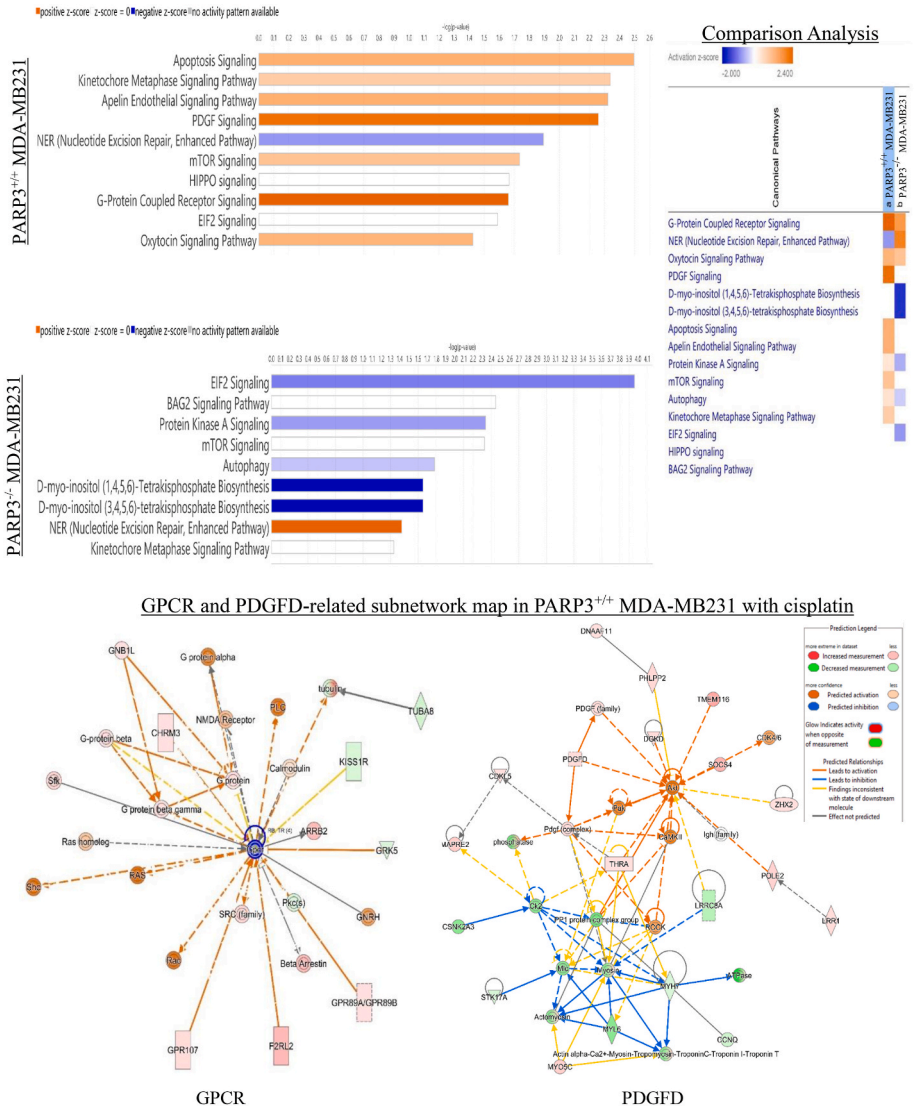

Fig. 4. Comparison of canonical pathways in *PARP3* wild-type and knockout MDA-MB-231 cells, following cisplatin exposure. The figure includes a comparative analysis of the canonical pathways between the two groups, with a specific focus on the subnetwork map of G-coupled protein receptor and PDGFD-related molecules in *PARP3* wild-type cells treated with cisplatin.

promising targets through survival analysis, we compared the mutation hotspots of 27 BER proteins across 23 cancer types. Consequently, we concentrated on *PARP3* due to its highest mutation frequency.

Cisplatin affects cancer cells by binding to specific sites in the DNA, *e.g.*, by binding to the N-7 positions of adenine and guanine [50]. These binding interactions result in the formation of interstrand and intra-strand crosslinks which impair DNA structure and DNA functions, including replication and transcription [51], leading to retarded cell growth and induction of cell death [52]. However, changes in the DNA binding sites due to mutations can alter cisplatin's ability to bind to DNA turning the expression of specific genes on or off and, thereby, resulting in non-desired changes in protein expression. This can increase toxicity to normal cells or lead to drug resistance in cancer cells. The application of combination therapies represents a common approach to dampen side effects of cisplatin on normal tissues and enhance cisplatin sensitivity towards tumor cells caused by cisplatin-caused DNA mutations. On the other hand, the identification of unwanted gene expression by computational methods, such as molecular docking, molecular dynamic, and machine learning, as well as experimental techniques may enable to design novel effective target-specific ligands as novel partners for cisplatin-based combination regimens in the future [46]. Another aspect in this context is the appearance of SNPs that also affect cisplatin-induced cytotoxicity by influencing gene expression [53]. In addition, integrated "-omics" analyses may considerably facilitate the identification of cisplatin-induced off-target effects, which may pave the way for gene-editing tools specifically targeting cancer cells and simultaneously sparing normal cells. Moreover, improvement drug delivery systems could reduce adverse effects of cisplatin by targeting only cancer cells [54].

Experimental determination of differences between mutant and wild-type proteins represents a fundamental step in understanding the influence of protein expression and variations [46]. Therefore, we conducted cytotoxic experiments to observe the consequences of *PARP3* inhibition in the presence of cisplatin. According to our microarray results, the increased expression of gene involved in nucleotide excision repair (NER) was caused from the inhibition of BER. Obviously, cells have multiple mechanisms to maintain genomic stability. If one mechanism is interrupted, another alternative mechanism may take over the protection of cellular integrity. It is apparent that there are more than 20 genes involved in BER genes, each performing a unique function. Obviously, each of them has distinct connections with the other neighbourhood genes. Our studies focussed only on the impact of *PARP3* on

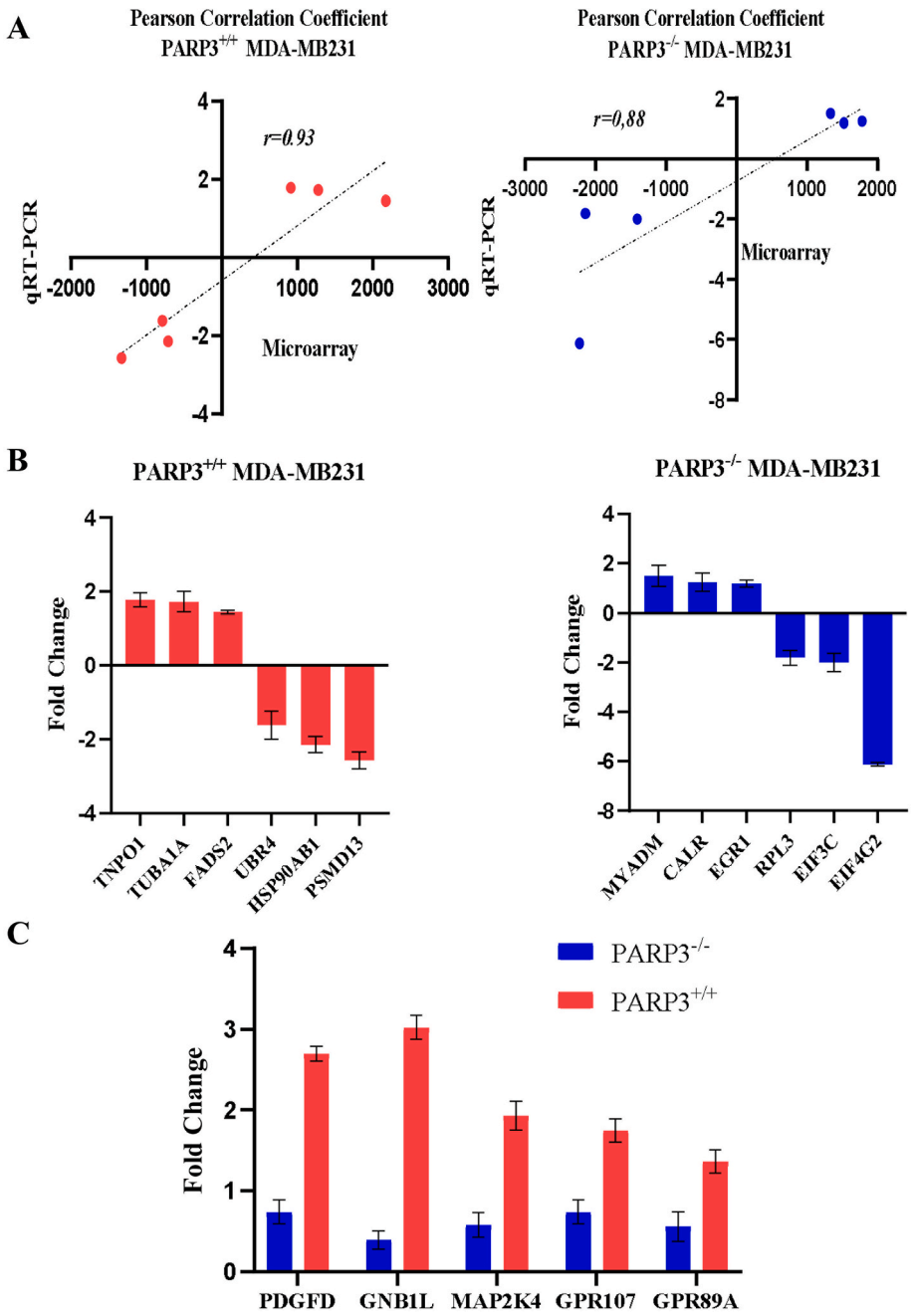

Fig. 5. A) Linear regressions and Pearson correlation coefficients for microarray and qRT-PCR data in *PARP3* wild-type and knockout MDA-MB-231 cells. B) Verification of the top three down- and up-regulated genes in these cells. C) Significant downregulation of *PDGFD, GNB1L, MAP2K4, GPR107*, and *GPR89A* genes in *PARP3* knockout MDA-MB-231 cells, with the opposite trend in the *PARP3* wild-type cells.

corresponding mechanisms by using microarray analyses. The other genes involved in BER were associated with various complex signaling pathways. Thus, blocking of distinct BER genes may result in various other molecular and cellular effects. For example, if NEIL3 has an impact on the PIK3K/AKT/mTOR signaling pathway, TDG is related to genes acting on cell cycle arrest, senescence, and death by mitotic alterations [55,56]. However, to obtain deeper information, comprehensive experimental analyses are required in the future.

The primary focus of our study was to demonstrate the alterations of neighbouring genes induced by the inhibition of *PARP3* in the response against cisplatin. The inhibition of *PARP3* plays a role the down-regulation of the mTOR signaling pathway, along with the restraint of TGFβ and reactive oxygen species (ROS)-driven epithelial-mesenchymal transition (EMT) [15,16]. Indeed, our data showed a downregulation of mTOR and apoptosis via *PARP3* blocking. Additionally, *PARP3* inhibition was found to suppress PDGF and G protein-coupled receptor (GPCR) signaling pathways, particularly affecting the expression of genes involved in the PDGF signaling pathway. The blocking of *TDG* and *NEIL3* were distinct consequences by affecting other signaling pathways. To understand the impact of *TGD* and *NEIL3* gene expression blocking, further experimental analyses are required.

Notably, PDGF assumes as modulator in the orchestration of diverse cellular processes, encompassing but not limited to cell proliferation, apoptotic regulation, cellular transformation, migration, invasion, angiogenesis, and the facilitation of metastasis [17]. Activation of PDGF fosters the survival and proliferation of cancer cells by engaging multiple oncogenic pathways such as phosphatidylinositol-3-kinase (PI3K/AKT), nuclear factor-κ B cells (NF-κB), Notch, extracellular

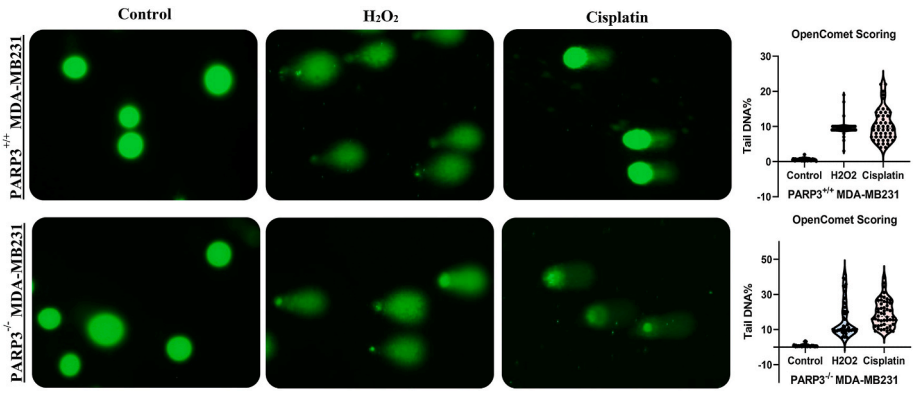

Fig. 6. Quantitative assessment of DNA damage using the alkaline comet assay, specifically single cell gel electrophoresis, following cisplatin exposure in *PARP3* wild-type and knockout MDA-MB-231 cells. The 'tail DNA%' parameter was quantified based on the analysis of 50 randomly selected cells, as illustrated in the accompanying violin plot.

signal-regulated kinase (ERK), mitogen-activated protein kinase (MAPK), and JAK-STAT [19,57–60].

The intricate interplay among various signaling pathways has a significant impact on protein-protein interactions. There exists a complex interplay among different signaling pathways, where the downregulation of one pathway exerts either a negative or positive influence on another. Illustrative examples on the relations between distinct signaling pathways have been published [61,62]. The efficient targeting to downregulate PI3K/AKT signaling revealed specific protein-protein interactions in the present of the inhibitor. The downregulation of PI3K/AKT has been considered as an alternative strategy to impede the growth of cancer cells by specific targeted ligands. Also, PDGF has a function in cancer progression by inducing proliferation, migration and cellular growth. The potential of PDGF as a therapeutic target is increasingly recognized. It is connected multiple signaling pathways responsible for cellular proliferation and growth. G protein-coupled receptors (GPCRs) is one of signal pathway affected by PDGF. In our studies, PDGF and GPCRs were downregulated through blocking of *PARP3* in breast cancer. Consequently, there are positive correlation between GPCRs, PDGF signaling pathways, and blocked *PARP3* expression. The development of potential ligands targeting PDGF is anticipated to inhibit cell proliferation by modulating the signaling pathways mentioned above.

In breast cancer, several studies showed the overexpression of PDGF as adverse prognostic factor [63,64]. Consequently, extensive research has focused on PDGF as a potential therapeutic target to combat cancer progression, as Its receptor and ligand play significant roles in drug resistance and oncogenesis [65,66]. Inhibition of PDGF, either directly or indirectly, holds promise as an approach in cancer treatment [67]. Our pathway analysis revealed that *PARP3* inhibition had a discernible impact on downregulating the PDGF signaling pathway.

Also, PDGF can be induced via GPCRs [68]. GPCRs are another modulators in tumor growth, angiogenesis, and metastasis, underscoring their significance as key players in cancer progression [69]. The upregulation of GPCR has profound effects on cancer-related signaling pathways, including AKT/mTOR, MAPKs, and the Hippo signaling pathway, which are intimately involved in cellular processes contributing to malignancy [70]. Therefore, comprehending the functional implications of GPCR in cancer drug treatment is of utmost importance in optimizing pharmacological strategies and identifying potential therapeutic targets [22]. In line with this, our study supports the proposition that *PARP3* knockdown, in the presence of cisplatin, affects GPCRs. We observed a lower function of GPCRs in *PARP3*$^{-/-}$ MDA-MB231 cells upon cisplatin exposure.

This was supported by robust evidence obtained through q-PCR verification, demonstrating the indirect influence of *PARP3* inhibition on afore-mentioned signal pathways involved in cancer progression. Notably, a pronounced upregulation was observed in the expression levels of *PDGFD, GNB1L, MAP2K4, GPR107*, and *GPR89A* genes if *PARP3* was present, as illustrated in Fig. 5C. In contrast, MDA-MB-231 breast cancer cells with the presence of *PARP3* inhibition exhibited a downregulation of these specific genes. This result indicates that knockout of *PARP3* suppressed the growth of MDA-MB-231 and increased cisplatin sensitivity. Moreover, less cisplatin concentration led to higher DNA damage in the *PARP3*$^{-/-}$ MDA-MB-231, which increased treatment efficiency at less side effects.

In conclusion, we demonstrated synthetic lethal interaction between GPCR, PDGF signaling pathways, and gene silencing of *PARP3*. In the cisplatin resistance, *PARP3* could be a promising target of a precision medicine approach. The combination of *PARP3* gene silencing and cisplatin drug may be a treatment method with fewer side effects by using lower doses of cisplatin concentration.

CRediT authorship contribution statement

Ayşegül Varol: Writing – review & editing, Writing – original draft, Validation, Software, Methodology, Investigation, Data curation, Conceptualization. **Sabine M. Klauck:** Writing – review & editing, Software, Methodology, Investigation, Data curation, Conceptualization. **Françoise Dantzer:** Methodology, Investigation, Conceptualization. **Thomas Efferth:** Writing – review & editing, Supervision, Project administration, Conceptualization.

Declaration of competing interest

The authors declare the following financial interests/personal relationships which may be considered as potential competing interests: Aysegul VAROL reports financial support was provided by Turkish Government (National Education Scholarship). If there are other authors, they declare that they have no known competing financial interests or personal relationships that could have appeared to influence the work reported in this paper.

Data availability

No data was used for the research described in the article.

Acknowledgement

We gratefully acknowledge the Microarray Unit of the Genomics and Proteomics Core Facility, German Cancer Research Center (DKFZ) Heidelberg, for providing excellent Expression Profiling service. A.V. is grateful for a stipend provided by the Turkish Government (National Education Scholarship).

Appendix A. Supplementary data

Supplementary data to this article can be found online at https://doi.org/10.1016/j.cbi.2024.111094.

References

[1] C.J. Norbury, I.D. Hickson, Cellular responses to DNA damage, Annu. Rev. Pharmacol. Toxicol. 41 (1) (2001) 367–401.
[2] G.-M. Li, Mechanisms and functions of DNA mismatch repair, Cell Res. 18 (1) (2008) 85–98.
[3] N. Chatterjee, G.C. Walker, Mechanisms of DNA damage, repair, and mutagenesis, Environ. Mol. Mutagen. 58 (5) (2017) 235–263.
[4] Y. Khazaei Monfared, et al., DNA damage by radiopharmaceuticals and mechanisms of cellular repair, Pharmaceutics 15 (12) (2023) 2761.
[5] L. Amable, Cisplatin resistance and opportunities for precision medicine, Pharmacol. Res. 106 (2016) 27–36.
[6] J. Liu, et al., Genetic polymorphisms of DNA repair pathways in sporadic colorectal carcinogenesis, J. Cancer 10 (6) (2019) 1417.
[7] H.E. Krokan, M. Bjørås, Base excision repair, Cold Spring Harbor Perspect. Biol. 5 (4) (2013) a012583.
[8] P. Fortini, et al., The base excision repair: mechanisms and its relevance for cancer susceptibility, Biochimie 85 (11) (2003) 1053–1071.
[9] U. Sattler, et al., Long-patch DNA repair synthesis during base excision repair in mammalian cells, EMBO Rep. 4 (4) (2003) 363–367.
[10] A. Gembka, et al., The checkpoint clamp, Rad9-Rad1-Hus1 complex, preferentially stimulates the activity of apurinic/apyrimidinic endonuclease 1 and DNA polymerase β in long patch base excision repair, Nucleic Acids Res. 35 (8) (2007) 2596–2608.
[11] S. O'Grady, et al., The role of DNA repair pathways in cisplatin resistant lung cancer, Cancer Treat Rev. 40 (10) (2014) 1161–1170.
[12] E. Belousova, A. Ishchenko, O. Lavrik, Dna is a new target of Parp3, Sci. Rep. 8 (1) (2018) 1–12.
[13] J.M. Rodriguez-Vargas, L. Nguekeu-Zebaze, F. Dantzer, PARP3 comes to light as a prime target in cancer therapy, Cell Cycle 18 (12) (2019) 1295–1301.
[14] H.L. Ko, E.C. Ren, Functional aspects of PARP1 in DNA repair and transcription, Biomolecules 2 (4) (2012) 524–548.
[15] O. Karicheva, et al., PARP3 controls TGFβ and ROS driven epithelial-to-mesenchymal transition and stemness by stimulating a TG2-Snail-E-cadherin axis, Oncotarget 7 (39) (2016) 64109.
[16] C. Beck, et al., PARP3, a new therapeutic target to alter Rictor/mTORC2 signaling and tumor progression in BRCA1-associated cancers, Cell Death Differ. 26 (9) (2019) 1615–1630.
[17] Z. Wang, et al., Emerging roles of PDGF-D signaling pathway in tumor development and progression, Biochim. Biophys. Acta Rev. Canc 1806 (1) (2010) 122–130.
[18] Z. Wang, et al., PDGF-D signaling: a novel target in cancer therapy, Curr. Drug Targets 10 (1) (2009) 38–41.
[19] Z. Wang, et al., Down-regulation of platelet-derived growth factor-D inhibits cell growth and angiogenesis through inactivation of Notch-1 and nuclear factor-κB signaling, Cancer Res. 67 (23) (2007) 11377–11385.
[20] C.-H. Heldin, Targeting the PDGF signaling pathway in tumor treatment, Cell Commun. Signal. 11 (2013) 1–18.
[21] R. Bar-Shavit, et al., G protein-coupled receptors in cancer, Int. J. Mol. Sci. 17 (8) (2016) 1320.
[22] Y. Liu, et al., G protein-coupled receptors as promising cancer targets, Cancer Lett. 376 (2) (2016) 226–239.
[23] E. Cerami, et al., The cBio cancer genomics portal: an open platform for exploring multidimensional cancer genomics data, Cancer Discov. 2 (5) (2012) 401–404.
[24] J. Gao, et al., Integrative analysis of complex cancer genomics and clinical profiles using the cBioPortal, Sci. Signal. 6 (269) (2013) pl1-pl1.
[25] J. O'brien, et al., Investigation of the Alamar Blue (resazurin) fluorescent dye for the assessment of mammalian cell cytotoxicity, Eur. J. Biochem. 267 (17) (2000) 5421–5426.
[26] K.J. Livak, T.D. Schmittgen, Analysis of relative gene expression data using real-time quantitative PCR and the 2− ΔΔCT method, Methods 25 (4) (2001) 402–408.
[27] B.M. Gyori, et al., OpenComet: an automated tool for comet assay image analysis, Redox Biol. 2 (2014) 457–465.
[28] G. Housman, et al., Drug resistance in cancer: an overview, Cancers 6 (3) (2014) 1769–1792.
[29] S. Tanida, et al., Mechanisms of cisplatin-induced apoptosis and of cisplatin sensitivity: potential of BIN1 to act as a potent predictor of cisplatin sensitivity in gastric cancer treatment, Int. J. Surg. Oncol. (2012) 2012.
[30] S.-H. Chen, J.-Y. Chang, New insights into mechanisms of cisplatin resistance: from tumor cell to microenvironment, Int. J. Mol. Sci. 20 (17) (2019) 4136.
[31] Q. Wang, P. Li, W. Wu, A systematic analysis of immune genes and overall survival in cancer patients, BMC Cancer 19 (2019) 1–9.
[32] D. Lebwohl, et al., Progression-Free survival: gaining on overall survival as a gold standard and AcceleratingDrug development, Cancer J. 15 (5) (2009) 386–394.
[33] R.J. Motzer, et al., Overall survival and updated results for sunitinib compared with interferon alfa in patients with metastatic renal cell carcinoma, J. Clin. Oncol. 27 (22) (2009) 3584.
[34] T. Adachi, et al., Oxaliplatin and molecular-targeted drug therapies improved the overall survival in colorectal cancer patients with synchronous peritoneal carcinomatosis undergoing incomplete cytoreductive surgery, Surg. Today 45 (2015) 986–992.
[35] R. Dienstmann, et al., Prediction of overall survival in stage II and III colon cancer beyond TNM system: a retrospective, pooled biomarker study, Ann. Oncol. 28 (5) (2017) 1023–1031.
[36] S.J. Cohen, et al., Relationship of Circulating Tumor Cells to Tumor Response, Progression-free Survival, and Overall Survival in Patients with Metastatic Colorectal Cancer, 2008.
[37] V. Gupta, et al., Survival prediction tools for esophageal and gastroesophageal junction cancer: a systematic review, J. Thorac. Cardiovasc. Surg. 156 (2) (2018) 847–856.
[38] L. Liu, et al., Breast cancer survival prediction using seven prognostic biomarker genes, Oncol. Lett. 18 (3) (2019) 2907–2916.
[39] H. Huang, Q. Hua, NEIL3 mediates lung cancer progression and modulates PI3K/AKT/mTOR signaling: a potential therapeutic target, Int. J. Genomics (2022) 2022.
[40] J.-J. Quan, J.-N. Song, J.-Q. Qu, PARP3 interacts with FoxM1 to confer glioblastoma cell radioresistance, Tumor Biol. 36 (2015) 8617–8624.
[41] G. Wang, et al., Comprehensive analysis of the prognostic value and biological function of TDG in hepatocellular carcinoma, Cell Cycle 22 (12) (2023) 1478–1495.
[42] Z. Song, et al., Poly (ADP-ribose) polymerase-3 overexpression is associated with poor prognosis in patients with breast cancer following chemotherapy, Oncol. Lett. 16 (5) (2018) 5621–5630.
[43] M.E. Dolan, Inhibition of DNA repair as a means of increasing the antitumor activity of DNA reactive agents, Adv. Drug Deliv. Rev. 26 (2–3) (1997) 105–118.
[44] C.G. Broustas, H.B. Lieberman, DNA damage response genes and the development of cancer metastasis, Radiat. Res. 181 (2) (2014) 111–130.
[45] A. Kumar, et al., Reduced expression of DNA repair genes (XRCC1, XPD, and OGG1) in squamous cell carcinoma of head and neck in North India, Tumor Biol. 33 (2012) 111–119.
[46] M. Petrosino, et al., Analysis and interpretation of the impact of missense variants in cancer, Int. J. Mol. Sci. 22 (11) (2021) 5416.
[47] V. Gotea, et al., The functional relevance of somatic synonymous mutations in melanoma and other cancers, Pigment Cell Melanoma Res. 28 (6) (2015) 673–684.
[48] R.R. Haraksingh, M.P. Snyder, Impacts of variation in the human genome on gene regulation, J. Mol. Biol. 425 (21) (2013) 3970–3977.
[49] B.S. Strauss, Frameshift mutation, microsatellites and mismatch repair, Mutat. Res. Rev. Mutat. Res. 437 (3) (1999) 195–203.
[50] Y. Mantri, S.J. Lippard, M.-H. Baik, Bifunctional binding of cisplatin to DNA: why does cisplatin form 1, 2-intrastrand cross-links with AG but not with GA? J. Am. Chem. Soc. 129 (16) (2007) 5023–5030.
[51] S. Rezaei, et al., Investigation on the effect of fluorescence quenching of calf thymus DNA by piperine: caspase activation in the human breast cancer cell line studies, DNA Cell Biol. 43 (1) (2024) 26–38.
[52] P.B. Tchounwou, et al., Advances in our understanding of the molecular mechanisms of action of cisplatin in cancer therapy, J. Exp. Pharmacol. (2021) 303–328.
[53] S.J. Shukla, et al., Susceptibility loci involved in cisplatin-induced cytotoxicity and apoptosis, Pharmacogenetics Genom. 18 (3) (2008) 253–262.
[54] M.A. Farooq, et al., Recent progress in nanotechnology-based novel drug delivery systems in designing of cisplatin for cancer therapy: an overview, Artif. Cell Nanomed. Biotechnol. 47 (1) (2019) 1674–1692.
[55] W. Wang, et al., NEIL3 contributes toward the carcinogenesis of liver cancer and regulates PI3K/Akt/mTOR signaling, Exp. Ther. Med. 22 (4) (2021) 1–11.
[56] P. Mancuso, et al., Thymine DNA glycosylase as a novel target for melanoma, Oncogene 38 (19) (2019) 3710–3728.
[57] D. Kong, et al., Mammalian target of rapamycin repression by 3, 3′-diindolylmethane inhibits invasion and angiogenesis in platelet-derived growth factor-D–overexpressing PC3 cells, Cancer Res. 68 (6) (2008) 1927–1934.
[58] M.-L. Vignais, et al., Platelet-derived growth factor induces phosphorylation of multiple JAK family kinases and STAT proteins, Mol. Cell Biol. 16 (4) (1996) 1759–1769.
[59] M.-L. Vignais, M. Gilman, Distinct mechanisms of activation of Stat1 and Stat3 by platelet-derived growth factor receptor in a cell-free system, Mol. Cell Biol. 19 (5) (1999) 3727–3735.
[60] N.A. Lokker, et al., Platelet-derived growth factor (PDGF) autocrine signaling regulates survival and mitogenic pathways in glioblastoma cells: evidence that the novel PDGF-C and PDGF-D ligands may play a role in the development of brain tumors, Cancer Res. 62 (13) (2002) 3729–3735.
[61] M. Kaffash, et al., Spectroscopy and molecular simulation on the interaction of Nano-Kaempferol prepared by oil-in-water with two carrier proteins: an investigation of protein–protein interaction, Spectrochim. Acta Mol. Biomol. Spectrosc. 309 (2024) 123815.
[62] Z. Malek-Esfandiari, et al., Molecular dynamics and multi-spectroscopic of the interaction behavior between bladder cancer cells and calf thymus DNA with rebeccamycin: apoptosis through the down regulation of PI3K/AKT signaling pathway, J. Fluoresc. 33 (4) (2023) 1537–1557.
[63] L. Seymour, W. Bezwoda, Positive immunostaining for platelet derived growth factor (PDGF) is an adverse prognostic factor in patients with advanced breast cancer, Breast Cancer Res. Treat. 32 (1994) 229–233.
[64] I. Carvalho, et al., Overexpression of platelet-derived growth factor receptor α in breast cancer is associated with tumour progression, Breast Cancer Res. 7 (5) (2005) 1–8.
[65] K. Pietras, et al., PDGF receptors as cancer drug targets, Cancer Cell 3 (5) (2003) 439–443.

[66] M.T. Weigel, et al., Preclinical and clinical studies of estrogen deprivation support the PDGF/Abl pathway as a novel therapeutic target for overcoming endocrine resistance in breast cancer, Breast Cancer Res. 14 (3) (2012) 1–15.
[67] P. Pandey, et al., New insights about the PDGF/PDGFR signaling pathway as a promising target to develop cancer therapeutic strategies, Biomed. Pharmacother. 161 (2023) 114491.
[68] J.-B. Demoulin, A. Essaghir, PDGF receptor signaling networks in normal and cancer cells, Cytokine Growth Factor Rev. 25 (3) (2014) 273–283.
[69] R.T. Dorsam, J.S. Gutkind, G-protein-coupled receptors and cancer, Nat. Rev. Cancer 7 (2) (2007) 79–94.
[70] M. O'Hayre, M.S. Degese, J.S. Gutkind, Novel insights into G protein and G protein-coupled receptor signaling in cancer, Curr. Opin. Cell Biol. 27 (2014) 126–135.

4.2. Inhibition of MSH6 augments the antineoplastic efficacy of cisplatin in non-small cell lung cancer as autophagy modulator

Contribution Statement

The study explores how MSH6 inhibition enhances the efficacy of cisplatin in non-small cell lung cancer by modulating autophagy-related pathways. MSH6 functions as a key regulator linking autophagy and cell death through major signaling routes such as mTOR, PI3K/Akt, and NRF2. Its inhibition sensitized cancer cells to cisplatin by reversing the pro-survival role of autophagy and promoting DNA damage and cell cycle arrest.

My main contribution includes conceptualization, experimental and bioinformatic analyses, data interpretation, and manuscript preparation. The findings identify MSH6 as a potential therapeutic target to overcome cisplatin resistance.

This article was written under the supervision of Prof. Dr. Thomas Efferth at the Department of Pharmaceutical Biology, Johannes Gutenberg University Mainz.

Authorship contribution: Ayşegül Varol: Writing – review & editing, Writing – original draft, Methodology, Investigation, Data curation, Conceptualization. **Joelle C. Boulos**: Methodology. **Chunmei Jin**: Methodology. **Sabine M. Klauck:** Writing – review & editing, Software, Methodology, Investigation, Data curation, Conceptualization. **Anatoly Zhitkovich:** Methodology, Investigation. **Thomas Efferth:** Writing – review & editing, Supervision, Project administration, Conceptualization.

Publication Information

Title: *Inhibition of MSH6 augments the antineoplastic efficacy of cisplatin in non-small cell lung cancer as autophagy modulator* **(DOI:** https://doi.org/10.1016/j.cbi.2024.111193)

Journal: *Chemico-Biological Interactions*

Volume: 402

Article Number: 111193

Year: 2024

Chemico-Biological Interactions 402 (2024) 111193

Contents lists available at ScienceDirect

Chemico-Biological Interactions

journal homepage: www.elsevier.com/locate/chembioint

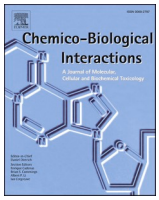

Research paper

Inhibition of MSH6 augments the antineoplastic efficacy of cisplatin in non-small cell lung cancer as autophagy modulator

Ayşegül Varol [a], Joelle C. Boulos [a], Chunmei Jin [a], Sabine M. Klauck [b], Anatoly Zhitkovich [c], Thomas Efferth [a,*]

[a] Department of Pharmaceutical Biology, Institute of Pharmaceutical and Biomedical Sciences, Johannes Gutenberg University-Mainz, 55128, Mainz, Germany
[b] Division of Cancer Genome Research, German Cancer Research Center (DKFZ) Heidelberg, National Center for Tumor Diseases (NCT), NCT Heidelberg, a Partnership Between DKFZ and University Hospital Heidelberg, 69120, Heidelberg, Germany
[c] Department of Pathology and Laboratory Medicine, Brown University, Providence, Rhode Island, 02903, USA

ARTICLE INFO

Keywords:
Chemotherapy
Drug resistance
Prognostic factors
Signal transduction
Survival analysis
Transcriptomics

ABSTRACT

The altered response to chemotherapeutic agents predominantly stems from heightened single-point mutations within coding regions and dysregulated expression levels of genes implicated in drug resistance mechanisms. The identification of biomarkers based on mutation profiles and expression levels is pivotal for elucidating the underlying mechanisms of altered drug responses and for refining combinatorial therapeutic strategies in the field of oncology. Utilizing comprehensive bioinformatic analyses, we investigated the impact of eight mismatch repair (MMR) genes on overall survival across 23 cancer types, encompassing more than 7500 tumors, by integrating their mutation profiles. Among these genes, *MSH6* emerged as the most predictive biomarker, characterized by a pronounced mutation frequency and elevated expression levels, which correlated with poorer patient survival outcomes.

The wet lab experiments disclosed the impact of *MSH6* in mediating altered drug responses. Cytotoxic assays conducted revealed that the depletion of *MSH6* in H460 non-small lung cancer cells augmented the efficacy of cisplatin, carboplatin, and gemcitabine. Pathway analyses further delineated the involvement of *MSH6* as a modulator, influencing the delicate equilibrium between the pro-survival and pro-death functions of autophagy.

Our study elucidates the intricate interplay between *MSH6*, autophagy, and cisplatin efficacy, highlighting *MSH6* as a potential therapeutic target to overcome cisplatin resistance. By revealing the modulation of autophagy pathways by *MSH6* inhibition, our findings offer insights into novel approaches for enhancing the efficacy of cisplatin-based cancer therapy through targeted interventions.

1. Introduction

Therapy resistance significantly contributes to treatment failure and disease recurrence in cancer [1,2]. Drug resistance, whether inherent or acquired, can arise from diverse mechanisms [3]. The biomedical community is actively engaged in ongoing endeavours directed towards identifying of component underlying resistance mechanisms and formulating novel drugs to surmount them [2]. Cisplatin resistance, a common form of cancer drug resistance, occurs due to reduced drug accumulation, increased detoxification activity, enhanced DNA repair capacity, and disrupted cell death signalling [4].

Among increased DNA repair function, the mismatch repair (MMR) system, renowned for its intricate defence against mutagenesis, stands as a profoundly conserved repair pathway across evolutionary scales [5,6]. The MMR mechanism is effectively responsible for the correction of base–base mismatches and insertion/deletion (I/D) mismatches that arise during the processes of replication and recombination in various organisms [7,8]. The malfunctioning of the MMR repair pathway fosters profound repair defects and progressive mutation accumulation in the genetic material [9]. Particularly, mutations within coding regions due to MMR failure affects the response to certain forms of chemotherapy by changing the function of tumor suppressor genes and proto-oncogenes [10,11]. Beyond its canonical role in DNA repair, MMR proteins orchestrate cellular responses to distinct forms of genotoxic insult, mediating either apoptotic cell death or cell cycle arrest [10,12–14]. The mutations and aberrant expression of MMR genes engender resistance to chemotherapeutic regimens by impeding damage-triggered apoptotic

* Corresponding author.
E-mail address: efferth@uni-mainz.de (T. Efferth).

https://doi.org/10.1016/j.cbi.2024.111193
Received 23 April 2024; Received in revised form 18 July 2024; Accepted 7 August 2024
Available online 20 August 2024

Abbreviations

MMR	Mismath repair
I/D	insertion/deletion
NSCLC	non-small cell lung cancer
5-FU	5-fluorouracil
BNIP3	Bcl-2 19-kDa interacting protein
shRNA	short hairpin RNA
IPA	Ingenuity Pathway Analysis software
PI3K/Akt	phosphatidylinositol 3 kinase
Nrf2	nuclear factor erythroid2-related factor2
q-PCR	quantitative polymerase chain reaction
cDNA	complementary DNA
PI	propidium iodide
ROS	reactive oxygen species
SNP	single nucleotide polymorphisms
TCGA	The Cancer Genome Atlas

cascades, thereby furnishing a selective advantage within cancer cell populations [10,11,15,16].

Currently, contemporary pharmacogenomic research has increasingly emphasized the investigation of single point mutations within coding regions that lead to adverse drug responses, with variations in drug responsiveness commonly observed across diverse populations [17]. The discernment of biomarkers in manner of mutation profile and expression level enables to enhance the refinement of combinatorial therapeutic approaches in the field of oncology [18]. To date, especially in the context of MMR, the presence of *MSH6* mutations was recognized as a significant factor contributing to the recurrence of glioma, development of acquired resistance to alkylating agents, and the induction of genome instability [19–21]. However, while significant biomarkers have been delineated concerning drug resistance, the precise impact of extant mutations on drug resistance at the level of the MMR mechanism remains incompletely understood.

Additionally, current research has highlighted the crucial role of autophagy as a key modulator in cisplatin drug resistance [1,22]. Autophagy has a dual role in cancer mechanism [23–25]. Autophagy activation impacts cancer cells in two distinct ways: promoting cell survival (pro-survival) or contributing to cell death (pro-death) [24,26]. Apart from the cell death role of autophagy, its protective function aids cancer cell survival by generating nutrients and energy during metabolic and oxidative stress [27]. It also eliminates damaged proteins and organelles, providing an additional energy source for tumor cells, enabling them to resist anticancer therapies [27,28]. The dual role of autophagy depends on genetic background, tumor stage, and type [25,29]. In certain cases, autophagy induction promotes cisplatin resistance, particularly in ovarian and lung cancers [30,31]. In this context, several potential strategies concentrate to inhibit autophagy to re-sensitize the resistant cancer cells to anticancer therapy [32]. Inhibition of autophagy enhanced the therapeutic efficacy of cisplatin and 5-fluorouracil (5-FU) in esophageal and colon cancer, respectively [33,34].

Multiple regulatory mechanisms tightly govern autophagy induction owing to its crucial role in maintenance of cellular balance [32,35]. Certain DNA-repair proteins play a crucial role in triggering autophagy following exposure to genotoxic stress [36]. Some evidence has demonstrated that following exposure to a genotoxic methylating agent, 6-thioguanine, DNA mismatch repair processes induce autophagy, and result in increased survival of colorectal and endometrial cancer cells in humans [37]. Furthermore, recent findings underscore the indispensable role of Bcl-2 19-kDa interacting protein 3 (BNIP3), a proapoptotic member of the BH3-only subfamily, in autophagy induction subsequent to MMR-mediated processing [38,39] However, the intricate interplay between autophagy and MMR still remains enigmatic [39]. The findings of the present investigation reveal the crosstalk between *MSH6* and autophagy. The inhibition of *MSH6* acts as a modulator between autophagy and cellular death, influencing several signalling pathways including the mTOR signalling pathway, PI3K/Akt, c-MYC, NRF-2 mediating oxidative signalling pathway etc. Notably, *MSH6* has an important function to orchestrate the bidirectional functionality of autophagy. The blocking of *MSH6* function results in the enhanced drug sensitivity for chemotherapy agents by changing the pro-survival role of autophagy.

In summary, our study sheds light on the intricate interplay of *MSH6* in the context of autophagy and chemotherapy efficacy. The findings underscore the need for a nuanced and personalized approach to therapeutic interventions, with *MSH6* emerging as a promising target to enhance the efficacy of cisplatin-based cancer therapy. Our studies open new avenues for the development of pharmaceutical agents specifically targeting *MSH6* to address the challenges posed by cisplatin resistance.

2. Material and methods

2.1. Mutation analyses

This study aimed to investigate the mutation profiles of eight mismatch repair (MMR) proteins across 23 different cancer types. The UniProt database was utilized to determine the domain sites associated with the MMR proteins and cBioPortal, an open-access platform for exploring cancer genomics data, provided the mutation data covering a date range from 2020 to 2021 [40,41]. The data of more than 7,500 tumor patients were used and classified into three categories: missense mutations, nonsense mutations, and frameshift mutations. We only focused on mutations inside domain sides of MMR proteins. The mutation frequency of the eight MMR proteins was analyzed and compared across the selected cancer types to identify common mutation patterns. Subsequently, a more in-depth analysis was performed on the *MSH6* protein to show the mutation distribution and genetic variation in 23 cancer types.

2.2. Survival analyses

To investigate the survival curve linked to the expression of the eight MMR genes at the mRNA level, we utilized the Cancer Genome Atlas (TCGA) dataset obtained from cBioportal (https://www.cbioportal.org; accessed between 2020 and 2021) as our primary data source. This dataset provided extensive information on 23 different cancer types, including the expression levels of MMR genes, along with five key parameters: age, race, gender, metastasis stage, and tumor stage [40]. To begin the analysis, we prepared individual Excel files for each parameter using the data from cBioportal. In these files, we labeled patient outcomes as "1″ for living patients and "0″ for deceased patients. As for the age parameter, we separately handled each of seven age ranges (10–20, 20–30, 30–40, 40–50, 50–60, 60–70, 70–80). Subsequently, we conducted Kaplan-Meier survival analyses on each MMR gene within the given context, utilizing the SPSS program (IBM Corp. Released 2015. IBM SPSS Statistics for Windows, Version 23.0. Armonk, NY: IBM Corp).

For statistical significance, we employed the "log-rank" test statistics. This allowed us to identify survival curves that showed significant differences. Specifically, we considered survival curves with a p-value below 0.05 as statistically significant. After conducting the analyses, we compared all the obtained survival curves and focused on the MMR gene that exhibited the highest impact on poor patient survival across the five parameters mentioned earlier.

2.3. MSH6 knockdown cancer cell line

In this study, the H460 cell line, obtained from the American Type Culture Collection (ATCC) and characterized by the absence of any DNA abnormalities, was utilized. Gene knockout of *MSH6* was executed

Table 1
Specific mutational hotspot sites and the mutation frequency therein of eight MMR genes.

Gene	Missense mutations	Nonsense mutations	Frameshift mutations	Mutation Hotspot Domain	Total mutation number
MSH3	4	1	30	MutS-II (MutS domain II) (366–522)	34
MSH6	9	4	17	MutS V (MutS domain V) (1075–1325)	30
MSH2	17	3	2	MutS III (MutS domain III) (306–610)	22
PMS2	7	–	–	HATPase_c_3 (histidine kinase) (34–139)	7
MLH1	7	2	–	DNA_repair (C terminal domain) (216–334)	9
EXO1	4	1	–	XPG_I (XPG I region) (139–225)	5
MLH3	8	–	1	MutL_C (MutL-C terminal dimerization domain (1217–1370)	9
RPA1	6	–	–	Replication factor-A C terminal domain (461–606)	6

following previously established protocols [42]. In brief, sustained depletion of protein levels was accomplished through the deployment of short hairpin RNA (shRNA) expressed from the pSUPERretro vector [42]. The plasmid underwent linearization using *Hin*dIII and *Bgl*II to facilitate the integration of annealed oligonucleotides targeting the mRNA sequence of interest. *MSH6*-targeting vectors were assembled utilizing 5′-gatccccggtgatccctctgagaactttcaagagaagttctcagagggatcaccttt ttggaaa-3' oligonucleotides. Cells expressing the vector were subjected to selection in the presence of 1.5 μg/mL puromycin [42].

2.4. Cytotoxicity assay

The cytotoxicity of the compounds was determined through the well-established resazurin reduction assay [43]. This assay enables the determination of viable cells by measuring the reduction of resazurin to resorufin. Specifically, the impact of cisplatin, carboplatin, and gemcitabine was investigated over a concentration range of 0.003 μM–100 μM, targeting both H460 wilt type and *MSH6-shRNA* transfected H460 cancer cell lines. To execute the experiments, $MSH6^{+/+}$ H460 and $MSH6^{-/-}$ H460 were seeded onto 96-well plates. Upon reaching approximately 70 %–80 % confluence, the cells were exposed to the specified compounds for a period of 72 h. Following this incubation, the cells were subjected to an additional 4-h incubation with 20 μL/well of resazurin (Sigma-Aldrich, Taufkirchen, Germany) diluted in double-distilled water (ddH_2O). The outcomes were recorded using the fluorescence wavelength of 544 nm and an emission wavelength of 590 nm, utilizing the advanced infinite M2000 ProTM plate reader (Tecan, Crailsheim, Germany). This reader enables precise and reliable measurements. To determine the inhibitory concentration required to achieve 50 % inhibition (IC_{50}), nonlinear regression analysis was performed using Microsoft Excel, a widely employed software tool for data analysis.

2.5. Microarray-based expression profiling for predicting canonical pathways

To discern the impact of *MSH6* absence in H460 cells on the canonical pathway, we conducted microarray hybridization expression analyses. Both $MSH6^{+/+}$ H460 and $MSH6^{-/-}$ H460 cell lines were subjected to distinct cisplatin concentrations (12.3 μM and 4.4 μM, respectively) for a 24-h period. Subsequently, we extracted total RNA using the InviTrap® Spin Universal RNA Mini Kit from Invitek Molecular, Berlin, Germany. Following this, complementary DNA (cDNA) was synthesized, labeled, and subjected to hybridization on Affymetrix GeneChips® utilizing the human Clariom S™ assay (Affymetrix, Santa Clara, CA, USA) at the Genomics and Proteomics Core Facility of the German Cancer Research Center (DKFZ, Heidelberg, Germany). We then observed the affected genes through Chipster software (version 3.16.3) (accessed on June 21, 2020), where we assessed their variable expression and significance based on the empirical Bayes *t*-test ($p < 0.05$).

To elucidate the canonical pathway affected by *MSH6* inhibition, we employed Ingenuity Pathway Analysis software (IPA) from Ingenuity Systems (Redwood City, CA, USA) using content version 51 963 813, released on July 31, 2023. IPA facilitated the assessment of changes in canonical pathways between the $MSH6^{+/+}$ H460 and $MSH6^{-/-}$ H460 cells following cisplatin exposure. To compare the effects of cisplatin exposure on $MSH6^{+/+}$ and $MSH6^{-/-}$ H460 cells, we conducted gene heatmap and canonical pathway analyses, utilizing activation z-scores and *p*-values as metrics.

2.6. Quantitative real-time q-PCR for validating relative gene expression

After identifying the canonical pathways associated with the absence of *MSH6*, we aimed to validate the microarray hybridization findings using the q-PCR technique. To achieve this, we designed primers using the Primer BLAST online tool (https://www.ncbi.nlm.nih.gov/tools/primer-blast/) (accessed in 2023) and acquired them from Eurofins Genomics (Ebersberg, Germany). The specific primers chosen for the study are displayed in Supplementary Table S2. The expression of *GAPDH* served as internal control. Next, we conducted q-PCR on the selected genes. In brief, we treated both H460 wild-type and *MSH6* stably knocked down H460 cancer cells with cisplatin concentrations equivalent to their respective IC_{50} values (12.3 μM and 4.4 μM) for a duration of 24 h. We performed total RNA extraction using the InviTrap® Spin Universal RNA Mini Kit (Invitek Molecular, Berlin, Germany). The conversion from mRNA to cDNA was achieved using the LunaScript® RT SuperMix Kit cDNA Synthesis Kit (New England Bio Labs, Darmstadt, Germany).

For gene amplification, we employed the EvaGreen master mix (5 × Hot Start Taq EvaGreen® q-PCR Mix (no ROX); Axon Labortechnik, Kaiserslautern, Germany) following the manufacturer's instructions. Q-PCR was carried out on a CFX384TM instrument (Bio-Rad, Munich, Germany) using a 38-well plate and running 40 cycles. The PCR run conditions comprised an initial denaturation phase at 95 °C for 15 s, followed by a gradient annealing step ranging from 62 °C to 47 °C for 30 s, and finally, an elongation step at 72 °C for 1 min. To determine the fold-change in gene expression, we used the comparative Cq ($2^{-\Delta\Delta Cq}$) method [44].

2.7. Western blotting

$MSH6^{+/+}$ and $MSH6^{-/-}$ H460 cancer cell lines were treated with cisplatin for the specified durations (24 h). After treatment, the cells were washed three times with PBS. Total proteins were extracted using the M-PER Mammalian Protein Extraction Reagent (Thermo Fisher Scientific, Darmstadt, Germany). For nuclear and cytoplasmic protein extraction, the NE-PER Nuclear and Cytoplasmic Extraction Reagents kit (Thermo Fisher Scientific) was utilized. Both extraction buffers contained 1 % Halt Protease Inhibitor Cocktail and phosphatase inhibitor

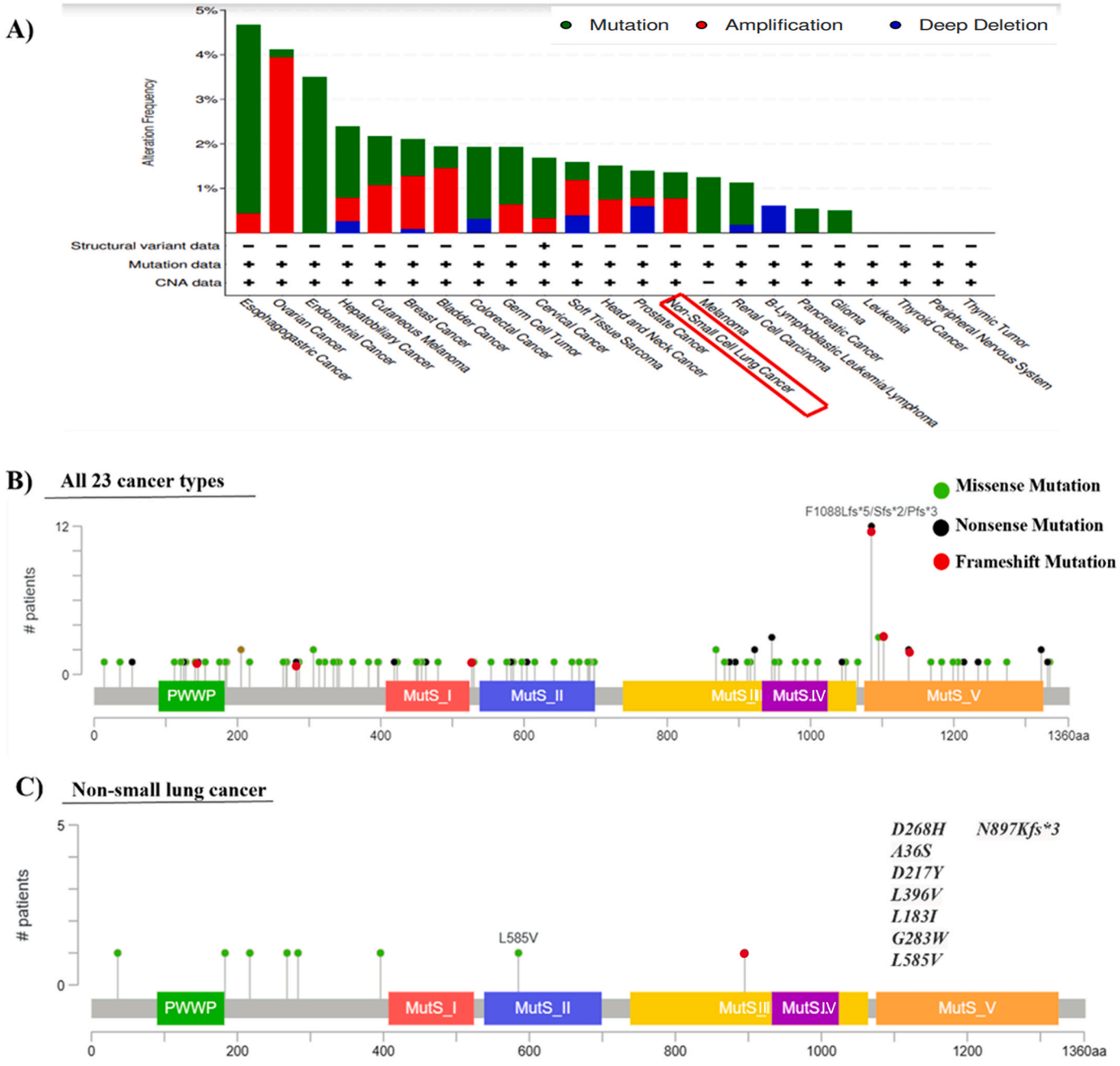

Fig. 1. Mutational analysis of the *MSH6* genes. **A)** The frequency of *MSH6* gene modifications in the specified cancer types. **B)** The distribution of mutations in the *MSH6* gene with its domains (PWWP, MutS I to V) in 23 cancer types. **C)** The distribution of mutation profiles of *MSH6* across non-small lung cancer cases.

(Thermo Fisher Scientific). Protein concentrations were measured with a Nanodrop spectrophotometer. Equal protein amounts (30 μg) were resolved by 10 % SDS-PAGE and transferred onto a polyvinylidene fluoride membrane (ROTI®PVDFR, Carl Roth, Karlsruhe, Germany). The membrane was blocked with TBST buffer containing 5 % bovine serum albumin (BSA) for 1 h. Subsequently, the membranes were incubated overnight at 4 °C with specific primary antibodies: anti-PTEN rabbit antibody (1:1000, Cell Signalling Technology, Leiden, The Netherlands), anti-RPTOR rabbit antibody (1:1000, Cell Signalling Technology), anti-ILC3-B rabbit antibody (1:1000, Cell Signalling Technology), anti-GAPDH rabbit antibody (1:1000, Cell Signalling Technology), and anti-β-actin rabbit antibody (1:1000, Cell Signalling Technology). The following day, the membrane was incubated with HRP-linked anti-mouse or anti-rabbit IgG (1:2000, Cell Signalling Technology) for 1 h at room temperature. Immunoreactive bands were detected using the Luminate™ Classico HRP substrate (Merck Millipore, Schwalbach, Germany) and visualized with an Alpha Innotech FluorChem Q system (Biozym, Oldendorf, Germany). Band intensities were quantified using ImageJ software (National Institutes of Health), with relative protein expression normalized to GAPDH or β-actin.

2.8. ROS detection

In a concise manner, $MSH6^{+/+}$ and $MSH6^{-/-}$ H460 cancer cell lines, at a density of 3×10^5 cells per well, were cultured and exposed to varying concentrations of cisplatin (respectively 12.3 μM for $MSH6^{+/+}$ H460 cells and 4.4 μM for $MSH6^{-/-}$ H460 cells) for durations of 24 h. Following treatment, cells were collected, PBS-washed, and

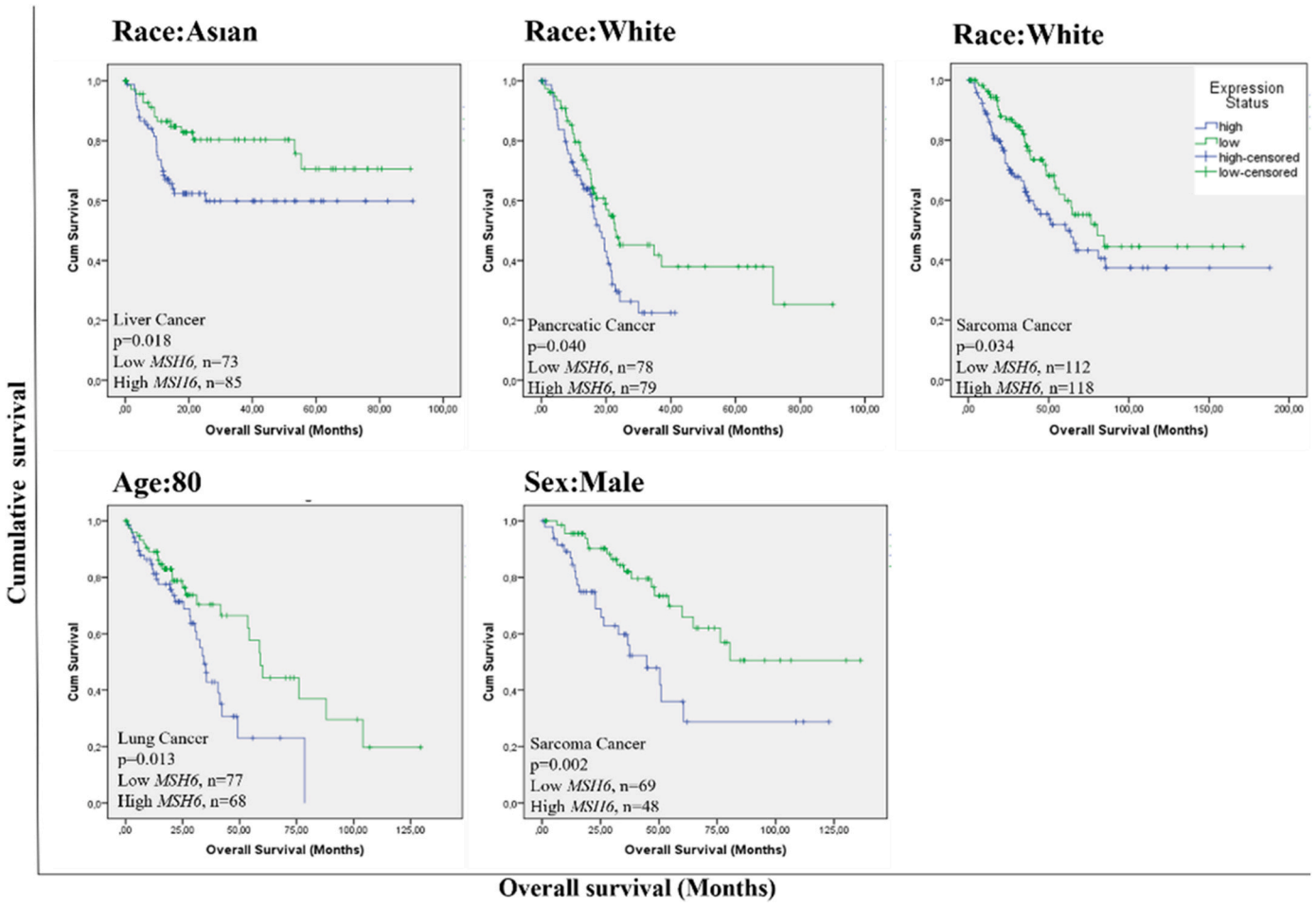

Fig. 2. Overall survival analyses of high *MSH6* expression resulting in poor survival in various cancer types considering distinct parameters.

subsequently resuspended in 1 mL PBS. The cells were then subjected to a 30-min incubation at 37 °C with 10 μM 2′7-dichlorodihydrofluorescein diacetate (H_2DCFH-DA) obtained from Sigma-Aldrich. As a positive control, H_2O_2 at a concentration of 50 μM (Sigma-Aldrich) for 15 h was used. We used 10 μL DAPI (50 μg/mL) for a live cell staining. For each sample, 20 000 cells were counted. The gate was based on forward and side scatter properties (FSC-A/SSC-A), the single cells were gated (FSC-A/FSC-H) in a linear manner to remove doublets or debris. We used VL 405 nm 445/45 filter to detect living cells by DAPI staining dye (DAPI negative cells) and BL 488 nm 525/45 filter for H_2DCFH-DA. Measurement of fluorescence intensity was conducted by using median fluorescence intensity of H_2DCFH-DA in NovoCyte Quanteon (Agilent) Flow Cytometer. The data were analyzed by the FlowJo software (version 10.8.1) (Celeza, Olten, Switzerland). Each experimental condition was independently replicated three times. GraphPad-Prism 6 (La Jolla, CA, USA) software was used to data analyses.

2.9. Cell cycle analysis

MSH6$^{+/+}$ H460 and *MSH6*$^{-/-}$ H460 cells, seeded at a density of 3 × 10^5 cells per well in 6-well plates, underwent treatment with distinct cisplatin concentrations (12.3 μM for *MSH6*$^{+/+}$ H460 cells and 4.4 μM for *MSH6*$^{-/-}$ H460 cells) for a 24 h incubation period. Subsequently, both cell lines were fixed with ethanol and stored at −20 °C for an additional 24 h. The fixed samples were then subjected to centrifugation (4000 rpm, 10 min) and re-suspended in 500 μL of cold PBS, supplemented with 20 μg/mL RNase (Roche Diagnostics, Mannheim, Germany). Following this, staining was performed using 50 μg/mL propidium iodide (PI) from Sigma-Aldrich. For each sample, 10 000 cells were counted. The gate was based on forward and side scatter properties (FSC–H/SSC-H), the single cells were gated (PI-YG561nm 615/20-A/PI-YG561nm 615/20-H) in a linear manner to remove doublets or debris. We used YG 561 nm 615/20 filter for PI staining dye. Measurement of the stained samples was carried out utilizing NovoCyte Quanteon (Agilent) Flow Cytometer. The resulting data underwent analysis using FlowJo software (version 10.8.1) (Celeza, Olten, Switzerland). Each experimental procedure was independently replicated three times. Data analysis was further conducted using GraphPad-Prism 6 (La Jolla, CA, USA) software for presentation and interpretation.

2.10. Single cell electrophoresis (comet assay)

The Oxiselect™ Comet Assay Kit (3-Well Slides) from Cell Biolabs/Biocat (Heidelberg, Germany), was employed to conduct the comet assay in this study. *MSH6*$^{+/+}$ H460 and *MSH6*$^{-/-}$ H460 cells were initially seeded at a density of 3 × 10^5 cells per well in 6-well plates. Subsequently, these cells were treated with cisplatin concentrations corresponding to their respective IC_{50} values (12.3 μM and 4.4 μM for 24 h) and H_2O_2 at a concentration of 50 μM for 15 min as a positive control.

After treatment, cells were collected, centrifuged at 3000 × *g* for 10 min, and reconstituted in PBS. Cell suspensions at a concentration of 1 × 10^5 cells/mL were mixed with molten agarose (at a ratio of 1:6) at 37 °C. The resulting mixtures were spread onto comet slides and incubated in darkness at 4 °C for 30 min. Slides were immersed in a pre-chilled lysis buffer (containing NaCl, EDTA solution, and 10 × lysis solution at pH

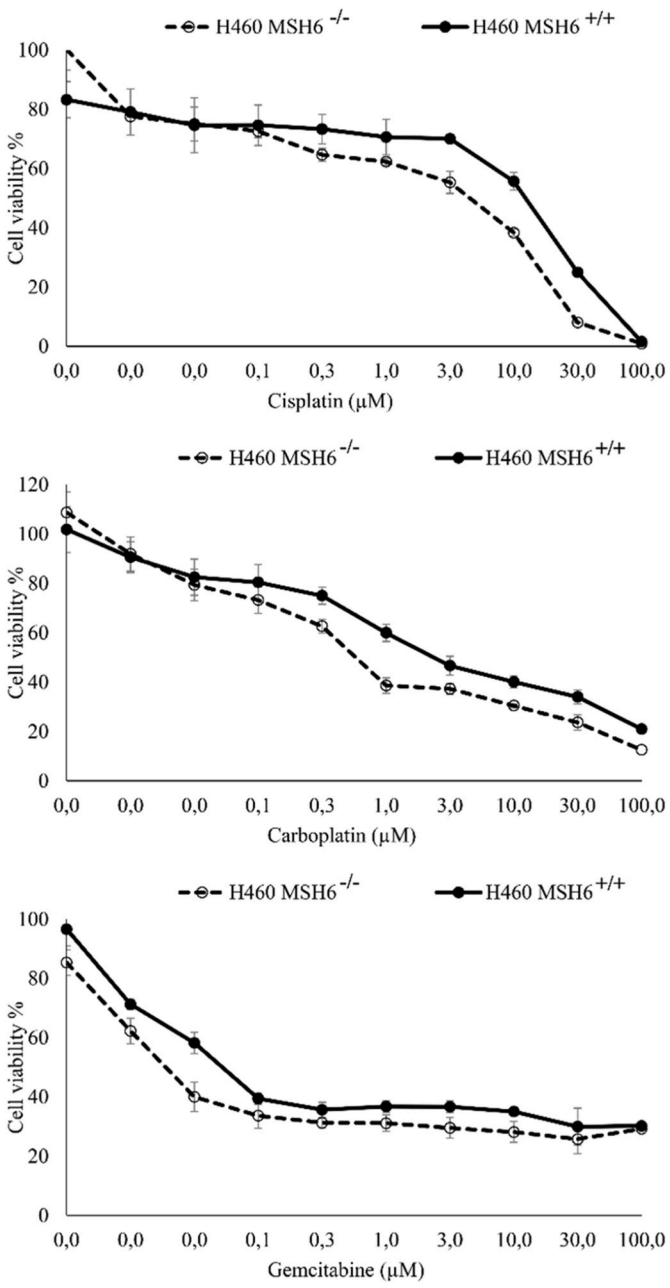

Fig. 3. The cell viability of *MSH6*$^{+/+}$ and *MSH6*$^{-/-}$ H460 cells by using different concentrations of cisplatin, carboplatin, or gemcitabine as measured by the resazurin assay.

10.0) for 1 h at 4 °C. Following lysis, slides were transferred to a pre-chilled alkaline electrophoresis solution buffer (containing NaOH, EDTA solution, and distilled water) for 40 min at 4 °C in darkness.

The slides were then placed in an electrophoresis chamber filled with the alkaline electrophoresis solution buffer, and electrophoresis was performed at 20 V for 20 min. After electrophoresis, slides underwent two washes with pre-chilled distilled water for 5 min each. Subsequently, slides were immersed in cold ethanol (70 %) for 5 min and air-dried. Once dried, 100 μL of Vista Green DNA dye (diluted at a ratio of 1:10 000 in TE buffer) was added to each slide and incubated for 15 min at room temperature. Fifty comets from each treatment group were randomly selected and analyzed using OpenComet, a software tool integrated within Image J, developed by the National Institutes of Health. Tail DNA% served as the parameter for quantifying DNA damage [45].

3. Results

3.1. Mutation analyses

We concentrated on mutations in coding regions of genes including missense, nonsense, and frameshift mutations. We determined the mutational hotspot sites for eight MMR genes based on the existing mutation data across 23 different cancer types to identify the most probable predictive target. As displaying in Table 1, *MSH3,* and *MSH6* contained the highest mutation numbers in comparison of specific mutational hotspot sites of the selected MMR genes. Particularly, our interest focused on the mutations of *MSH6* and lung cancer (Fig. 1) after having performed the survival analyses.

3.2. Survival analyses

We performed survival analyses to identify the genes whose high expression resulted in poor survival in 23 cancer types. To determine the right targets, we handled the impact of various factors including age, race, gender, metastasis stage, and tumor stage. The summarized results, available in Supplementary Table S1 and Supplementary Fig. S1, may serve as a valuable reference investigating the intricate relationship between MMR gene expression and its prognostic implications in cancer. It is evident from Fig. S1 in the supplement that the mRNA expression level of MMR genes is completely different according to cancer type and the analyzed parameters. These valuable data highlight the inevitability of individual therapy. Comparative bioinformatic analyses pinpointed *MSH6* and *EXO1* as notably promising targets. The data acquired revealed that increased expression of *EXO1* was linked to unfavorable survival outcomes across all five parameters, encompassing age, race, gender, tumor stage, and metastasis stage. In addition, the high expression of *MSH6* emerged as a noteworthy factor contributing to diminished survival rates, particularly within the parameters of age, race and gender as shown in Fig. 2. We therefore focused on *MSH6*, considering mutation and survival analyses across 23 cancer types.

3.3. Cytotoxicity assays

The cytotoxicity assay was conducted using cisplatin, carboplatin, and gemcitabine. We compared the differences between the *MSH6*$^{+/+}$ H460 and the *MSH6*$^{-/-}$ H460 cell lines. Upon treatment for 72 h, the *MSH6*$^{-/-}$ H460 cells exhibited diminished growth compared to the wild-type cells in response to the aforementioned drugs (cisplatin, carboplatin, and gemcitabine).

Specifically, the *MSH6*$^{-/-}$ H460 cells demonstrated IC_{50} values at a cisplatin concentration of 4.4 ± 0.5 μM, a carboplatin concentration of 0.5 ± 0.09 μM, and a gemcitabine concentration of 0.018 ± 0.004 μM. In comparison, the wild-type cells exhibited IC_{50} values at a cisplatin concentration of 12.3 ± 0.3 μM, a carboplatin concentration of 2.4 ± 0.5 μM, and a gemcitabine concentration of 0.051 ± < 0.01 μM (Fig. 3).

3.4. Microarray hybridization-based expression profiling for predicting canonical pathways

After comprehensive bioinformatic analyses, we performed microarray hybridization analyses for expression profiling to reveal the molecular relationships between *MSH6* inhibition and drug activities. We compared two groups, namely *MSH6*$^{+/+}$ H460 and *MSH6*$^{-/-}$ H460 cells following exposure to cisplatin by using Ingenuity Pathway Analysis (IPA).

The canonical pathways obtained from microarray analyses showed that the inhibition of *MSH6* changed the balance of mechanisms playing a role in the response given against cisplatin. In Fig. 4, the comparative analysis clearly reflects the differences between the two groups and mechanisms affected by cisplatin. The canonical pathways of cisplatin-treated *MSH6*$^{+/+}$ H460 and *MSH6*$^{-/-}$ H460 cells (Fig. 4) exhibited

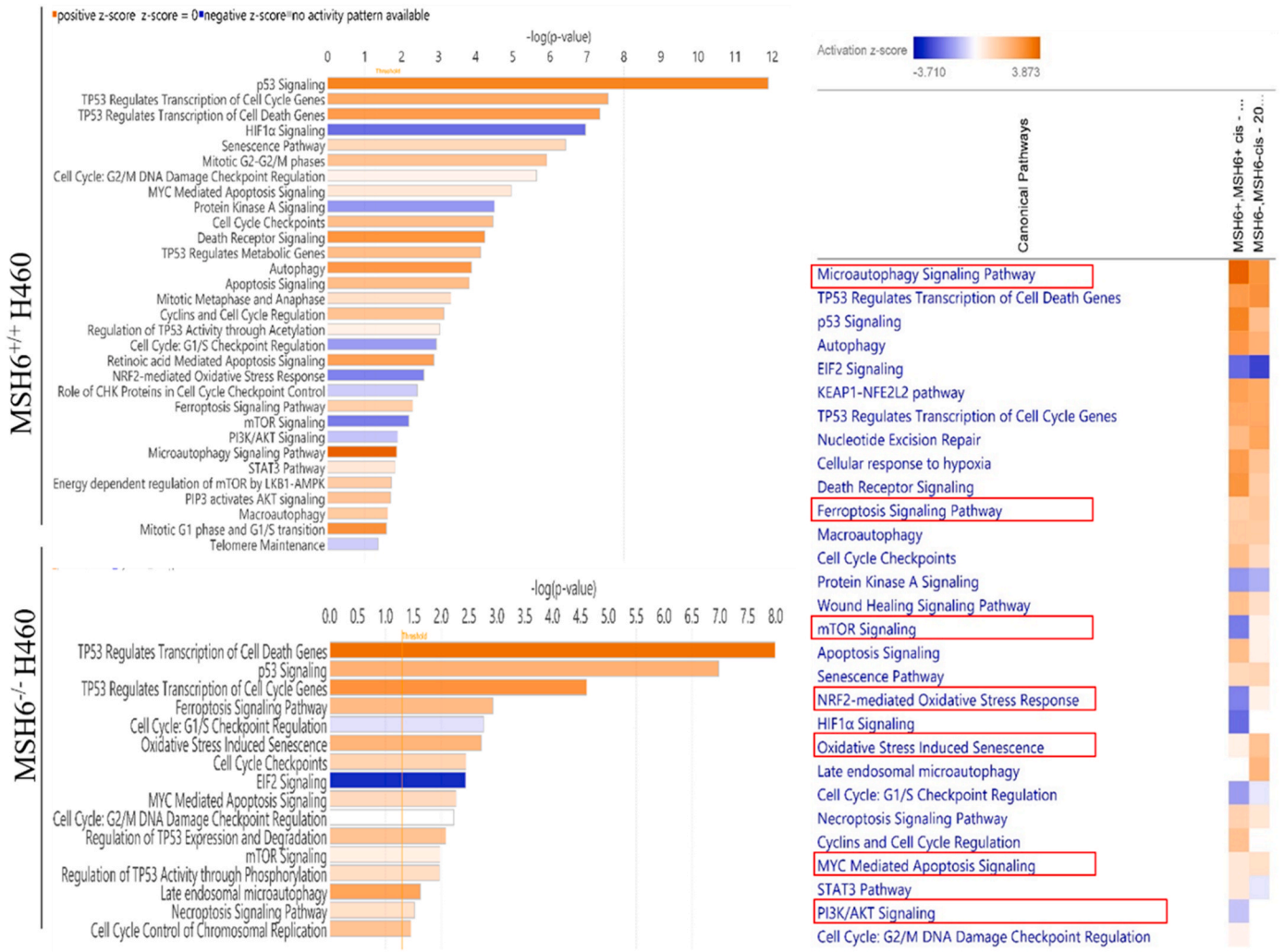

Fig. 4. Canonical pathway analysis of *MSH6*$^{-/-}$ H460 and *MSH6*$^{+/+}$ H460 cells following cisplatin exposure as assessed by microarray hybridization. The figure includes a comparative analysis of the canonical pathways between the two groups.

prominent differences through their activation z-scores belonging to various mechanisms. For *MSH6*$^{+/+}$ H460, an inhibition of the m-TOR signalling pathway was observed, which resulted in enhanced autophagy activation (Fig. 5), particularly the microautophagy signalling pathway (Fig. 4). In addition, the downregulation of NRF2-mediated oxidative stress response, HIF1α, PI3K/AKT, and protein kinase A was seen in *MSH6*$^{+/+}$ H460 cells as major differences compared to *MSH6*$^{-/-}$ H460 cells. In the absence of *MSH6*, the oxidative stress-induced senescence signalling was activated. Furthermore, we observed a changed activation of MYC-mediated apoptosis and ferroptosis displayed by the absence of *MSH6*. Especially, the altered expression of BAX and BCL-2 considerably affected MYC-mediated apoptosis. The expression of BAX increased in *MSH6*$^{-/-}$ H460 cells in response to cisplatin.

3.5. Quantitative real-time q-PCR for validating relative gene expression

To verify the microarray hybridization findings, we completed q-PCR by using top three up and down-regulated genes for the *MSH6*$^{-/-}$ and *MSH6*$^{+/+}$ H460 cell lines, respectively. All genes presented with a good Pearson correlation coefficient of microarray- and q-PCR-based expression (Fig. 6A and B). Then, specific autophagy-related genes (*PTEN, MAP1LC3B, RPTOR*, and *PIK3R1*) have been selected. These genes were previously identified through microarray analysis as being differently regulated in response to cisplatin exposure when *MSH6* is inhibited. In *MSH6*$^{-/-}$ H460 cells, *PTEN* and *MAP1LC3B* exhibited decreased expression compared to the *MSH6*$^{+/+}$ H460 cell line (Fig. 6C). In contrast, *RPTOR* and *PIK3R1* showed increased expression levels in *MSH6*$^{-/-}$ H460 cells in comparison to the wild-type cells.

3.6. Western blotting

To assess the impact of *MSH6* gene inhibition, western blotting was employed to examine the expression levels of PTEN, ILC3B–I, ILC3B-II, and RPTOR, revealing alterations in autophagy activation in both cell lines (Fig. 7). Specifically, *MSH6*$^{+/+}$ H460 and *MSH6*$^{-/-}$ H460 cancer cell lines were treated with cisplatin at IC_{50} values of 12.3 ± 0.3 μM and 4.4 ± 0.5 μM, respectively. Notably, in the absence of MSH6, the protein expression of PTEN and ILC3B–I/II decreased, whereas the expression level of RPTOR increased.

3.7. ROS detection

To identify the impact of *MSH6* gene inhibition on the defense against reactive species, following cisplatin exposure, the ROS level was determined in *MSH6*$^{+/+}$ and *MSH6*$^{-/-}$ H460 cell lines. The identified ROS level is nearly identical in each group of cell lines despite using less cisplatin concentration in the *MSH6*$^{-/-}$ H460 cancer cell lines (Fig. 8). However, the response to increased ROS levels was different for both of the cell lines analyzing the obtained microarray data. Particularly the

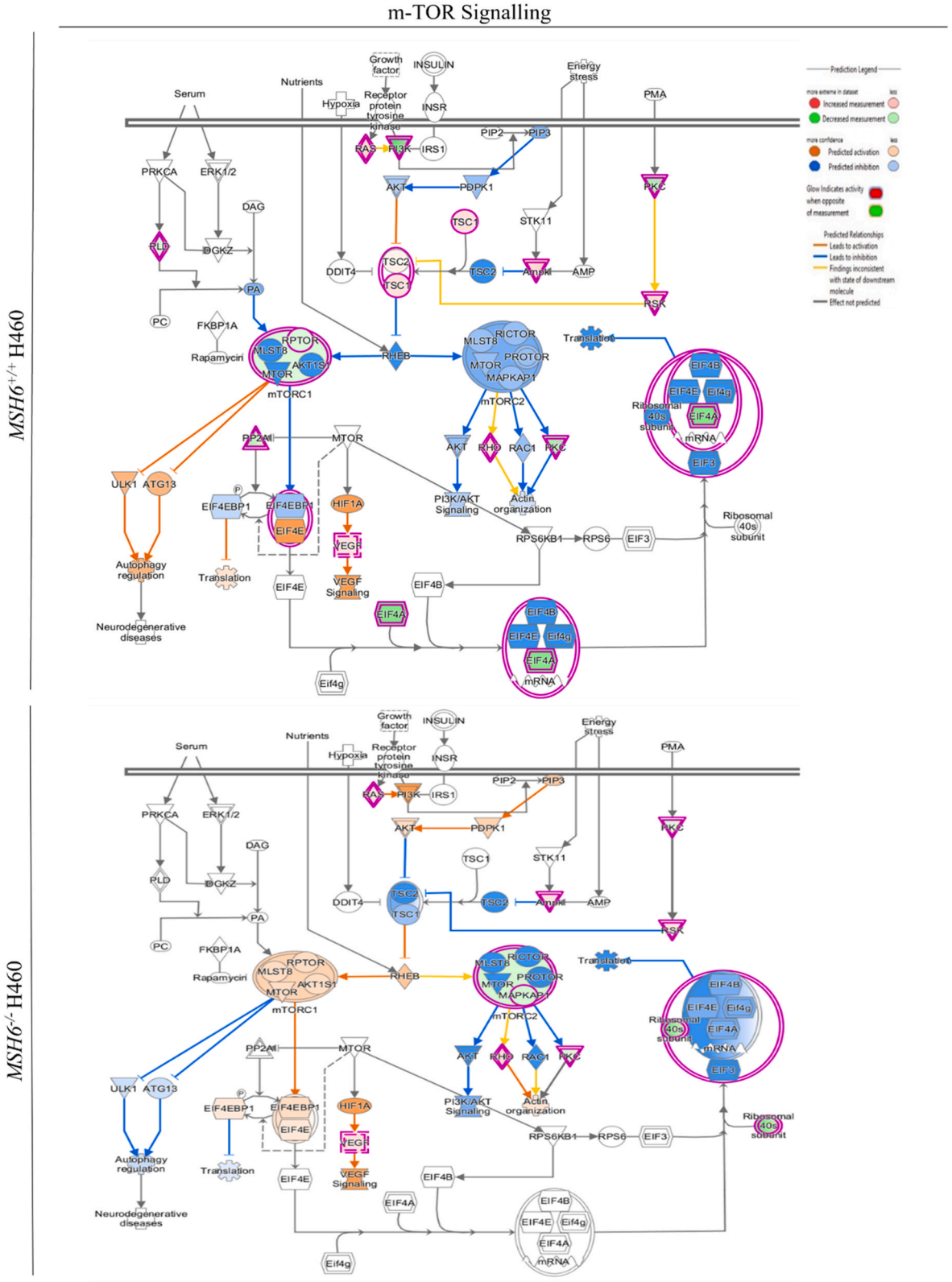

Fig. 5. Intricate cellular responses to cisplatin exposure and comparative assessment of mTOR signalling pathway alterations in *MSH6*$^{+/+}$ H460 and *MSH6*$^{-/-}$ H460 cells, respectively as assessed by microarray hybridization.

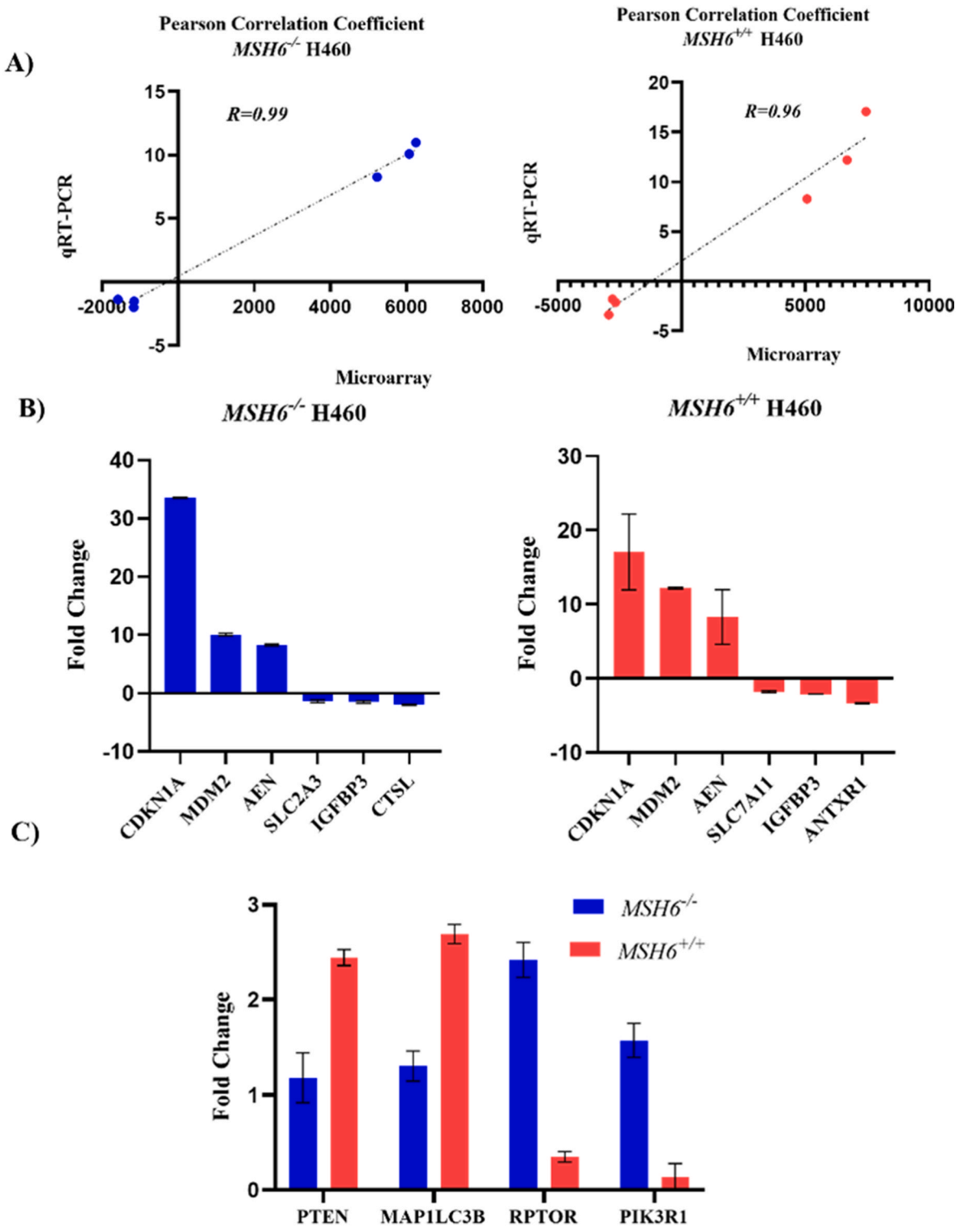

Fig. 6. mRNA expression *MSH*$^{-/-}$ *H460 wild-type and MSH*$^{+/+}$ *H460 cells:* **A)** Linear regressions and Pearson correlation coefficients for microarray hybridization and q-PCR data. **B)** Verification of the top three up- and down-regulated genes by q-PCR in these cell lines. **C)** Significant downregulation of *PTEN, MAP1LC3B,* and upregulation of *RPTOR* and *PIK3R1* genes in *MSH6*$^{-/-}$ H460 cancer cells with the opposite trend in *MSH*$^{+/+}$ H460 wild-type cells.

expression of NRF2-mediated oxidative stress response signalling pathway related genes was altered.

3.8. Cell cycle analysis

MSH6 inhibition maintained the cell cycle arrest effect of cisplatin even at low concentrations. If considering both groups, *MSH6*$^{+/+}$ and *MSH6*$^{-/-}$ H460 cancer cell lines, following exposure to different IC_{50} value of cisplatin, the effect of cisplatin on the cell cycle was nearly identical (Fig. 9A and B). Particularly, *MSH6*$^{-/-}$ H460 cells exhibited a significant S-phase arrest in response to cisplatin, indicating that the effect of the drug did not disappear even at low doses (Fig. 9C and D). These findings suggest that *MSH6* inhibition potentiates the cell cycle-arresting effects of cisplatin.

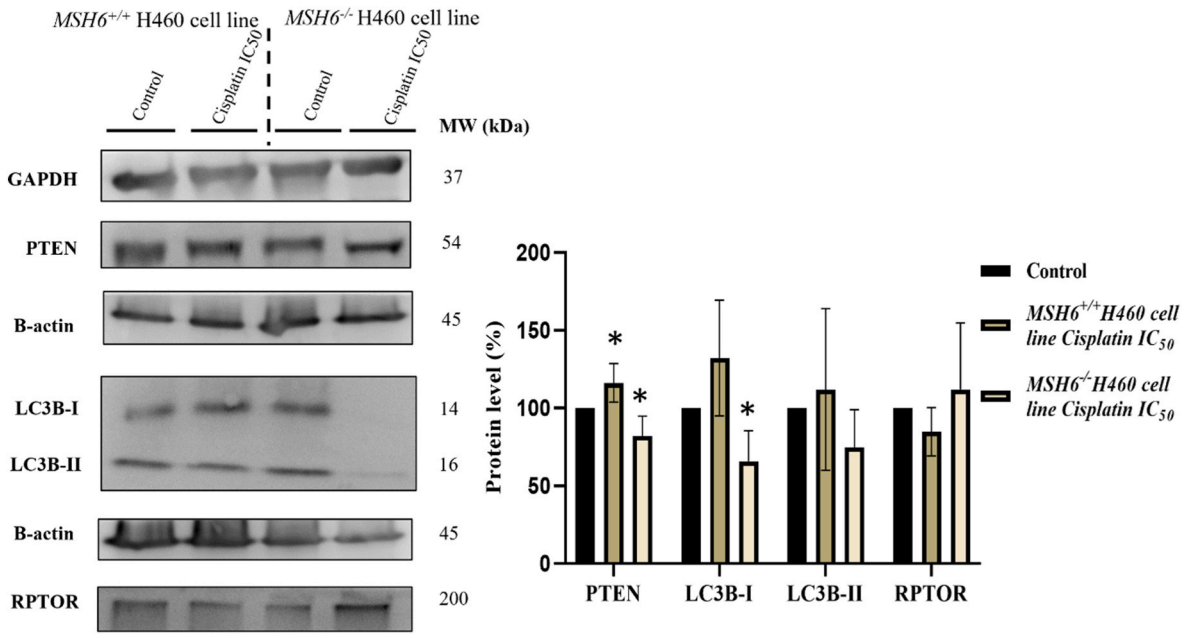

Fig. 7. Western blot analysis of PTEN, RPTOR, and ILC3B-I-II in *MSH6*$^{+/+}$ H460 and *MSH6*$^{-/-}$ H460 cells upon cisplatin exposure (* $p < 0.05$).

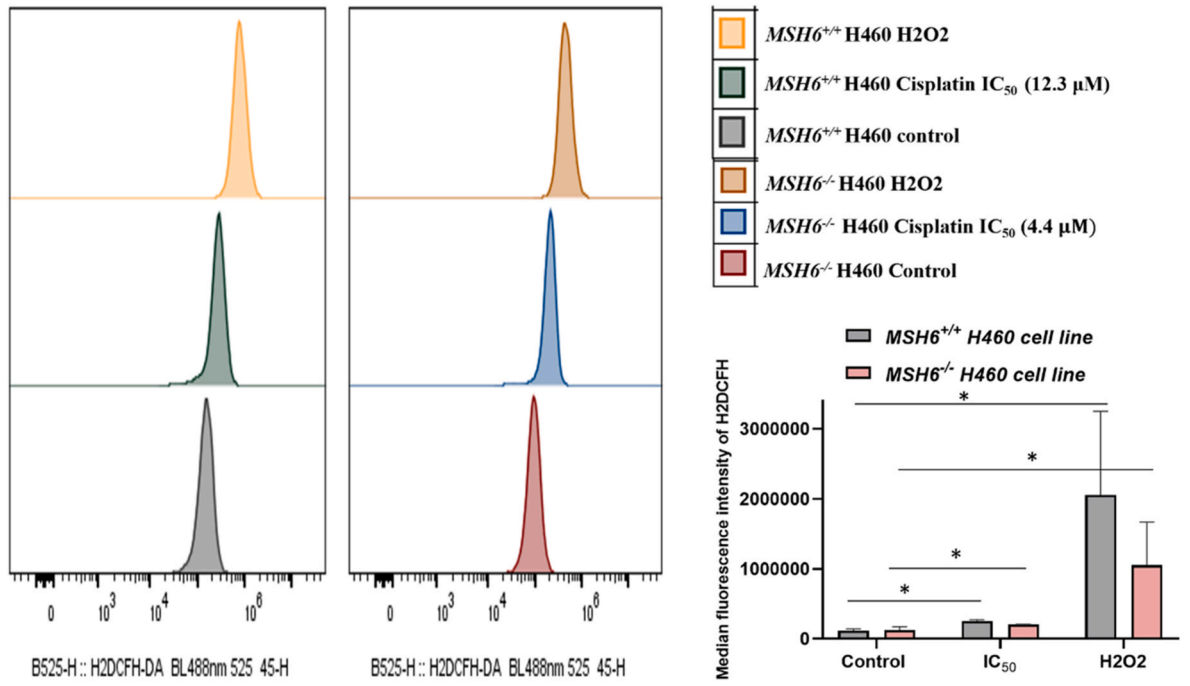

Fig. 8. ROS levels in *MSH6*$^{+/+}$ and *MSH6*$^{-/-}$ H460 cancer cell lines, respectively following cisplatin exposure (* $p < 0.05$).

3.9. Single cell electrophoresis (comet assay)

In order to assess DNA damage in *MSH6*$^{+/+}$ H460 and *MSH6*$^{-/-}$ H460 cells, we utilized the alkaline comet assay. A discernible disparity in the DNA damage profiles was observed with *MSH6*$^{-/-}$ H460 cells manifesting heightened susceptibility to cisplatin-induced damage at a concentration of 4.4 µM. In comparison, the wild-type cell line exhibited a reduced percentage of DNA damage even upon exposure to a higher cisplatin concentration (12.3 µM), as depicted in Fig. 10. This observed discrepancy suggests that the absence of *MSH6* renders cells considerably vulnerable to cisplatin.

4. Discussion

The intricacies of DNA mismatch repair (MMR) play a pivotal role in maintaining genomic stability, acting as a safeguard against deleterious consequences arising from genetic aberrations [46,47]. MMR is responsible for keeping mutation rates at an acceptably low level by correcting mistake in the genetic material [7,47]. If the mismatch repair mechanism is functionally impaired, a profound defect in repair processes ensues, leading to an escalation in the incidence of base substitutions, accumulation of DNA replication errors, and the emergence of a mutator phenotype [47]. Therefore, mismatch repair defects are known as a major reason of various hereditary disease and sporadic

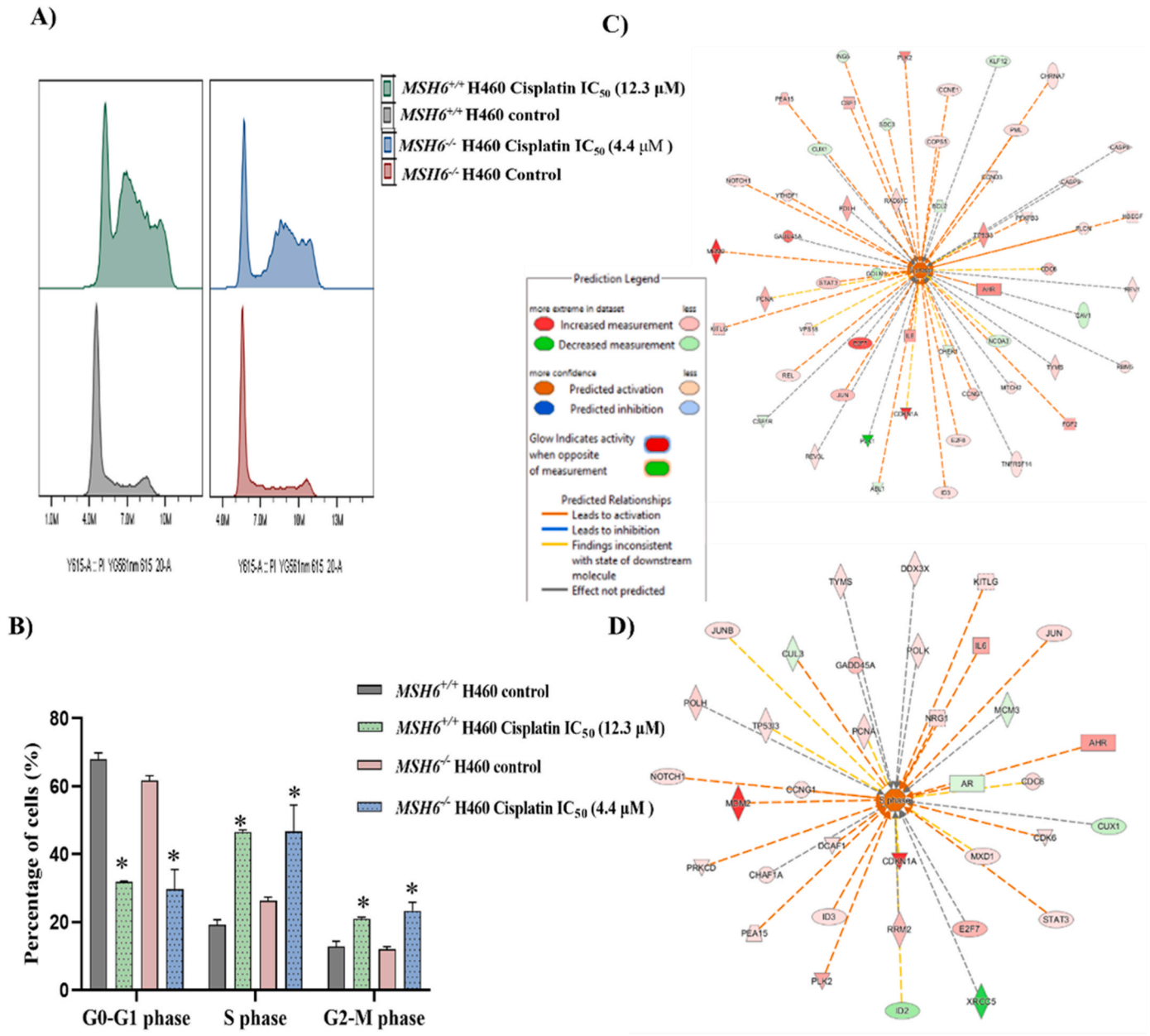

Fig. 9. Effect of MSH6 on the cisplatin-induced S-phase arrest of the cycle. A-B) Flow cytometric cell cycle analysis in *MSH6* $^{+/+}$ and *MSH6* $^{-/-}$ H460 cancer cell lines treated with IC_{50} concentration of cisplatin. Statistical significance was analyzed using Student's t-test, $*p < 0{,}05$ **C-D)** The figures obtained from microarray analysis data show the altered gene related to S-phase after cisplatin treatment for **C)** the *MSH6* $^{+/+}$ H460 cell line, and for **D)** the *MSH6* $^{-/-}$ H460 cell line, respectively.

human cancers, with colon and endometrial cancers exemplifying such manifestations due to mutations in genes encoding mismatch repair proteins [8,48,49].

Also, the augmented mutation incidence resulting from MMR deficiencies becomes a crucial factor in the development of resistance in mammalian cells against cytotoxic impacts induced by diverse DNA damaging agents [50]. The deficiency in MMR functionality amplifies mutation rates in coding regions and disrupts regulatory sequences in other genes, consequently rendering tumor cells more susceptible against the effects of therapeutic drugs [51]. Gene mutations, pre-existing in the tumor or acquired during therapy, stand out as significant contributors to drug resistance in cancer therapy [52]. This underscores the need for understanding these variations in designing rational combinational therapies to counter resistant mutations that promote tumor growth [53]. The identification of SNP profiles in distinct cancer cases enhances personalized treatment strategies and facilitates the discovery of cancer-specific biomarkers [54,55]. Our comprehensive analysis of single point mutations within the MMR genes highlights *MSH6* and *MSH3* due to the existent highest mutation numbers in hotspots site across 23 cancer types.

Additionally, we sought to pinpoint the key determinants affecting patient survival within the context of the mismatch repair (MMR) system. To achieve this, we conducted a comprehensive analysis by comparing overall survival curves across 23 distinct cancer types, considering five essential parameters. Notably, our investigation singled out *MSH6* and *EXO1* as particularly compelling targets for further exploration. Our findings revealed that heightened expression of *EXO1* was consistently associated with adverse survival outcomes across all five parameters, encompassing age, race, gender, tumor stage, and metastasis stage. Concurrently, elevated expression of *MSH6* emerged as

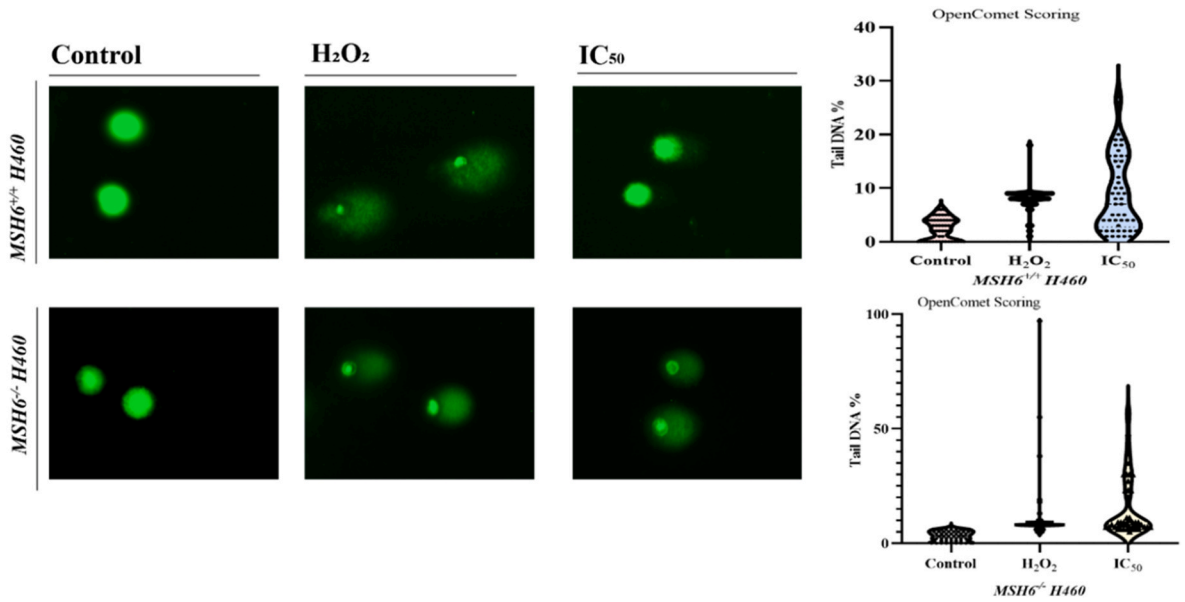

Fig. 10. Quantitative assessment of DNA damage using the alkaline comet assay following cisplatin exposure in *MSH6*$^{+/+}$ and *MSH6*$^{-/-}$ H460 cells. The 'tail DNA%' parameter was quantified based on the analysis of 50 randomly selected cells as illustrated in the accompanying violin plot.

a significant contributor to reduced survival rates, particularly within the parameters of age, race, and gender. This multifaceted exploration underscores the intricate interplay of various factors within the MMR system, emphasizing the need for a nuanced and personalized approach to prognostication in the clinical setting. The obtained data, through comprehensive analysis of overall survival and mutation patterns, provided valuable insights for future investigations and therapeutic strategies in this specific context (as shown in Supplementary Table S1 and Supplementary Fig. S1).

Additionally, if comparing different cancer types, the high expression of MSH6 led to reduced survival primarily in liver, sarcoma, pancreatic, and lung cancers. At this point, our focus directed these four cancer types. However, among these cancer types, lung cancer exhibited the highest frequency of mutations in MSH6, particularly in the coding site (as seen in Fig. 1A). In this study, we preferred *MSH6* and its association with lung cancer as focal point. Lung cancer, categorically segregated into non-small cell lung cancer (NSCLC) and small cell lung cancer, represents the predominant contributor to global cancer-related mortality [56]. Currently, molecular profiling directs the therapeutic approach for NSCLC. However, in cases where specific genetic aberrations are not identified, platinum-based anticancer regimens remain the conventional norm [57,58]. Even though an initial positive response to platinum-based chemotherapy is observed in roughly 20–40 % of advanced NSCLC patients, the durability of these responses tends to be transient [59]. After choosing *MSH6* as target, we aimed at revealing a relationship between *MSH6* and chemotherapy drug efficiency in non-small lung cancer. Obtained data showed that the absence of *MSH6* enhance drug activity for cisplatin, carboplatin, and gemcitabine. To demonstrate the reason underlying increased drug sensitivity, we focused on cisplatin and completed microarray hybridization analyses. These transcriptomic analyses illustrated the modulator role of *MSH6* between autophagy and cellular death. Canonical analyses of the *MSH6*$^{+/+}$ H460 cancer cell lines displayed a significant downregulation of the mTOR signalling pathway, PI3K/Akt, HIF1α, and NRF2-mediated oxidative stress response signalling. This signalling pathways downregulation contributed to the induction of autophagy activation in *MSH6*$^{+/+}$ H460 cells, particularly microautophagy. In the absence of *MSH6*, the response of the H460 cell line against cisplatin was completely different.

The intricate involvement of autophagy in cancer biology manifests through its dichotomous nature, wherein it exerts dual effects by either bolstering cancer cell viability (pro-survival) or facilitating cellular demise (pro-death) [26,32]. In the pro-survival role, it serves to curtail carcinogenesis by facilitating the removal of impaired mitochondria, specifically engaging in mitophagy to mitigate the production of elevated levels of reactive oxygen species (ROS) [22,28]. The complex interplay between the pro-survival role of autophagy and DNA repair mechanisms, particularly in the context of MMR, remains mystery [39]. While the exact dynamics between autophagy and MMR are not fully elucidated, scientific studies highlighted the indispensability of MMR for autophagy activation in response to certain chemotherapies, such as nucleoside analogs, 6-thioguanine (6-TG) and 5-FU [38,39,60]. Remarkably, certain scientific investigations posit that the induction of autophagy, instigated by MMR, may function as a pro-survival mechanism within neoplastic cells, impeding the apoptotic cascade triggered by chemotherapeutic interventions [39,60]. Our findings confirm this, showing that *MSH6* activated autophagy and suppressed other cell death signalling pathways. At this point, the pro-survival role of autophagy led to increased drug sensitivity by promoting cancer growth. In considering genes related to cisplatin treatment for both groups, we observed the changed activation of MYC-mediated apoptosis and ferroptosis signalling upon *MSH6* inhibition.

In the *MSH6*$^{+/+}$ H460 cell line exposed to cisplatin, the diminished activation of ferroptosis can be attributed to the concurrent downregulation of the NRF-2 signalling pathway. RF2 is known as a master regulator of redox homoeostasis [61]. Conventionally, wild-type H460 cells were expected to manifest heightened activation of genes associated with both NRF2 and ferroptosis signalling pathways in response to elevated levels of ROS induced by increased cisplatin concentrations. The observed deviation from this anticipated response challenges established paradigms. Presently, the scientific community advocates for NRF2 downregulation as a prospective therapeutic strategy in cancer treatment [61]. According to this hypothesis, the downregulation of NRF2 signalling results in augmented intracellular ROS levels within cancer cells, consequently inducing apoptosis. However, a delicate interplay between NRF2 and autophagy may exist. The escalation of ROS through NRF2 downregulation might impact the pro-survival function of autophagy. In this paradoxical scenario, our findings provide supportive evidence indicating an augmented microautophagy activation through the downregulation of the NRF-2 signalling pathway

in *MSH6*$^{+/+}$ H460 cells exposed to cisplatin. Therefore, ROS-mediated protective autophagy assumes a pivotal role, rendering cancer cells more resilient to the cytotoxic effects of cisplatin. In contrast, the dynamics shift distinctly in the presence of *MSH6* inhibition. The blocking of *MSH6* combined with cisplatin reverses the pro-survival influence of autophagy, heightening the sensitivity of the cancer cell line to drug-induced cytotoxicity. This observation suggests a promising avenue for therapeutic interventions targeting *MSH6* to augment the efficacy of cisplatin-based chemotherapy in cancer treatment.

In our investigation, we expanded our exploration to discern the repercussions of *MSH6* absence on the cell cycle and DNA damage, particularly in the context of lower cisplatin concentrations. Notably, our findings revealed that even with diminished doses of cisplatin, the *MSH6*$^{-/-}$ H460 cell line exhibited a sustained S-phase arrest effect. The observed maintenance of S-phase arrest in the absence of *MSH6* could be evidence for the utilization of lower cisplatin doses in patient treatment. This prospect is significant as it implies that the inhibition of *MSH6* expression might be a strategic approach in the future, potentially reducing side effects associated with conventional cisplatin treatments and addressing challenges related to drug resistance. Furthermore, the heightened occurrence of DNA damage in the absence of *MSH6*, even with lower doses of cisplatin, underscores the development of treatment strategies targeting *MSH6* by using cisplatin. Overall, by targeting *MSH6* in lung cancer cells, our study provides insights that could influence the development of more effective and personalized strategies in cisplatin-based cancer therapy.

CRediT authorship contribution statement

Ayşegül Varol: Writing – review & editing, Writing – original draft, Methodology, Investigation, Data curation, Conceptualization. **Joelle C. Boulos:** Methodology. **Chunmei Jin:** Methodology. **Sabine M. Klauck:** Writing – review & editing, Software, Methodology, Investigation, Data curation, Conceptualization. **Anatoly Zhitkovich:** Methodology, Investigation. **Thomas Efferth:** Writing – review & editing, Supervision, Project administration, Conceptualization.

Declaration of competing interest

The authors declare the following financial interests/personal relationships which may be considered as potential competing interests:

Aysegul VAROL reports that financial support was provided by the Turkish Government (National Education Scholarship). The other authors declare that they have no competing financial interests or personal relationships that could influence the work reported in this paper.

Data availability

The data that has been used is confidential.

Acknowledgement

We gratefully acknowledge the Microarray Unit of the Genomics and Proteomics Core Facility, German Cancer Research Center (DKFZ) (Heidelberg, Germany) for providing excellent mRNA expression profiling service. We thank Flow Cytometry Core Facility at the Institute of Molecular Biology (IMB, Mainz, Germany) for their kind training and technical support. A.V. is grateful for a stipend provided by the Turkish Government (National Education Scholarship).

Appendix A. Supplementary data

Supplementary data to this article can be found online at https://doi.org/10.1016/j.cbi.2024.111193.

The authors declare that they have no known competing financial interests or personal relationships that could have appeared to influence the work reported in this paper.

References

[1] C.K. Das, M. Mandal, D. Kögel, Pro-survival autophagy and cancer cell resistance to therapy, Cancer Metastasis Rev. 37 (2018) 749–766.
[2] M. Nikolaou, et al., The challenge of drug resistance in cancer treatment: a current overview, Clin. Exp. Metastasis 35 (2018) 309–318.
[3] X. Sui, et al., Autophagy and chemotherapy resistance: a promising therapeutic target for cancer treatment, Cell Death Dis. 4 (10) (2013) e838 e838.
[4] S.-H. Chen, J.-Y. Chang, New insights into mechanisms of cisplatin resistance: from tumor cell to microenvironment, Int. J. Mol. Sci. 20 (17) (2019) 4136.
[5] P. Hsieh, Molecular mechanisms of DNA mismatch repair, Mutat. Res. DNA Repair 486 (2) (2001) 71–87.
[6] M.A. Sanders, et al., Life without mismatch repair, bioRxiv (2021), https://doi.org/10.1101/2021.04.14.437578.
[7] T.A. Kunkel, D.A. Erie, DNA mismatch repair, Annu. Rev. Biochem. 74 (2005) 681–710.
[8] G.-M. Li, Mechanisms and functions of DNA mismatch repair, Cell Res. 18 (1) (2008) 85–98.
[9] P. Peltomäki, DNA mismatch repair and cancer, Mutat. Res. Rev. Mutat. Res. 488 (1) (2001) 77–85.
[10] D. Gupta, C.D. Heinen, The mismatch repair-dependent DNA damage response: mechanisms and implications, DNA Repair 78 (2019) 60–69.
[11] L. Dong, et al., Biomarkers for chemotherapy and drug resistance in the mismatch repair pathway, Clin. Chim. Acta (2023) 117338.
[12] R.P. Topping, J.C. Wilkinson, K.D. Scarpinato, Mismatch repair protein deficiency compromises cisplatin-induced apoptotic signaling, J. Biol. Chem. 284 (21) (2009) 14029–14039.
[13] L. Stojic, R. Brun, J. Jiricny, Mismatch repair and DNA damage signalling, DNA Repair 3 (8–9) (2004) 1091–1101.
[14] Z. Li, A.H. Pearlman, P. Hsieh, DNA mismatch repair and the DNA damage response, DNA Repair 38 (2016) 94–101.
[15] R. Fishel, Signaling mismatch repair in cancer, Nat. Med. 5 (11) (1999) 1239–1241.
[16] A. Fedier, D. Fink, Mutations in DNA mismatch repair genes: implications for DNA damage signaling and drug sensitivity, Int. J. Oncol. 24 (4) (2004) 1039–1047.
[17] D.K. Ray, et al., Unraveling the genetic code: pharmacogenomics' role in personalized drug responses, J. Pharma Insight Res. 1 (2) (2023) 15–20.
[18] E.H. Stover, et al., Biomarkers of response and resistance to DNA repair targeted therapies, Clin. Cancer Res. 22 (23) (2016) 5651–5660.
[19] C. Hunter, et al., A hypermutation phenotype and somatic MSH6 mutations in recurrent human malignant gliomas after alkylator chemotherapy, Cancer Res. 66 (8) (2006) 3987–3991.
[20] S. Yip, et al., MSH6 mutations arise in glioblastomas during temozolomide therapy and mediate temozolomide resistance, Clin. Cancer Res. 15 (14) (2009) 4622–4629.
[21] C. Xie, et al., Association of MSH6 mutation with glioma susceptibility, drug resistance and progression, Mol. Clin. Oncol. 5 (2) (2016) 236–240.
[22] B.M. Gąsiorkiewicz, et al., Autophagy modulating agents as chemosensitizers for cisplatin therapy in cancer, Invest. N. Drugs 39 (2) (2021) 538–563.
[23] E.-L. Eskelinen, The dual role of autophagy in cancer, Curr. Opin. Pharmacol. 11 (4) (2011) 294–300.
[24] K. Dalby, et al., Targeting the pro-death and pro-survival functions of autophagy as novel therapeutic strategies in cancer, Autophagy 6 (3) (2010) 322–329.
[25] S.S. Singh, et al., Dual role of autophagy in hallmarks of cancer, Oncogene 37 (9) (2018) 1142–1158.
[26] M. Russo, G.L. Russo, Autophagy inducers in cancer, Biochem. Pharmacol. 153 (2018) 51–61.
[27] A. Kumar, U.K. Singh, A. Chaudhary, Targeting autophagy to overcome drug resistance in cancer therapy, Future Med. Chem. 7 (12) (2015) 1535–1542.
[28] C.W. Yun, S.H. Lee, The roles of autophagy in cancer, Int. J. Mol. Sci. 19 (11) (2018) 3466.
[29] A. Eisenberg-Lerner, A. Kimchi, The paradox of autophagy and its implication in cancer etiology and therapy, Apoptosis 14 (2009) 376–391.
[30] L. Bao, et al., Induction of autophagy contributes to cisplatin resistance in human ovarian cancer cells, Mol. Med. Rep. 11 (1) (2015) 91–98.
[31] B. Sirichanchuen, T. Pengsuparp, P. Chanvorachote, Long-term cisplatin exposure impairs autophagy and causes cisplatin resistance in human lung cancer cells, Mol. Cell. Biochem. 364 (2012) 11–18.
[32] S. Chen, et al., Autophagy is a therapeutic target in anticancer drug resistance, Biochim. Biophys. Acta Rev. Cancer 1806 (2) (2010) 220–229.
[33] D. Liu, et al., Inhibition of autophagy by 3-MA potentiates cisplatin-induced apoptosis in esophageal squamous cell carcinoma cells, Med. Oncol. 28 (2011) 105–111.
[34] J. Li, et al., Inhibition of autophagy by 3-MA enhances the effect of 5-FU-induced apoptosis in colon cancer cells, Ann. Surg Oncol. 16 (2009) 761–771.
[35] L. Galluzzi, et al., Autophagy in malignant transformation and cancer progression, EMBO J. 34 (7) (2015) 856–880.
[36] D. Zhang, et al., The interplay between DNA repair and autophagy in cancer therapy, Cancer Biol. Ther. 16 (7) (2015) 1005–1013.
[37] X. Zeng, et al., DNA mismatch repair initiates 6-thioguanine–induced autophagy through p53 activation in human tumor cells, Clin. Cancer Res. 13 (4) (2007) 1315–1321.

[38] X. Zeng, T.J. Kinsella, BNIP3 is essential for mediating 6-thioguanine-and 5-fluorouracil-induced autophagy following DNA mismatch repair processing, Cell Res. 20 (6) (2010) 665–675.
[39] L.R. Gomes, C.F. Menck, G.S. Leandro, Autophagy roles in the modulation of DNA repair pathways, Int. J. Mol. Sci. 18 (11) (2017) 2351.
[40] E. Cerami, et al., The cBio cancer genomics portal: an open platform for exploring multidimensional cancer genomics data, Cancer Discov. 2 (5) (2012) 401–404.
[41] J. Gao, et al., Integrative analysis of complex cancer genomics and clinical profiles using the cBioPortal, Sci. Signal. 6 (269) (2013) pl1-pl1.
[42] M.F. Reynolds, et al., Rapid DNA double-strand breaks resulting from processing of Cr-DNA cross-links by both MutS dimers, Cancer Res. 69 (3) (2009) 1071–1079.
[43] J. O'brien, et al., Investigation of the Alamar Blue (resazurin) fluorescent dye for the assessment of mammalian cell cytotoxicity, Eur. J. Biochem. 267 (17) (2000) 5421–5426.
[44] K.J. Livak, T.D. Schmittgen, Analysis of relative gene expression data using real-time quantitative PCR and the 2− ΔΔCT method, Methods 25 (4) (2001) 402–408.
[45] B.M. Gyori, et al., OpenComet: an automated tool for comet assay image analysis, Redox Biol. 2 (2014) 457–465.
[46] J. Zhou, et al., Evolving insights: how DNA repair pathways impact cancer evolution, Cancer Biol. Med. 17 (4) (2020) 805.
[47] B.D. Harfe, S. Jinks-Robertson, DNA mismatch repair and genetic instability, Annu. Rev. Genet. 34 (1) (2000) 359–399.
[48] P. Modrich, R. Lahue, Mismatch repair in replication fidelity, genetic recombination, and cancer biology, Annu. Rev. Biochem. 65 (1) (1996) 101–133.
[49] K. Tamura, et al., Genetic and genomic basis of the mismatch repair system involved in Lynch syndrome, Int. J. Clin. Oncol. 24 (9) (2019) 999–1011.
[50] R.R. Iyer, et al., DNA mismatch repair: functions and mechanisms, Chem. Rev. 106 (2) (2006) 302–323.
[51] M.M. de las Alas, et al., Loss of DNA mismatch repair: effects on the rate of mutation to drug resistance, J. Natl. Cancer Inst. 89 (20) (1997) 1537–1541.
[52] N. Chatterjee, T.G. Bivona, Polytherapy and targeted cancer drug resistance, Trends in cancer 5 (3) (2019) 170–182.
[53] N.C. Turner, J.S. Reis-Filho, Genetic heterogeneity and cancer drug resistance, Lancet Oncol. 13 (4) (2012) e178–e185.
[54] J.J. McCarthy, R. Hilfiker, The use of single-nucleotide polymorphism maps in pharmacogenomics, Nat. Biotechnol. 18 (5) (2000) 505–508.
[55] C. Rodríguez-Antona, M. Taron, Pharmacogenomic biomarkers for personalized cancer treatment, J. Intern. Med. 277 (2) (2015) 201–217.
[56] R.L. Siegel, et al., Cancer statistics, 2021, Ca-Cancer J. Clin. 71 (1) (2021) 7–33.
[57] R. Ruiz-Cordero, W.P. Devine, Targeted therapy and checkpoint immunotherapy in lung cancer, Surgical pathology clinics 13 (1) (2020) 17–33.
[58] F. Yang, et al., Insight into autophagy in platinum resistance of cancer, Int. J. Clin. Oncol. 28 (3) (2023) 354–362.
[59] M. Circu, et al., Modulating lysosomal function through lysosome membrane permeabilization or autophagy suppression restores sensitivity to cisplatin in refractory non-small-cell lung cancer cells, PLoS One 12 (9) (2017) e0184922.
[60] X. Zeng, T.J. Kinsella, A novel role for DNA mismatch repair and the autophagic processing of chemotherapy drugs in human tumor cells, Autophagy 3 (4) (2007) 368–370.
[61] P. Basak, et al., Perspectives of the Nrf-2 signaling pathway in cancer progression and therapy, Toxicol Rep 4 (2017) 306–318.

4.3. Comprehensive transcriptomic analysis in wild-type and ATM knockout lung cancer cells: Influence of cisplatin on oxidative stress-induced senescence

Contribution Statement

This article presents a comprehensive transcriptomic analysis demonstrating the influence of ATM gene knockout on cisplatin sensitivity and cell death pathways in lung cancer cells. The study shows that loss of ATM function enhances cisplatin-induced cytotoxicity by activating alternative cell death mechanisms such as oxidative stress-induced senescence and necroptosis, with a key regulatory interplay involving NRF2 signaling. These results suggest that targeting ATM and associated pathways could provide innovative strategies to overcome drug resistance and advance personalized cancer treatments tailored to individual tumor profiles.

Authorship contribution: Ayşegül Varol: Writing – review & editing, Writing – original draft, Methodology, Investigation, Data curation, Conceptualization. **Sabine M. Klauck:** Writing – review & editing, Software, Methodology, Investigation, Data curation, Conceptualization. **Susan P. Lees-Miller**: Methodology, Investigation. **Thomas Efferth:** Writing – review & editing, Supervision, Project administration, Conceptualization.

Publication Information

Title: *Comprehensive transcriptomic analysis in wild-type and ATM knockout lung cancer cells: Influence of cisplatin on oxidative stress-induced senescence (***(DOI:** https://doi.org/10.1016/j.cbi.2025.111563)

Journal: *Chemico-Biological Interactions*

Volume: 418

Article Number: 111563

Year: 2025

Chemico-Biological Interactions 418 (2025) 111563

Contents lists available at ScienceDirect

Chemico-Biological Interactions

journal homepage: www.elsevier.com/locate/chembioint

Research paper

Comprehensive transcriptomic analysis in wild-type and ATM knockout lung cancer cells: Influence of cisplatin on oxidative stress-induced senescence

Ayşegül Varol [a], Sabine M. Klauck [b], Susan P. Lees-Miller [c], Thomas Efferth [a,*]

[a] Department of Pharmaceutical Biology, Institute of Pharmaceutical and Biomedical Sciences, Johannes Gutenberg University-Mainz, 55128, Mainz, Germany
[b] Division of Cancer Genome Research, German Cancer Research Center (DKFZ) Heidelberg, National Center for Tumor Diseases (NCT), NCT Heidelberg, a partnership between DKFZ and University Hospital Heidelberg, 69120, Heidelberg, Germany
[c] Department of Biochemistry and Molecular Biology, Robson DNA Science Centre, Charbonneau Cancer Institute, Cumming School of Medicine, University of Calgary, 3330 Hospital Drive NW, Calgary, AB, T2N 1N4, Canada

ARTICLE INFO

Keywords:
Chemotherapy resistance
Personalized cancer therapy
Prognostic biomarkers signal transduction
Survival analysis
Transcriptomics

ABSTRACT

Genetic mutations and impaired DNA repair mechanisms in cancer not only facilitate tumor progression but also reduce the effectiveness of chemotherapeutic agents, particularly cisplatin. Combination therapy has emerged as a promising strategy to overcome resistance. Comprehensive transcriptomic analyses, supported by integrated comparative bioinformatics and experimental approaches, are essential for identifying biomarkers and novel therapeutic targets underlying drug resistance. In this study, we performed overall survival and mutation analyses, examining 23 double-strand break repair proteins across more than 7500 tumors spanning 23 distinct cancer types. Our findings identify ATM (ataxia-telangiectasia mutated) as a key protein with the highest mutation frequency.

Using CRISPR/Cas9, we investigated the effects of ATM mutations on signalling pathways that influence the cellular response to cisplatin. ATM knockout enhanced cisplatin cytotoxicity by activating alternative cell death pathways, including oxidative stress-induced senescence and necroptosis. Microarray analysis revealed a regulatory interplay between ATM and NRF2 in the activation of oxidative stress-induced senescence. Specifically, ATM knockout promoted senescence by increasing reactive oxygen species (ROS) accumulation and down-regulating NRF2 expression.

To enhance combination therapy, integrating genetic profiling with advanced tools such as CRISPR/Cas9 to target oxidative stress-induced senescence may provide innovative strategies to overcome drug resistance, thereby advancing personalized cancer treatment. These approaches lay the foundation for the development of personalized cancer therapies tailored to the unique mutational landscape of individual patients, offering promising prospects for improving treatment outcomes.

1. Introduction

DNA damage is an inevitable consequence of cellular metabolism, resulting from both endogenous factors such as reactive oxygen species (ROS) and exogenous factors such as ultraviolet (UV) radiation [1–3]. This damage can manifest in single-strand breaks (SSBs) and double-strand breaks (DSBs), which are among the most detrimental forms of DNA lesions [4,5]. To maintain genomic stability and preserve cellular function, mammalian cells employ a complex DNA damage response (DDR), which halts the cell cycle and initiates repair mechanisms to restore the integrity of the genome [5,6]. However, if these repair mechanisms fail or are overwhelmed, mutations can accumulate,

Abbreviations: ATM, Ataxia-telangiectasia mutated; cDNA, Complementary DNA; DRM, DNA repair mechanism; DDR, DNA damage response; DSB, Double-strand breaks; H_2DCFH-DA, 2′7-Dichlorodihydrofluorescein diacetate; IPA, Ingenuity Pathway Analysis; NRF2, Nuclear factor (erythroid-derived 2)-like 2; PI, Propidium iodide; PBS, Phosphate-buffered saline; PS, Phosphatidyl serine; ROS, Reactive oxygen species; SA-β-gal, Senescence-associated β-galactosidase; SSB, Single-strand breaks; TCGA, The Cancer Genome Atlas; UV, Ultraviolet radiation.

* Corresponding author.
E-mail address: efferth@uni-mainz.de (T. Efferth).

https://doi.org/10.1016/j.cbi.2025.111563
Received 28 February 2025; Received in revised form 30 April 2025; Accepted 15 May 2025
Available online 16 May 2025

leading to cellular dysfunction and contributing to the development of age-related diseases and cancer [7]. Cancer progression is driven by the accumulation of genetic mutations, as well as the impairment of key defence systems, including DNA repair mechanisms and cellular death pathways [8]. While the individual impact of these mutations may be minimal, their cumulative effects can significantly alter cellular function, making them crucial drivers of cancer initiation and progression [8]. Moreover, the presence of mutations leads to resistance to cancer therapies, particularly chemotherapeutic agents [9].

Cisplatin resistance is one of the most common challenges encountered in cancer chemotherapy [10]. Cisplatin induces cell cycle arrest and apoptosis by binding to DNA and forming crosslinks [11,12]. However, its effectiveness is often limited by drug resistance, which can result from mutations in drug target sites or changes in related cellular pathways [13]. Especially, acquired mutations in DNA repair and cell death genes can reduce cisplatin sensitivity, prompting the exploration of combination therapy as a strategy to overcome resistance. Successful combination therapy requires identifying biomarkers to develop drugs that bypass resistance mechanisms and improve treatment outcomes.

An integrated approach that combines biomarker expression profiling with genetic polymorphism analysis is crucial for accurately assessing a patient's drug resistance status. The impact of specific biomarkers can vary depending on tumor type, stage, metastasis, and patient-specific factors such as age, gender, and genetic background. To avoid the identification of conflicting or unreliable biomarkers, a comprehensive bioinformatic analysis is necessary. In this regard, we conducted a thorough investigation into the mutations and survival data of 23 proteins involved in the double-strand break DNA repair (DSB) mechanism across 23 distinct cancer types. Using theedistinct parameters, we identified mutation hotspots in protein-coding regions, with particular focus on missense, nonsense, and frameshift mutations. Our analysis revealed ATM (ataxia-telangiectasia mutated) as a key protein with the highest mutation frequency, particularly missense mutations, which varied across different cancer types. Notably, these mutations were observed in a subset of lung cancer patient samples, positioning ATM as a potentialcandidate for a predictive biomarker in lung cancer.

Additionally, we explored the effect of 23 distinct DNA repair proteins on survival across multiple cancer types by encompassing more than 7500 patient samples. We found that several biomarkers with high expression levels were associated with poor survival outcomes, particularly in lung, kidney, breast, and liver cancers. These findings highlight the need for personalized therapeutic approaches that take into account the unique mutational and expression profiles of individual patients.

The advent of CRISPR/Cas9 gene-editing technology has garnered significant attention in the scientific community for its potential to manipulate the genome in cancer cells [14]. The CRISPR/Cas9 platform provides a powerful tool to investigate the functional roles of specific genes or mutations in the context of cancer development [15–17]. By utilizing CRISPR/Cas9-based ATM knockout lung cancer cells, we assessed how targeting ATM influences cisplatin sensitivity. In the presence of ATM, cell death pathways, particularly apoptosis and autophagy, are activated in response to cisplatin exposure. However, the activation of cell death pathways was observed at higher doses of cisplatin. This suggests that existing mutations in ATM could restrict the proper response of these signalling pathways, leading to reduced sensitivity to cisplatin.

In contrast, the knockout of ATM through combination therapy has activated alternative cell death pathways. In particular, oxidative stress-induced senescence and necroptosis have been identified as key mechanisms responsible for the increased cisplatin sensitivity observed by ATM knockout. Oxidative stress, which results from an imbalance between the production of reactive oxygen species (ROS) and the antioxidant defence system, can trigger senescence, a stable arrest of the cell cycle that plays an important role in tumor suppression. Focusing on the genes or pathways that drive oxidative stress-induced cellular senescence could provide new opportunities for inhibiting cancer progression and overcoming drug resistance [18].

In our study, we performed microarray hybridization and bioinformatic analyses to uncover the interaction between ATM and nuclear factor (erythroid-derived 2)-like 2 (NRF2), a key regulator of the antioxidant response. Our findings are consistent with the existing knowledge in the literature [19,20]. Additionally, it demonstrates that senescence induced by oxidative damage is regulated through NRF2 and ATM signalling pathways. The suppression of NRF2, either directly or indirectly, significantly promoted cellular senescence, highlighting its potential as a therapeutic target for overcoming cisplatin resistance [21].

Thus, understanding the complex interplay between DNA repair, cell death pathways, and drug resistance mechanisms is essential for developing more effective cancer therapies. The integration of novel technologies such as CRISPR/Cas9 with biomarker profiling offers exciting prospects for personalized medicine, contributing ultimately to improve outcomes for those with cancer.

2. Material and methods

2.1. Determination of mutational hotspot sites

We determined the mutational hotspot sites in 23 genes involved in DSB. The UniProt database and cBioPortal, an open-access platform for exploring cancer genomics data, open the opportunity to detect the domains for each gene [22,23]. The sequence data of more than 7500 tumor patients were classified into three categories: missense mutations, nonsense mutations, and frameshift mutations.

Initially, data were downloaded from the open-access databases on the cBioPortal website (https://www.cbioportal.org/) by entering 23 different cancer studies and gene names. Subsequently, a more in-depth analysis was performed separately for each of the 23 genes. Rather than focusing on the total number of mutations found for each gene, the analysis specifically identified the number of missense, nonsense, and frameshift mutations in the domain regions. After determining the total number of mutations in the different domain regions, each gene was compared, and regions with a high density of mutations were identified. Supplementary Table S1 presents a representative example of the mutation analysis of the ATM gene obtained via the cBioportal platform. Our focus directed to those genes with the highest mutational hotspots, and *ATM* has been selected.

2.2. Overall survival analysis

To assess the survival probability of cancer patients associated with the mRNA expression of 23 DSB genes, we utilized the Cancer Genome Atlas (TCGA) dataset obtained from cBioportal (https://www.cbioportal.org; accessed between 2020 and 2021) as our primary data source. The TCGA dataset provided comprehensive information on 23 different cancer types, encompassing the expression levels of 23 distinct DSB genes, as well as five pathoclinical key parameters: age, race, gender, metastasis, and tumor stage. Combining multiple existing cohorts into a single, unified dataset can significantly support the identification and validation of reliable prognostic biomarkers [24]. For this purpose, we have performed survival analyses using the Kaplan-Meier (KM) plotter, a platform for performing survival analysis using transcriptomic data of large patient cohorts.

At the outset of the analysis, separate Excel files were generated for each parameter using data obtained from cBioPortal. Within these files, patient outcomes were encoded as "1" for surviving patients and "0" for deceased patients. Regarding the age parameter, each of the seven age groups (10–20, 20–30, 30–40, 40–50, 50–60, 60–70, 70–80) was analyzed separately. Subsequently, we conducted Kaplan-Meier survival analyses for each DSB gene (as stated in a previous [25]), utilizing the SPSS program (IBM Corp. Released 2015. IBM SPSS Statistics for Windows, Version 23.0. Armonk, NY: IBM Corp).

Table 1
Selected primer for qPCR experiment.

Gene Symbol	Forward Primer	Reverse Primer
GAPDH	TTCGACAGTCAGCCGCATCT	CCGACCTTCACCTTCCCCAT
CDKN2A	CTGCCCAACGCACCGAATAG	CCACCAGCGTGTCCAGGAAG
IL8	CTTTCCACCCCAAATTTATCAAAG	CAGACAGAGCTCTCTTCCATCAGA
IL6	CCGGGAACGAAAGAGAAGCT	GCGCTTGTGGAGAAGGAGTT

To determine the statistical significance, we employed the "log-rank" test statistics. By applying this statistical test, we identified survival curves that exhibited noteworthy differences. Specifically, we considered survival curves with a *p*-value below 0.05 as statistically significant. We selected the cancer types most affected by genes responsible for poor patient survival.

2.3. Knockout of ATM using CRISPR/nCas9-mediated genome editing

Gene knockout of ATM was conducted as previously described (performed by Dr. Yaping Yu at the Center for Genome Engineering, Cumming School of Medicine, University of Calgary) [26]. The CRISPR-Cas9 system was employed to delete ATM using the pSpCas9 (BB)-2A-GFP (pX458) plasmid, incorporating a short guide RNA sequence targeting exon 9 of ATM (5′-TACGTTCCCCATGTCGCTGT-3′). All short guide oligonucleotides were synthesized, annealed, and inserted into the pX458 plasmid, with successful cloning verified through DNA sequencing at the University of Calgary's DNA laboratory.

Forty-eight hours following transfection of A549 CRISPR-ATM cells, the cells were collected, and genomic DNA was extracted utilizing the KAPA Express Extract Kit (Kapa Biosystems) in accordance with the manufacturer's guidelines. PCR was performed to amplify genomic DNA fragments of ATM surrounding the short guide RNA target site.

2.4. Cytotoxicity assay

To detect the cytotoxicity of anticancer drugs, we used the resazurin reduction assay, which measures the cellular metabolic activity rather than direct cytotoxicity and is influenced by stress responses such as senescence or growth arrest, which may not involve immediate apoptosis or necrosis [27,28]. Specifically, the impact of cisplatin, carboplatin, and 5-fluorouracil was investigated over a concentration range of 0.003–100 μM, targeting both $ATM^{+/+}$ A549 and $ATM^{-/-}$ A549 cancer cell lines. To execute the experiments, the cells were seeded into 96-well plates, and upon reaching 70 %–80 % confluence, they were treated with the drugs for 72 h. Subsequently, the cells were incubated for 4 h with 20 μL resazurin (Sigma-Aldrich, Taufkirchen, Germany) per well, diluted in double-distilled water (ddH_2O). The fluorescence was detected using an excitation wavelength of 544 nm and an emission wavelength of 590 nm with the Infinite M2000 Pro™ plate reader (Tecan, Crailsheim, Germany). IC_{50} values were calculated using nonlinear regression analysis in Microsoft Excel.

2.5. Microarray-based expression profiling for predicting canonical pathways

To investigate the transcriptomic landscape of *ATM*-driven gene regulation in A549 cells, we performed microarray hybridization expression analyses. Both $ATM^{+/+}$ and $ATM^{-/-}$ A549 cells were exposed to IC_{50} concentrations of cisplatin (9.91 μM and 3.36 μM, respectively) for 24 h. After treatment, total RNA was extracted using the InviTrap® Spin Universal RNA Mini Kit from Invitek Molecular (Berlin, Germany). The extracted RNA was then converted to complementary DNA (cDNA), labeled, and hybridized onto Affymetrix GeneChips® using the human ClariomS™ assay (Affymetrix, Santa Clara, CA, USA) at the Genomics and Proteomics Core Facility of the German Cancer Research Center (DKFZ, Heidelberg, Germany). The gene expression was analyzed with Chipster software (version 3.16.3, https://chipster.csc.fi/) (accessed on June 21, 2020), focusing on differential expression and statistical significance determined by the empirical Bayes *t*-test ($p < 0.05$).

Chipster software is an open-source software used for bioinformatics analyses. Specifically, Chipster can be employed for the comparison of data derived from different databases. For instance, it can be used for differential expression analysis to compare gene expression levels. In our study, we initially prepared data from $ATM^{+/+}$ and $ATM^{-/-}$ A549 cells without cisplatin treatment using the Chipster software and visualized the results through the IPA (Ingenuity Pathway Analysis) software from Ingenuity Systems (Redwood City, CA, USA, content version 51963813, released on July 31, 2023) (Fig. 4). Subsequently, we compared the data from cisplatin-treated $ATM^{+/+}$ A549 cells with that of wild-type A549 cells not exposed to any treatment using the Chipster software and uploaded IPA software to visualized (corresponding to the $ATM^{+/+}$ A549 data shown in Fig. 5). The same analysis was also applied to compare cisplatin-treated $ATM^{-/-}$ A549 cells with untreated counterparts (corresponding to the $ATM^{-/-}$ A549 data shown in Fig. 5). We compared the impact of cisplatin on these cell lines by generating gene expression-based heatmaps and analyzed canonical signalling pathways using activation z-scores and p-values as key metrics.

2.6. Quantitative real-time q-PCR for validating relative gene expression

After performing transcriptomic analyses, our objective was to validate the microarray hybridization findings through q-PCR analysis. For this purpose, we designed primers using the Primer BLAST online tool (https://www.ncbi.nlm.nih.gov/nucleotide/, accessed in 2023) and obtained them from Eurofins Genomics (Ebersberg, Germany). The specific primers selected for the study are listed in Table 1. The expression of *GAPDH* was selected as an internal control.

Subsequently, we treated $ATM^{+/+}$ and $ATM^{-/-}$ A549 cancer cells with cisplatin concentrations equivalent to their respective IC_{50} values of 9,91 μM and 3,36 μM, respectively, for 24 h. Total RNA extraction was performed using the InviTrap® Spin Universal RNA Mini Kit (Invitek Molecular, Berlin, Germany), followed by mRNA to cDNA conversion using the LunaScript® RT SuperMix Kit cDNA Synthesis Kit (New England Bio Labs, Darmstadt, Germany).

For gene amplification, we utilized the EvaGreen master mix (5 × Hot Start Taq EvaGreen® q-PCR Mix (no ROX); Axon Labortechnik, Kaiserslautern, Germany) following the manufacturer's instructions. Q-PCR was conducted on a CFX384TM instrument (Bio-Rad, Munich, Germany) using a 38-well plate and running 40 cycles. The PCR run conditions included an initial denaturation phase at 95 °C for 15 s, followed by a gradient annealing step ranging from 62 °C to 47 °C for 30 s, and finally, an elongation step at 72 °C for 1 min. To determine the fold-change in gene expression, we employed the comparative Cq (2-ΔΔCq) method [29].

2.7. Cell cycle analysis

Cells were seeded at a density of 3×10^5 cells per well in 6-well plates and treated with distinct cisplatin concentrations (9.91 μM for $ATM^{+/+}$ A549 cells and 3.36 μM for $ATM^{-/-}$ A549 cells) for 24 h. Following treatment, both cell lines were fixed with ethanol and stored at −20 °C for an additional 24 h. Fixed samples were then subjected to centrifugation (4000 rpm, 10 min) and re-suspended in 500 μL of cold

PBS supplemented with 20 μg/mL RNase (Roche Diagnostics, Mannheim, Germany). Then, we used 50 μg/mL propidium iodide (PI) (Sigma-Aldrich, Darmstadt, Germany) for staining. Stained samples were measured using a NovoCyte Quanteon flow cytometer (Agilent) and data analysis was performed using FlowJo software (version 10.8.1) (BD Life Sciences). For each sample, 10,000 cells were recorded. The gating was performed by forward and side scatter properties (FSC–H/SSC-H), and further gating for single cells (PI-YG561nm 615/20-A/PI-YG561nm 615/20-H) in a linear manner was applied to remove doublets or debris. PI staining was detected using a 561 nm laser and 615/20BP filter. Each experimental procedure was independently replicated three times. Data analysis was further completed using GraphPad Prism 6 (La Jolla, CA, USA) software for presentation and interpretation.

2.8. Detection of apoptosis

Apoptotic and necrotic cell populations were assessed and quantified using Annexin V/PI staining, following established protocols [30]. This methodology was recently described in detail in our prior study [31]. Annexin V is a calcium-dependent phospholipid-binding protein that interacts specifically with phosphatidylserine (PS). During the initiation of apoptosis, PS translocates from the inner leaflet of the plasma membrane to the extracellular surface. Propidium iodide (PI), a membrane-impermeable dye, is excluded by viable or early apoptotic cells with intact membranes, but it intercalates with DNA in cells undergoing late apoptosis or necrosis, emitting red fluorescence.

$ATM^{+/+}$ A549 and $ATM^{-/-}$ A549 cancer cells were exposed to varying concentrations of cisplatin (9.91 μM and 3.36 μM, respectively) for 72 h. Subsequently, the cells were stained with Annexin V and PI (BioVersion/Biocat, Heidelberg, Germany) under dark conditions and analyzed using a BD Accuri™ C6 Flow Cytometer. Each experiment was independently conducted in triplicate to ensure reproducibility.

2.9. Detection of reactive oxygen species

We investigated the response of $ATM^{+/+}$ and $ATM^{-/-}$ A549 cancer cells in terms of the generation of reactive oxygen species (ROS). Cells were cultured at a density of 3×10^5 cells per well and exposed them to varying concentrations of cisplatin (9.91 μM for $ATM^{+/+}$ A549 cells and 3.36 μM for $ATM^{-/-}$ A549 cells) for 24 h. Following treatment, cells were collected, washed with PBS, and resuspended in 1 mL PBS. To assess oxidative stress, cells were incubated at 37 °C for 30 min with 10 μM 2′7-dichlorodihydrofluorescein diacetate (H_2DCFH-DA) from Sigma-Aldrich. As a positive control, cells were treated with 50 μM H_2O_2 for 15 min. Live cell staining was performed using 10 μL of DAPI (50 μg/mL). The fluorescence intensity was measured using the median fluorescence intensity of H_2DCFH-DA in a NovoCyte Quanteon flow cytometer (Agilent). The data analysis was performed using FlowJo software (version 10.8.1) (BD Life Sciences). 20,000 cells were recorded for each sample by flow cytometry. Single cells were gated based on forward and side scatter properties (FSC-A/SSC-A), and further gating (FSC-A/FSC-H) in a linear manner was applied to remove doublets or debris. Living cells, indicated by DAPI negative staining, were detected using a 405 nm laser and 445/45BP filter, while H_2DCFH-DA fluorescence was detected using a 488 nm laser and 525/45BP filter. Each experimental condition was independently replicated three times, and data were analyzed using GraphPad Prism 6 software.

2.10. Detection of cellular senescence

To assess cellular senescence in the absence of *ATM*, we employed the senescence-associated β-galactosidase (SA-β-gal) staining protocol using a commercially available kit (Senescence β-Galactosidase Staining Kit, Cell Signalling Technology, Hitchin, Herts, UK Cat no. #9860) [32]. $ATM^{-/-}$ and $ATM^{+/+}$ A549 cancer cell lines were seeded at a density of 3×10^5 cells per well in 6-well plates. After a 24 h incubation, the cell

Table 2
Specific mutational hotspot sites and the mutation frequency therein of 23 DSB-related genes.

Gene	Missense	Nonsense	Frameshift	Mutation Hotspots Domain	Total mutation number
ATM	44	2	3	PI3_PI4_kinase domain (2714–2961)	49
ATR	37	3	3	PI3_PI4_kinase domain (2323–2567)	43
BLM	29	0	3	DEAD/DEAH box helicase (671–838)	32
PRKDC	21	3	1	NUC194 domain (1814–2209)	25
XRCC4	20	0	2	DNA double-strand break repair and V(D)J recombination protein XRCC4 (1–334)	22
XRCC5	15	1	4	Ku70/ku80 β_barrel domain (252–453)	20
XRCC6	14	0	4	Ku70/ku80 N_terminal α/βdomain (37–255)	18
RAD54L	17	0	1	SNF2 family N-terminal domain (156–463)	18
XRCC2	14	1	2	RAD51 (43–205)	17
RAD54B	11	5	1	RAD51 (83–338)	17
RAD51	15	1	1	RAD51 (83–338)	17
RAD50	13	1	2	AAA domain (6–262)	16
WRN	12	2	1	DEAD/DEAH box helicase (551–710)	15
LIG4	11	1	1	DNA ligase N-terminus (14–209)	13
NBN	7	1	2	Nbs1 (683–746)	10
MRE11	7	1	0	MRE11 DNA-binding presumed domain (294–461)	8
DCLR1B	8	0	0	β-Lactamase superfamily domain (23–148)	8
RAD52	6	0	1	RAD52/22 family double-strand break repair protein (35–180)	7
SETMAR	6	0	1	SET domain (150–262)	7
NHEJ1	4	1	0	XLF cernunos, XRCC4-like factor, NHEJ component (11–172)	5
DCLR1A	3	2	0	DNA repair metallo-β-lactamase (914–1019)	5
XRCC3	3	0	2	RAD51 (64–338)	5
APLF	2	1	0	Zinc finger motif (377–402)	3

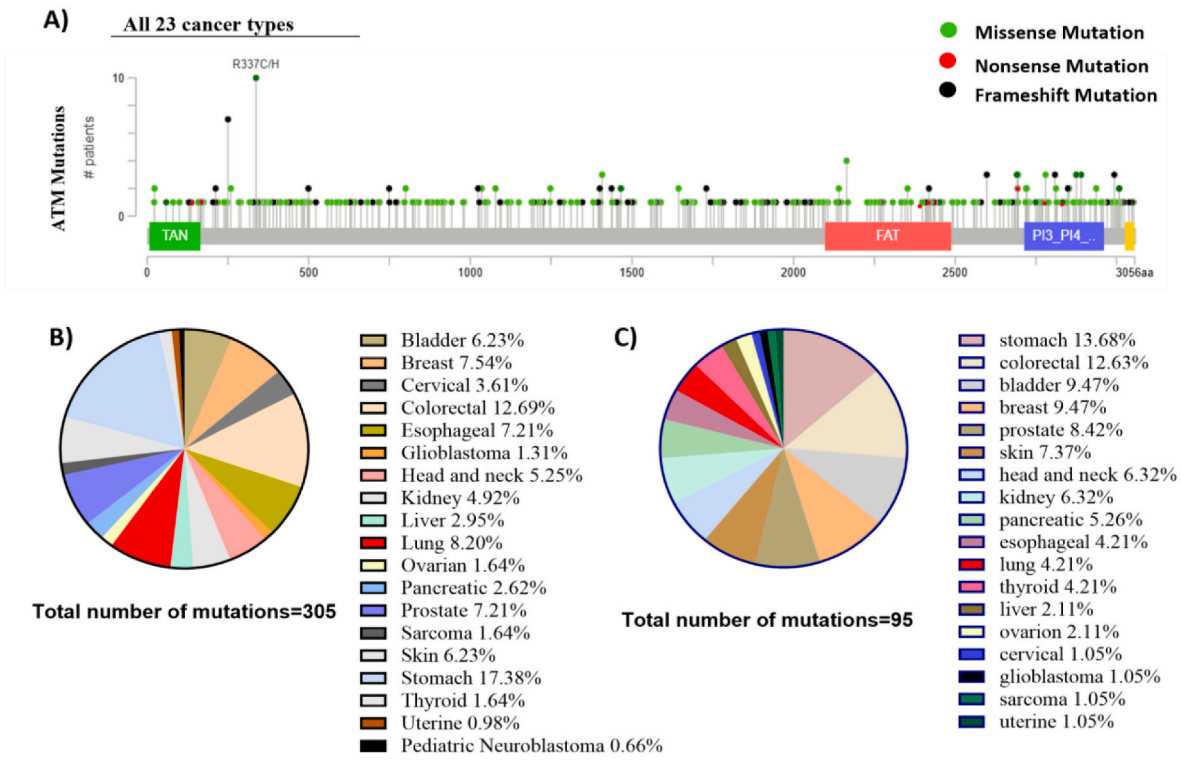

Fig. 1. Gene mutation analysis across 23 different cancer types. (A) The distribution of mutation profiles associated with *ATM. (*B) Percentage distribution of total mutations in the *ATM* gene, including both coding and non-coding regions. (C) Percentage distribution of mutations located exclusively in the coding regions of the *ATM* gene.

lines were exposed to distinct concentrations of cisplatin (9.91 μM for $ATM^{+/+}$ A549 cells and 3.36 μM for $ATM^{-/-}$ A549 cells) for 24 h. Following the treatment, the growth medium was aspirated, and the cells were rinsed twice with 1X phosphate-buffered saline (PBS). Subsequently, cells were fixed by adding 1 mL of 1X Fixative Solution per well and incubated at room temperature for 10–15 min. After fixation, the cells were washed twice with 1X PBS. Next, 1 mL of β-galactosidase staining solution was added to each well, and the plates were incubated at 37 °C overnight in a dry, CO_2-free incubator. Finally, the stained cells were examined under a light microscope equipped with a camera, using a 10 × or higher objective lens. For each of sample, we selected more than 5 images to calculate the percentage of senescent cells. The percentage of SA-β-gal-positive cells (blue staining) was calculated by counting the number of positive cells *versus* the total number of cells, with a minimum of 100 cells counted per condition.

2.11. Single cell electrophoresis (comet assay)

We utilized the comet assay (by using the Oxiselect™ Comet Assay Kit (3-Well Slides) from Cell Biolabs/Biocat (Heidelberg, Germany). $ATM^{+/+}$ A549 cells and $ATM^{-/-}$ A549 cells were initially seeded at a density of 3×10^5 cells per well in 6-well plates. These cells were then treated with cisplatin concentrations corresponding to their respective IC_{50} values (9.91 μM for $ATM^{+/+}$ A549 cell and 3.36 μM for $ATM^{-/-}$ A549 cell 24 h) and H_2O_2 (as a positive control) at a concentration of 50 μM for 15 min.

Following treatment, cells were collected, centrifuged at 3000×*g* for 10 min, and reconstituted in PBS. Cell suspensions at a concentration of 1×10^5 cells/mL were mixed with molten agarose (at a ratio of 1:6) at 37 °C. The resulting mixtures were spread onto comet slides and incubated in darkness at 4 °C for 30 min. Slides were then immersed in a pre-chilled lysis buffer (containing NaCl, EDTA solution, and 10 × lysis solution at pH 10.0) for 1 h at 4 °C. After lysis, slides were transferred to a pre-chilled alkaline electrophoresis solution buffer (containing NaOH, EDTA solution, and distilled water) for 40 min at 4 °C in darkness.

The slides were placed in an electrophoresis chamber filled with the alkaline electrophoresis solution buffer, and electrophoresis was conducted at 20 V for 20 min. After electrophoresis, slides underwent two washes with pre-chilled distilled water for 5 min each. Subsequently, slides were immersed in cold ethanol (70 %) for 5 min and air-dried. Once dried, 100 μL of Vista Green DNA dye (diluted at a ratio of 1:10,000 in TE buffer) was added to each slide and incubated for 15 min at room temperature. Fifty comets from each treatment group were randomly selected and analyzed using OpenComet, a software tool integrated within Image J, developed by the National Institutes of Health. Tail DNA% served as the parameter for quantifying DNA damage [33]. The images obtained showed comets which were captured using a 10 × objective lens, highlighting detailed structural and compositional features.

3. Results

3.1. Determination of mutational hotspot sites

We concentrated on mutations in domain site to detect most predictive biomarker in cancer patients. We determined mutation hotspot sites for 23 genes involved in DSB. Finally, we focused on ATM as the most probable predictive target. As displayed in Table 2, *ATM* contained the highest mutation numbers in comparison of specific mutational hotspot sites of the selected 23 genes involved in DBS. Supplementary Table 1 provides a more detailed representation of the *ATM* mutation analysis derived from the 23 selected cancer cases. Additionally, Fig. 1A visually illustrates the distribution of ATM mutations across the 23 cancer cases. Fig. 1B illustrates the percentage distribution of total mutations observed in both coding and non-coding regions of the *ATM* gene across 23 distinct cancer types. In this study, however, we primarily focused on mutations located within the coding regions. Accordingly, Fig. 1C presents the percentage-based frequency of

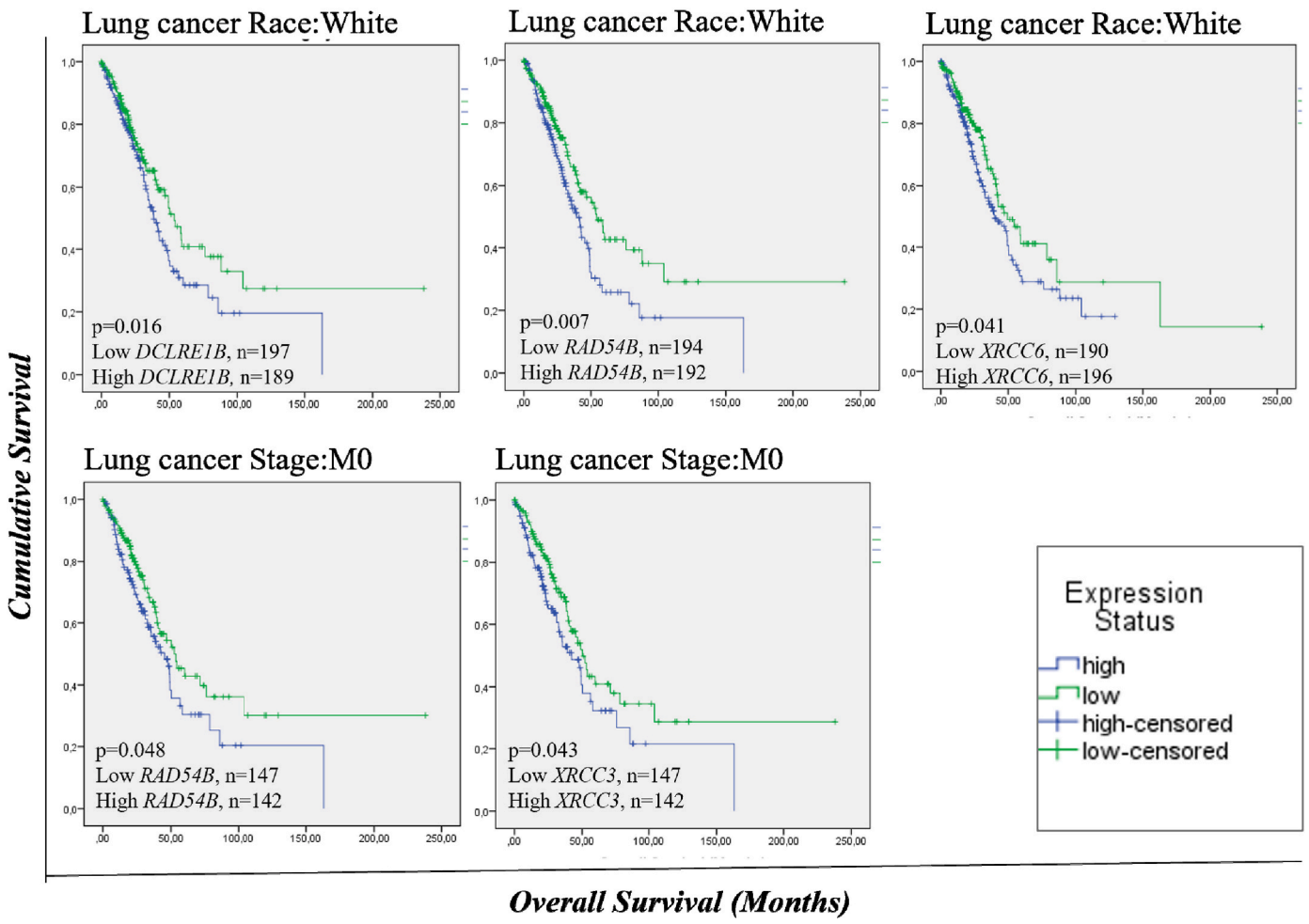

Fig. 2. Biomarkers associated with poor patient survival in lung cancer, as identified through overall survival analysis, are presented ($p < 0.05$)

mutations identified exclusively in the coding regions.

3.2. Overall survival analyses

To identify effective biomarkers, we investigated DSB repair genes with high expression levels associated with poor survival across 23 distinct cancer types. The identified biomarkers are presented in Supplementary Fig. S1. These findings emphasize the substantial biological diversity among cancer types and the context-dependent nature of prognostic biomarkers. Notably, a higher number of prognostic biomarkers were identified in kidney, breast, liver, sarcoma, lung, thyroid, and cervical cancers, suggesting these malignancies may involve more complex and heterogeneous biological mechanisms. Our aim was to focus on one of the cancer types with the highest number of identified prognostic biomarkers, making lung cancer the focal point of this study. Given its clinical significance, lung cancer was selected as the primary focus of this study. The biomarkers identified through survival analysis for lung cancer are presented in Fig. 2.

3.3. Cytotoxicity assay

The cytotoxicity assay was conducted using cisplatin, carboplatin, and 5-fluorouracil. We compared the differences between the $ATM^{+/+}$ A549 and $ATM^{-/-}$ A549 cell lines. Upon treatment for 72 h, the $ATM^{-/-}$ A549 cells exhibited diminished cell viability compared to the wild-type cells in response to the afore-mentioned drugs (cisplatin, carboplatin, and 5-fluorouracil).

Specifically, the $ATM^{-/-}$ A549 cells demonstrated IC_{50} values at a cisplatin concentration of 3.36 ± 1.31 μM, a carboplatin concentration of 14.5 ± 12.55 μM, and a 5-fluorouracil concentration of 0.5 ± 0.08 μM. In comparison, the wild-type cells exhibited IC_{50} values at a cisplatin concentration of 9.91 ± 2.5 μM, a carboplatin concentration of 39.3 ± 4.3 μM, and a 5-fluorouracil concentration of 1.7 ± 0.6 μM (Fig. 3).

3.4. Microarray-based mRNA expression profiling for predicting canonical signalling pathways

For comprehensive transcriptomic analysis of ATM, we performed microarray hybridization-based expression profiling analyses and consecutive Ingenuity Pathway Analysis (IPA). Firstly, to investigate the effects of ATM knockout by using CRISPR/Cas9 technologies, we compared mutant and wild-type A549 cancer cells without cisplatin exposure using IPA analysis (Fig. 4). The absence of ATM impacted signalling pathways involved in cancer cell proliferation, ultimately leading to the suppression of cellular proliferation. It was clearly observed that the NRF2-mediated oxidative stress response, mTOR, EIF2, NOTCH4, and WNT/β-catenin signalling pathways were down-regulated by ATM knockout.

To comprehensively elucidate the mechanisms underlying the enhancement of cisplatin sensitivity through ATM knockout, we conducted a microarray hybridization expression profiling analysis via IPA to compare mutant and wild-type A549 cancer cells under treatment with cisplatin (Fig. 5). The data obtained indicate that, in the presence of ATM, cisplatin response predominantly activated pathways related to autophagy, intrinsic pathway for apoptotic signalling, and MYC-

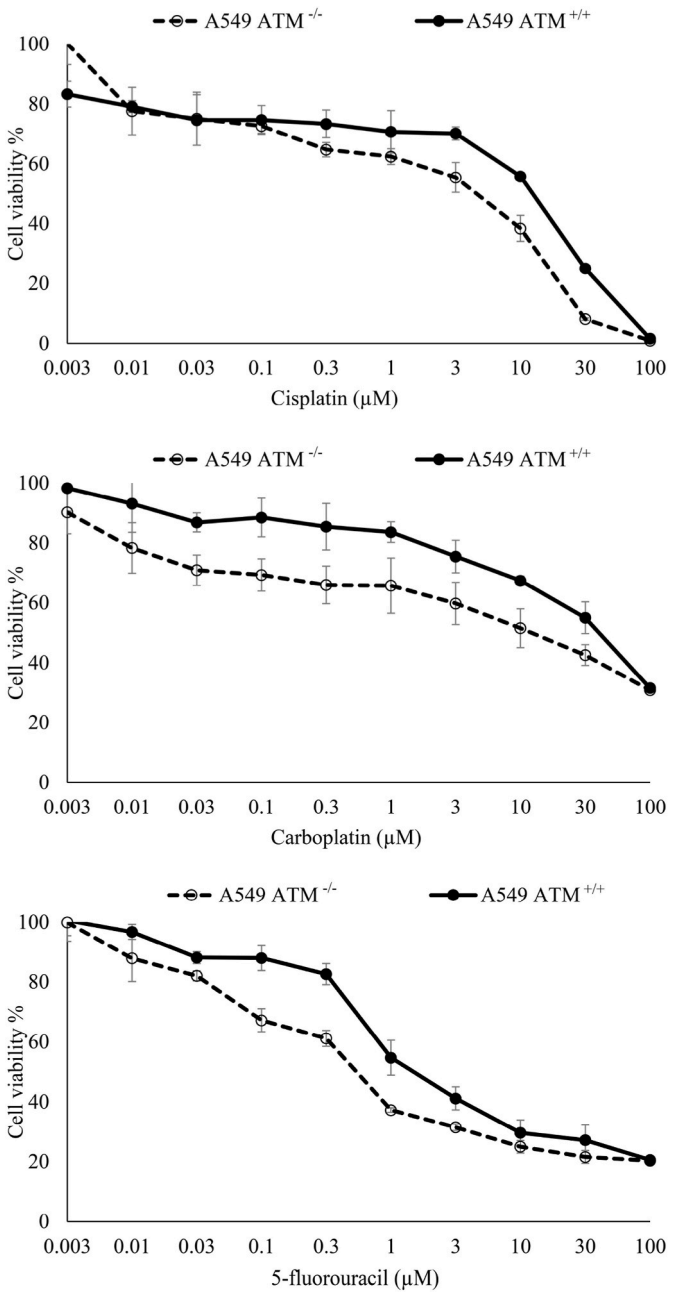

Fig. 3. The cell viability of $ATM^{+/+}$ and $ATM^{-/-}$ A549 cells by using different concentrations of cisplatin, carboplatin, and 5-fluorouracil.

mediated apoptotic signalling. However, in the absence of ATM, the cellular response to the drug shifted, leading to an increased activation of alternative cell death pathways. As illustrated in Fig. 5, despite lower concentrations of cisplatin, the activation of necroptosis, oxidative stress induced senescence and ferroptosis cell death signalling pathways was heightened, while the sub-pathways of autophagy, such as mitophagy and macroautophagy, appear to lose their influence. Especially, oxidative stress-induced senescence promotes cancer cell death, potentially mediated by the downregulation of NRF2. ATM may exert its effects on ROS through its interaction with NRF2, which could influence senescence triggered by oxidative stress.

At this point, mutations present in the ATM gene may render the response to cisplatin more resistant and lead to the activation of cell death signalling pathways only at higher concentrations of cisplatin. In the context of treatment development, employing combination therapies that target distinct cell death pathways through different agents may represent a promising strategy rather than increasing drug dose concentrations.

3.5. Quantitative real-time q-PCR for validating relative gene expression

To validate the microarray hybridization findings, we selected three upregulated and three downregulated genes from both sets including $ATM^{-/-}$ A549 and $ATM^{+/+}$ A549 and performed quantitative PCR (qPCR). The qPCR results were compared with the microarray data, and linear regression analysis along with Pearson correlation coefficients were calculated (Fig. 6A and B). The results were consistent with and supportive of the microarray data. To demonstrate the activation of the oxidative stress induced senescence signalling under ATM knockout, qPCR was performed after cisplatin exposure for two and experimental sets. In the *ATM* knockout A549 cancer cells following cisplatin exposure, the results revealed an upregulation in the expression of *CDKN2A, IL8*, and *IL6,* which play active roles in the oxidative stress-induced senescence signalling pathway (Fig. 6C). Particularly, IL8 and IL6 are two well-characterized factors involved in senescence [34,35].

3.6. Cell cycle analysis

ATM is an important part of cell cycle machinery. Thus, possible mutations in *ATM* result in a change of the cell cycle process upon specific cellular stimuli. Especially, the altered cellular responses after drug treatment by existing mutations may open opportunities for cancer cells to resist the detrimental effects of anticancer drugs. In the absence of functional ATM, cisplatin-induced S-phase arrest decreased, but G2/M arrest considerably increased even at low cisplatin concentrations (Fig. 7).

3.7. Apoptosis

To investigate the effect of ATM knockout on apoptosis, we performed an Annexin-V apoptosis assay. Following cisplatin exposure, an increase in necrosis was observed under ATM knockout, whereas apoptosis was more pronounced in wild-type cells (Fig. 8).

After cisplatin exposure, the percentage of necrotic (dead) cells increased from 50.8 % to 60.3 % in $ATM^{-/-}$ A549 cells, whereas in $ATM^{+/+}$ A549 cells, the percentage of necrotic (dead) cells rose from 6.11 % to 19.6 %. In $ATM^{-/-}$ A549 cells, apoptotic cells slightly decreased from 2.44 % to 0.94%. In contrast, in $ATM^{+/+}$ A549 cells, apoptotic cells increased from 0.46 % to 5.84 %. These values represent the average of three repetitions conducted at different times.

3.8. Detection of reactive oxygen species

We investigated the relation between *ATM* knockout and ROS by different cisplatin concentrations. We measured increased ROS levels depending on *ATM* knockout despite the exposure to only low concentration of cisplatin (Fig. 9). By employing the microarray hybridization technology, gene expression patterns were scrutinized to unravel the intricate interplay between *ATM* knockout and the cellular defence mechanisms against ROS. Our findings suggest that *ATM* knockout disrupted the intricate network of genes involved in ROS defence, thereby compromising the cell's ability to combat oxidative stress.

3.9. Detection of cellular senescence

To determine the effect of *ATM* knockout on cellular senescence, we performed β-galactosidase (β-Gal) staining. Despite exposure to lower concentrations of cisplatin under *ATM* knockout, cellular senescence was enhanced (Fig. 10). The percentage of cells exhibiting senescence was higher under *ATM* knockout.

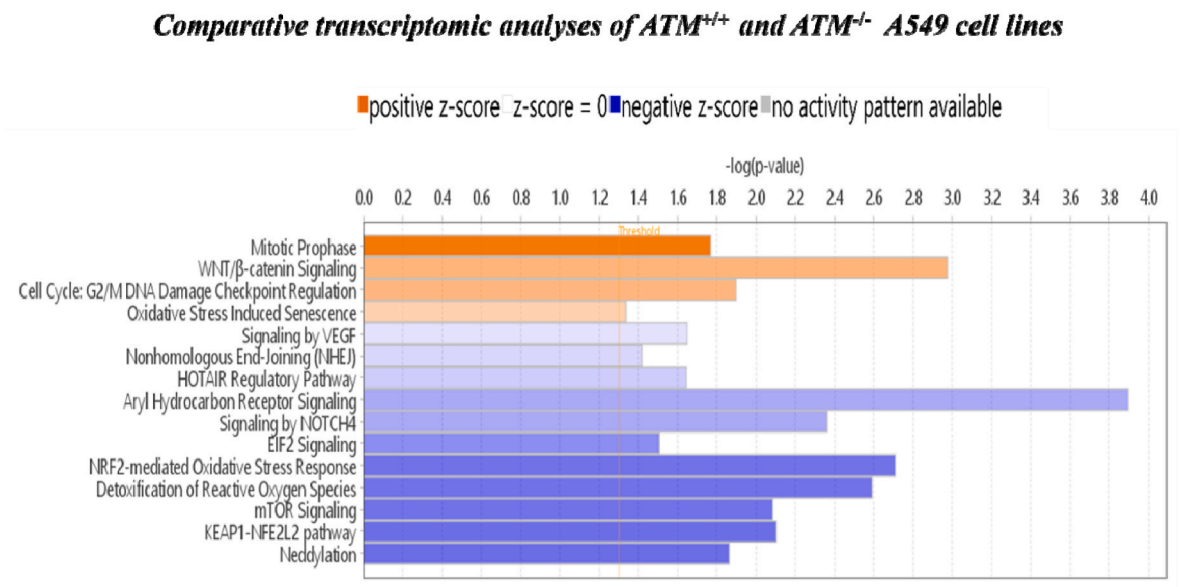

Fig. 4. Canonical pathway analysis of $ATM^{-/-}$ and $ATM^{+/+}$ A549 cells without cisplatin exposure.

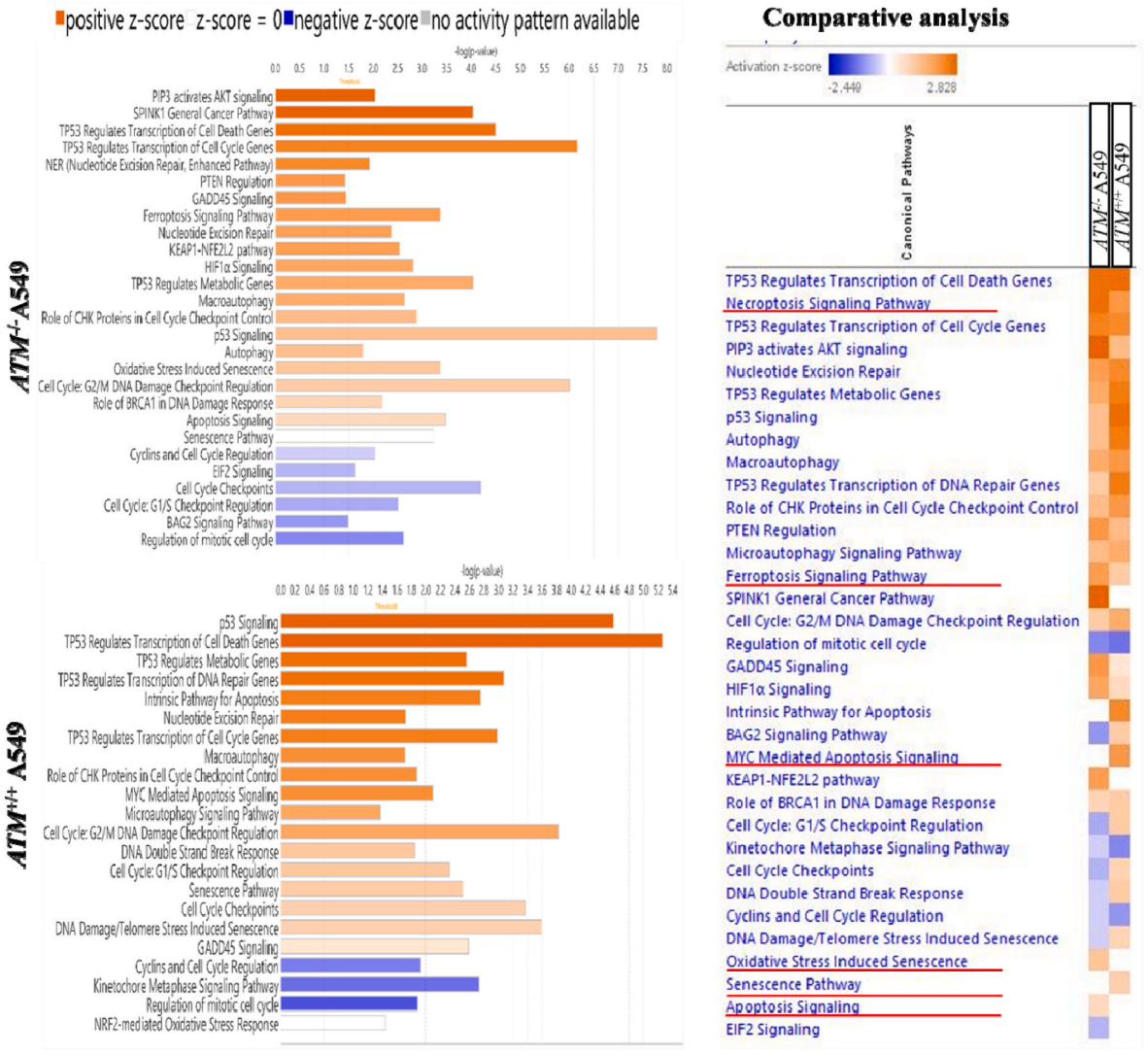

Fig. 5. Canonical pathway analysis of $ATM^{-/-}$ and $ATM^{+/+}$ A549 cells following cisplatin exposure. The figure includes a comparative analysis of the canonical pathways between the two groups.

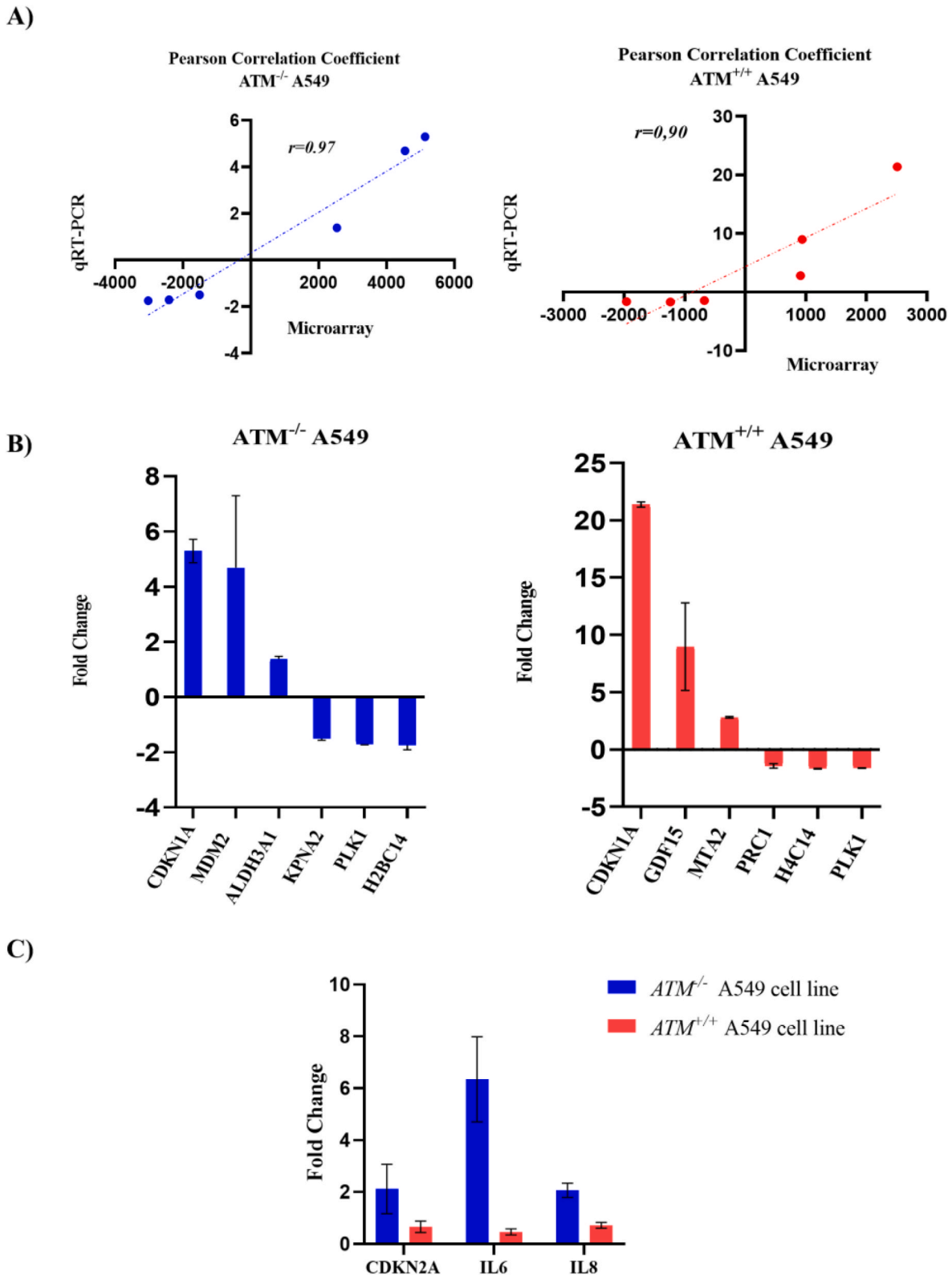

Fig. 6. A) Linear regressions and Pearson correlation coefficients for microarray and q-PCR data in $ATM^{-/-}$ A549 wild-type and $ATM^{+/+}$ A549 cells. **B)** Verification of the top three up and down-regulated genes by q-PCR in these cells. **C)** Significant upregulation of *CDKN2A, IL8* and *IL6* genes in $ATM^{-/-}$ A549 cancer cells, with the opposite trend in the A549 wild-type cells following cisplatin exposure.

3.10. Single cell electrophoresis (comet assay)

In order to assess DNA damage in $ATM^{+/+}$ A549 and $ATM^{-/-}$ A549 cells, we utilized the alkaline comet assay (as shown in Fig. 11). Especially, the alkaline comet assay is employed to assess oxidative DNA damage. Knockout of the *ATM* gene leads to a ROS increase, which exacerbated oxidative DNA damage, further supporting the tail formation observed in the comet assay. Moreover, the absence of *ATM*

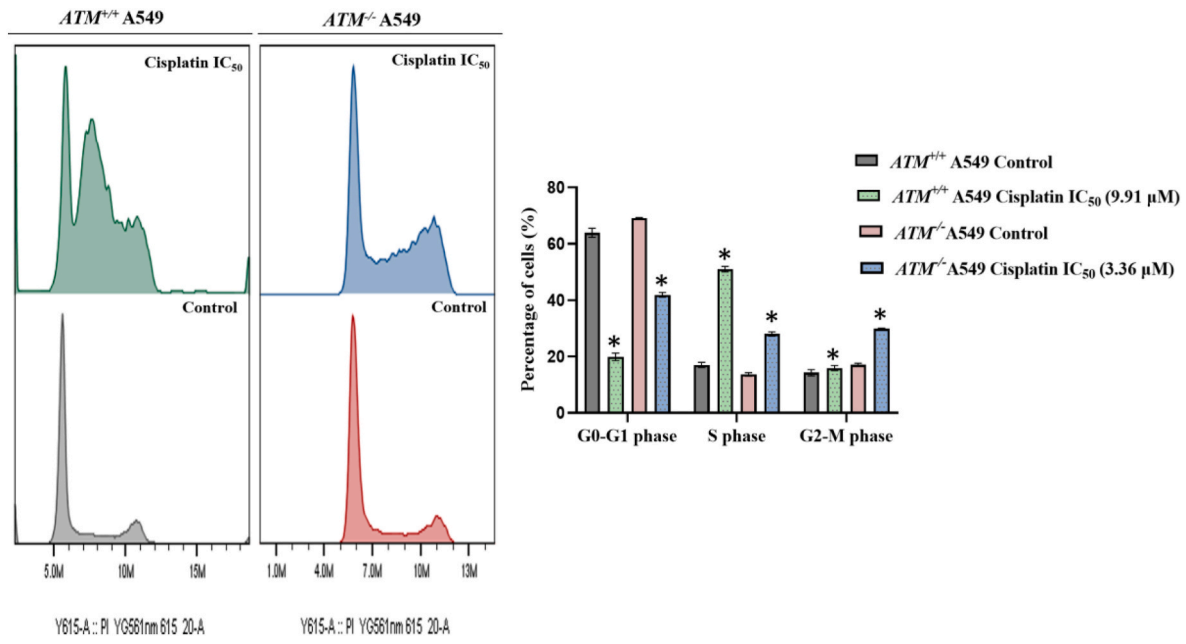

Fig. 7. Flow cytometric cell cycle analysis in $ATM^{+/+}$ and $ATM^{-/-}$ A549 cancer cell lines treated with the IC_{50} concentration of cisplatin. The statistical significance was analyzed using Student's t-test ($^*p < 0{,}05$).

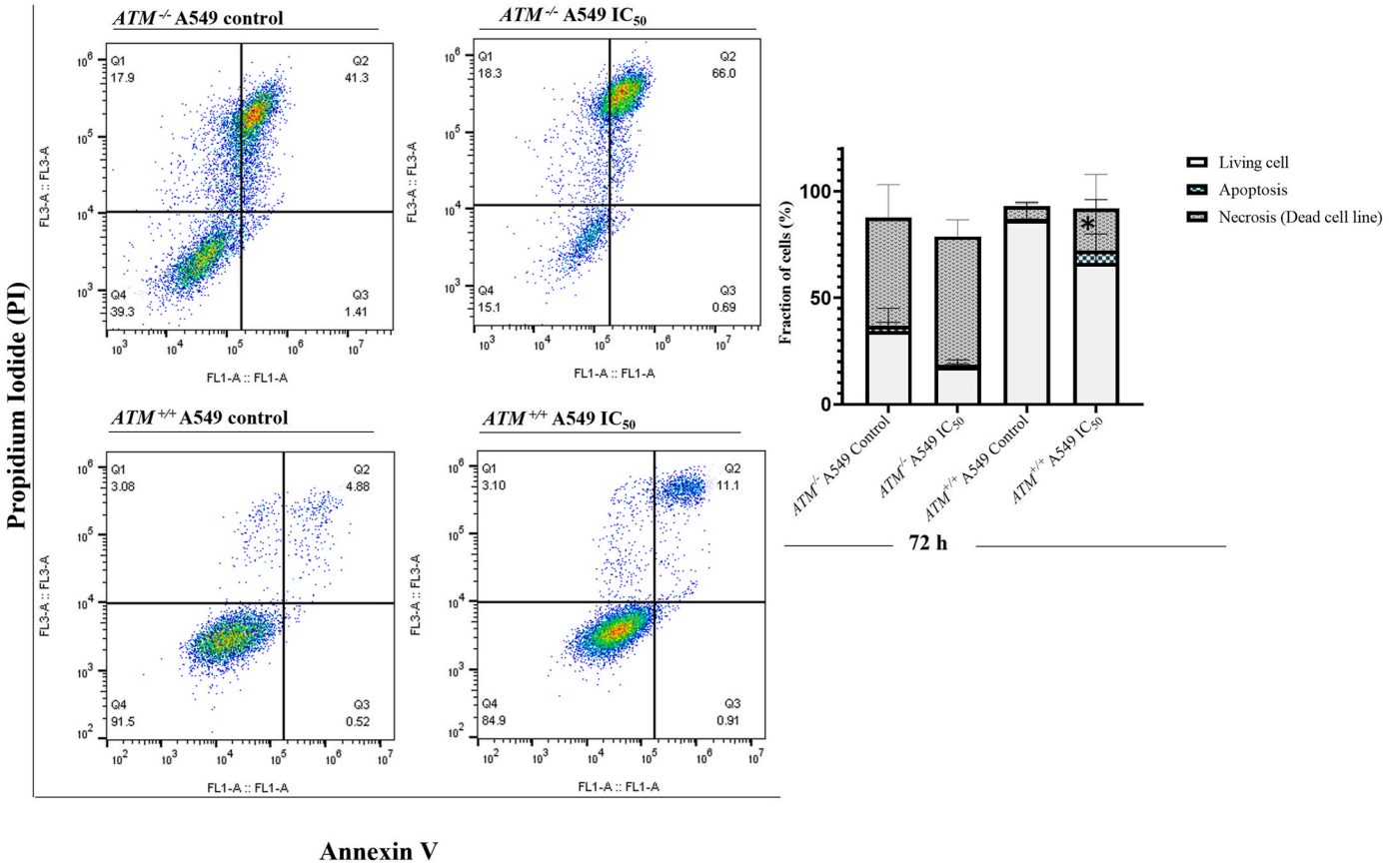

Fig. 8. Flow cytometric analysis for apoptosis in $ATM^{+/+}$ and $ATM^{-/-}$ A549 cancer cell lines treated with the IC_{50} concentration of cisplatin. The statistical significance was analyzed using Student's t-test ($^*p < 0{,}05$).

rendered cells more susceptible to the elevated ROS levels in the presence of cisplatin. The ATM knockout led to a significant increase in the tail moment of cells in the comet assay following cisplatin exposure. In contrast, we also observed a relatively lower comet tail moment in $ATM^{+/+}$ A549 cells. Cisplatin-induced DNA damage typically results in a reduced tail moment due to the formation of interstrand crosslinks. However, cisplatin not only causes DNA damage through the formation of interstrand crosslinks but also induces oxidative stress by increasing

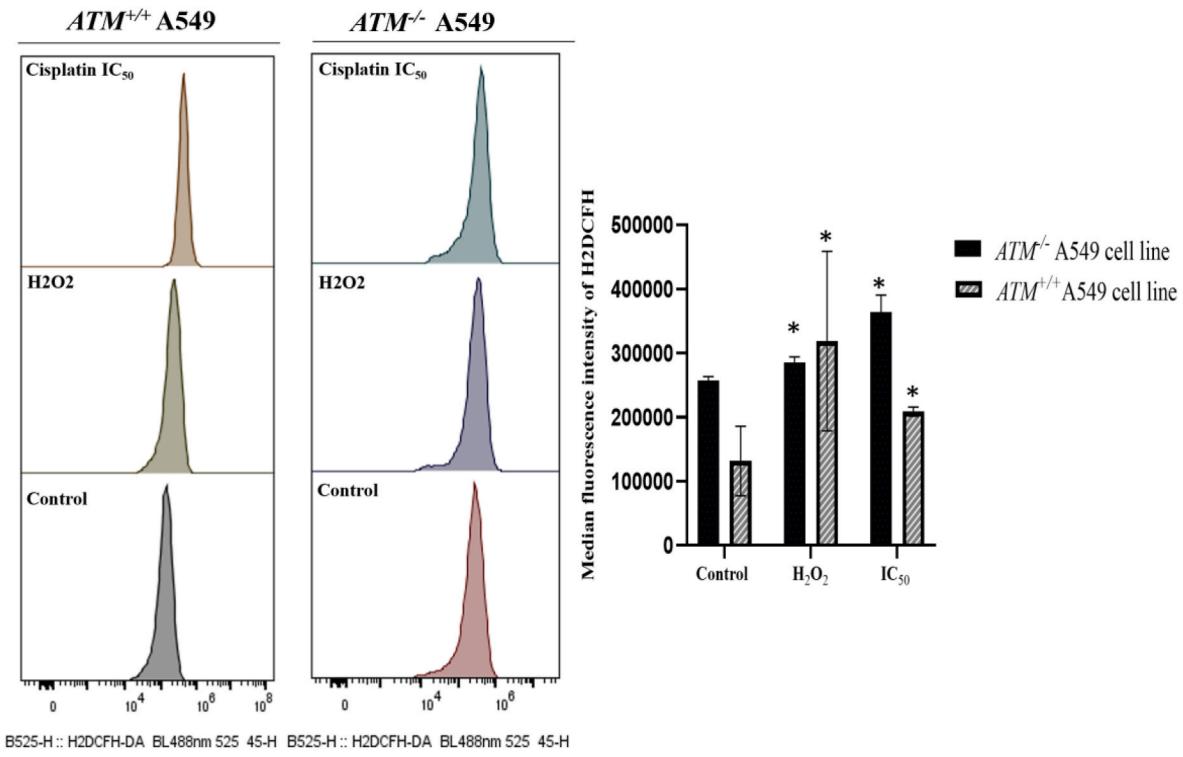

Fig. 9. Flow cytometric analysis to detect ROS levels in $ATM^{+/+}$ and $ATM^{-/-}$ A549 cancer cell lines treated with IC_{50} concentrations of cisplatin. The statistical significance was analyzed using Student's t-test ($*p < 0,05$).

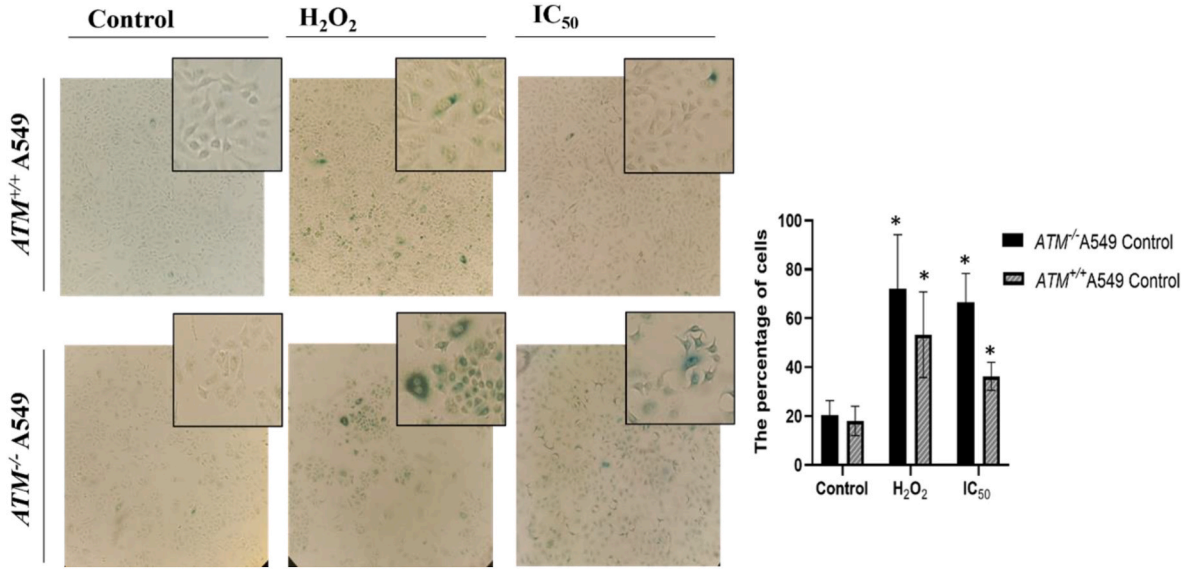

Fig. 10. Quantitative assessment of cellular senescence by staining senescence-associated β-galactosidase, following cisplatin exposure in $ATM^{+/+}$ and $ATM^{-/-}$ A549 cells.

ROS production, which may contribute to further DNA damage.

Our acquired data revealed a discernible disparity in the DNA damage profiles, with the $ATM^{-/-}$ A549 cell line manifesting heightened susceptibility to cisplatin-induced damage at a concentration of 3.36 μM. In comparison, the wild-type cell line exhibited a reduced percentage of DNA damage even upon exposure to a higher cisplatin concentration (9.91 μM). This observed discrepancy suggests that the absence of *ATM* renders cells considerably vulnerable to cisplatin.

4. Discussion

ATM, a key member of the phosphatidylinositol-3 kinase-related kinase (PIKK) family, plays a crucial role in the DNA damage response (DDR) by phosphorylating over 700 proteins, including p53, CHK2, and MDM2 [36–39]. These phosphorylations initiate signalling pathways such as apoptosis, senescence, and autophagy, maintaining cellular homeostasis [40]. However, arising mutations in *ATM* disrupt these mechanisms, contributing to aging, cancer progression, and therapy resistance.

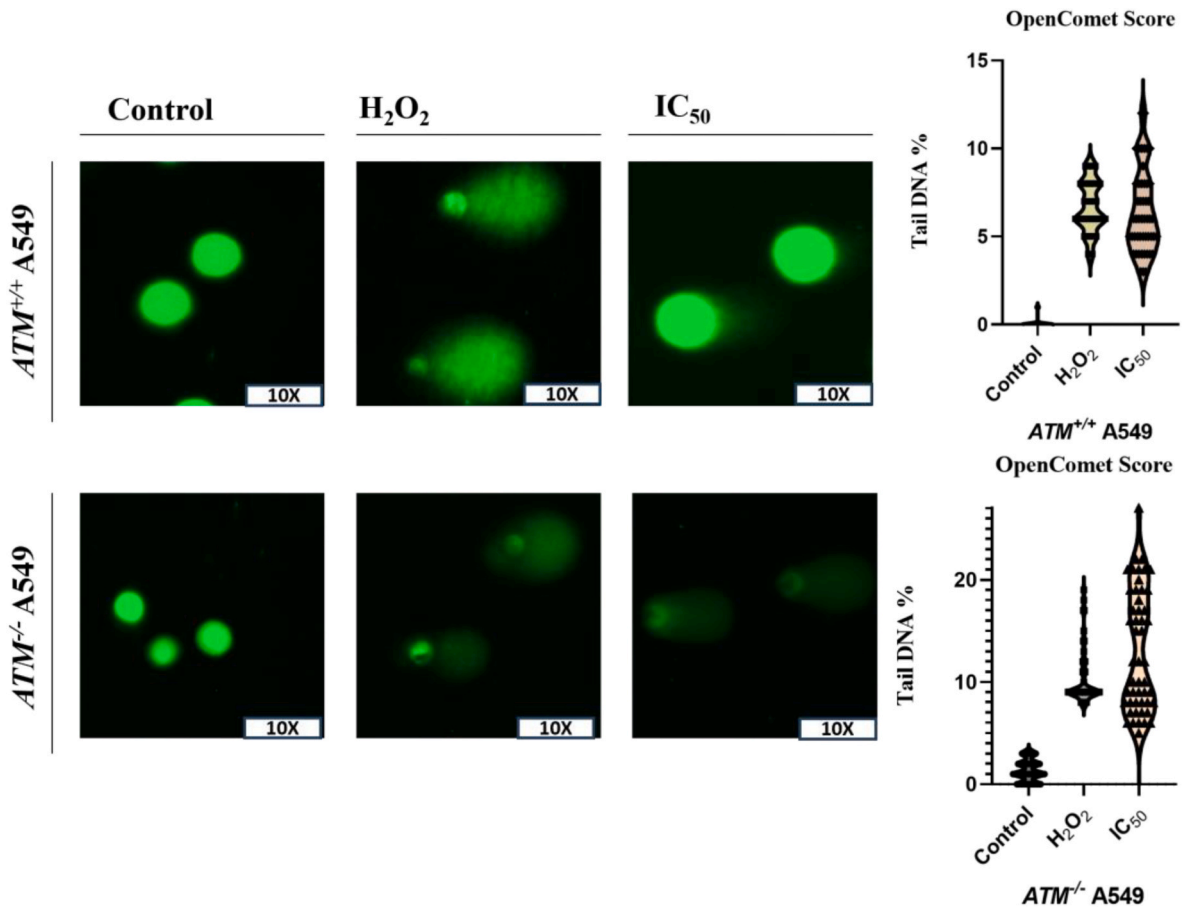

Fig. 11. Quantitative assessment of DNA damage using the alkaline comet assay, specifically single cell gel electrophoresis, following cisplatin exposure in $ATM^{+/+}$ and $ATM^{-/-}$ A549 cells. The 'tail DNA%' parameter was quantified based on the analysis of 50 randomly selected cells, as illustrated in the accompanying violin plot.

Whole-genome sequencing studies reveal that *ATM* mutations, particularly missense variants within the kinase domain, are prevalent in therapy-resistant cancers [39,41,42]. These mutations reduce ATM's kinase activity or protein expression, leading to impaired DDR and drug resistance [39,43]. However, the effect of mutations on drug resistance remains elusive. Hence, we performed a comparative analysis of multiple datasets in this study to select most predictive biomarkers in 23 cancer types. A comprehensive mutational analysis of 23 proteins involved in DSB mechanism was conducted across over 7500 tumors representing distinct cancer types in three parameters. The findings revealed that ATM exhibit the highest mutation frequency among the analyzed proteins. Particularly, missense mutations were observed to be the predominant type in ATM protein rather than frameshift and nonsense mutations. Mutation analysis executed via c-BioPortal reveals that the highest frequency of mutations in coding regions is observed in stomach, colorectal, bladder, breast, prostate, kidney, skin, head and neck, and lung cancer cases. These findings highlight the complex heterogeneity of various cancer cases, emphasizing the importance of tailoring treatment strategies based on cancer type. This underscores the necessity of developing personalized therapeutic approaches for effective cancer treatment management.

In addition, we conducted comprehensive bioinformatic analyses by using c-BioPortal to evaluate the effects of 23 proteins involved in the DSB mechanism across 23 different cancer types. From a broad perspective, our findings revealed that the high expression of identified biomarkers was associated with poor survival in liver, kidney, breast, and lung cancer cases according to various parameters (as shown in Supplementary Fig. 1). In the obtained data set, we observed that high expression of *ATM* was linked to poor survival exclusively in breast cancer. For lung cancer, the high expression of *RAD54B, XRCC6, XRCC3*, and *DCLRE1B* was identified as biomarkers associated with poor survival outcomes in distinct parameters (as shown in Fig. 2).

Platinum-based chemotherapies are cornerstone treatments for various cancers, exerting their cytotoxic effects primarily through DNA damage and the induction of apoptosis [44,45]. Prolonged use of platinum-based drug exposure increases mutation rates, altering drug responses and enabling cancer survival via alternative pathways. The most detrimental consequence of mutations is the limitation of cisplatin efficacy due to the development of resistance [46]. Combination therapies can delay resistance, but validating biomarkers as drug targets by experimental studies is necessary [47]. Therefore, we performed cytotoxic experiments to observe the consequences of *ATM* knockout in the presence of cisplatin. The results demonstrated that *ATM* knockout enhances cisplatin sensitivity. Considering the heterogeneity of mutations across different cancer types, experimental analyses tailored to specific cancer types are likely to provide greater opportunities for the development of personalized treatments.

Mechanistic insights from expression profiling data disclose the underlying mechanisms of increased cisplatin sensitivity. [48–52]. Senescence is a complex phenotype characterized by distinct changes in morphology, gene expression, metabolism, and other biological processes that occur in a time-dependent manner [53]. Cellular senescence is a fundamental stress response program that has evolved to serve specific physiological functions, including embryonic development and wound healing [54]. Currently, senescence is recognized as a highly dynamic state that is neither strictly irreversible nor fully reversible [54]. While *ATM* knockout has been previously shown to suppress senescence, our transcriptomic analysis reveals that ATM knockout

activates the oxidative damage induced senescence signalling pathway [48,55]. This activation occurs through an imbalance in cell death mechanisms caused by increased reactive oxygen species (ROS) levels.

In the presence of ATM, apoptosis is the predominant response to cisplatin treatment. However, *ATM* knockout shifts the balance, promoting necroptosis, ferroptosis, and oxidative damage-induced senescence. ATM acts as a defence mechanism, maintaining ROS levels within a manageable range [56]. If inhibited, ROS levels rise, triggering alternative cell death pathways to restore cellular homeostasis. Despite lower cisplatin concentrations, ROS accumulation was significantly higher in *ATM* knockout cells compared to wild-type A549 cancer cells, enhancing cisplatin sensitivity through oxidative damage-induced senescence.

To further investigate these mechanisms, we employed Ingenuity Pathway Analysis (IPA) and Chipster software to identify key genes involved. Our findings reveal a critical interplay between ATM and nuclear factor (erythroid-derived 2)-like 2 (NRF2). NRF2 is known as a central transcription regulator of the antioxidant response [57–59]. *NRF2* downregulation following *ATM* knockout reduces cellular resilience to oxidative stress, exacerbating ROS accumulation. Previously, *NRF2* inhibition suppressed the DNA damage response (DDR) by downregulating *ATM* and *ATR* expression, highlighting a critical feedback loop essential for maintaining cellular integrity [59]. However, there is no evidence of regulatory crosstalk between ATM and oxidative stress induced senescence through NRF2 downregulation.

The key point here is that prolonged cisplatin exposure, resulting in an increased mutation rate, may lead to changes in the drug's response. One of the potential reasons for resistance may be the inability of apoptotic signalling pathways to function as required in the presence of ATM. Existed mutations associated with ATM may hinder the cellular response to the administered drug. However, a potential solution to acquired resistance in cancer patients could be the activation of other cell death pathways through modified combination therapy strategies.

CRediT authorship contribution statement

Ayşegül Varol: Writing – review & editing, Writing – original draft, Methodology, Investigation, Data curation, Conceptualization. **Sabine M. Klauck:** Writing – review & editing, Software, Methodology, Investigation, Data curation, Conceptualization. **Susan P. Lees-Miller:** Methodology, Investigation. **Thomas Efferth:** Writing – review & editing, Supervision, Project administration, Conceptualization.

Declaration of competing interest

The authors declare the following financial interests/personal relationships which may be considered as potential competing interests: Aysegul Varol reports financial support was provided by Turkish Government (National Education Scholarship). If there are other authors, they declare that they have no known competing financial interests or personal relationships that could have appeared to influence the work reported in this paper.

Acknowledgement

We gratefully acknowledge the Microarray Unit of the Genomics and Proteomics Core Facility, German Cancer Research Center (DKFZ) Heidelberg, for providing excellent Expression Profiling service. We thank the Flow Cytometry Core Facility at the Institute of Molecular Biology (IMB, Mainz, Germany) for their kind training and technical support to complete the detection of reactive oxygen species and cell cycle experiments. A.V. is grateful for a stipend provided by the Turkish Government (National Education Scholarship).

Appendix A. Supplementary data

Supplementary data to this article can be found online at https://doi.org/10.1016/j.cbi.2025.111563.

Data availability

Data will be made available on request.

References

[1] B.N. Ames, Mutagenesis and carcinogenesis: endogenous and exogenous factors, Environ. Mol. Mutagen. 14 (S16) (1989) 66–77.
[2] R. De Bont, N. Van Larebeke, Endogenous DNA damage in humans: a review of quantitative data, Mutagenesis 19 (3) (2004) 169–185.
[3] A.M. Weber, A.J. Ryan, ATM and ATR as therapeutic targets in cancer, Pharmacol. Therapeut. 149 (2015) 124–138.
[4] N. Chatterjee, G.C. Walker, Mechanisms of DNA damage, repair, and mutagenesis, Environ. Mol. Mutagen. 58 (5) (2017) 235–263.
[5] A. Turchick, et al., Selective inhibition of ATM-dependent double-strand break repair and checkpoint control synergistically enhances the efficacy of ATR inhibitors, Mol. Cancer Therapeut. 22 (7) (2023) 859–872.
[6] X. Wu, et al., DNA damage response (DDR): a link between cellular senescence and human cytomegalovirus, Virol. J. 20 (1) (2023) 250.
[7] G.-M. Li, Mechanisms and functions of DNA mismatch repair, Cell Res. 18 (1) (2008) 85–98.
[8] C.D. McFarland, et al., Impact of deleterious passenger mutations on cancer progression, Proc. Natl. Acad. Sci. 110 (8) (2013) 2910–2915.
[9] C. Holohan, et al., Cancer drug resistance: an evolving paradigm, Nat. Rev. Cancer 13 (10) (2013) 714–726.
[10] A.-M. Florea, D. Büsselberg, Cisplatin as an anti-tumor drug: cellular mechanisms of activity, drug resistance and induced side effects, Cancers 3 (1) (2011) 1351–1371.
[11] A. Eastman, The mechanism of action of cisplatin: from adducts to apoptosis. Cisplatin: Chemistry and Biochemistry of a Leading Anticancer Drug, 1999, pp. 111–134.
[12] L.F. Qin, I.O. Ng, Induction of apoptosis by cisplatin and its effect on cell cycle-related proteins and cell cycle changes in hepatoma cells, Cancer Lett. 175 (1) (2002) 27–38.
[13] M. Kartalou, J.M. Essigmann, Mechanisms of resistance to cisplatin, Mutat. Res. Fund Mol. Mech. Mutagen 478 (1–2) (2001) 23–43.
[14] K. naidu gopal Hariprabu, M. Sathya, S. Vimalraj, CRISPR/Cas9 in cancer therapy: a review with a special focus on tumor angiogenesis, Int. J. Biol. Macromol. 192 (2021) 913–930.
[15] M. Vaghari-Tabari, et al., CRISPR/Cas9 gene editing: a new approach for overcoming drug resistance in cancer, Cell. Mol. Biol. Lett. 27 (1) (2022) 49.
[16] A.A. Aljabali, M. El-Tanani, M.M. Tambuwala, Principles of CRISPR-Cas9 technology: advancements in genome editing and emerging trends in drug delivery, J. Drug Deliv. Sci. Technol. (2024) 105338.
[17] A. Saber, et al., CRISPR/Cas9 for overcoming drug resistance in solid tumors, Daru 28 (2020) 295–304.
[18] D. Li, et al., Interactions between oxidative stress and senescence in cancer: mechanisms, therapeutic implications, and future perspectives, Redox Biol. 73 (2024) 103208.
[19] B. Li, et al., Distinct roles of c-Abl and Atm in oxidative stress response are mediated by protein kinase C δ, Gene Dev. 18 (15) (2004) 1824–1837.
[20] A. Agathanggelou, et al., Targeting the Ataxia Telangiectasia Mutated-null phenotype in chronic lymphocytic leukemia with pro-oxidants, Haematologica 100 (8) (2015) 1076.
[21] C. Yu, J.-H. Xiao, The Keap1-Nrf2 system: a mediator between oxidative stress and aging, Oxid. Med. Cell. Longev. 2021 (1) (2021) 6635460.
[22] E. Cerami, et al., The cBio cancer genomics portal: an open platform for exploring multidimensional cancer genomics data, Cancer Discov. 2 (5) (2012) 401–404.
[23] J. Gao, et al., Integrative analysis of complex cancer genomics and clinical profiles using the cBioPortal, Sci. Signal. 6 (269) (2013) pl1-pl1.
[24] B. Győrffy, Integrated analysis of public datasets for the discovery and validation of survival-associated genes in solid tumors, Innovation 5 (3) (2024).
[25] A. Varol, et al., Enhancing cisplatin drug sensitivity through PARP3 inhibition: the influence on PDGF and G-coupled signal pathways in cancer, Chem. Biol. Interact. (2024) 111094.
[26] N.R. Jette, et al., Combined poly-ADP ribose polymerase and ataxia-telangiectasia mutated/Rad3-related inhibition targets ataxia-telangiectasia mutated-deficient lung cancer cells, Br. J. Cancer 121 (7) (2019) 600–610.
[27] J. O'brien, et al., Investigation of the Alamar Blue (resazurin) fluorescent dye for the assessment of mammalian cell cytotoxicity, Eur. J. Biochem. 267 (17) (2000) 5421–5426.
[28] J. Petiti, L. Revel, C. Divieto, Standard operating procedure to optimize resazurin-based viability assays, Biosensors 14 (4) (2024) 156.
[29] K.J. Livak, T.D. Schmittgen, Analysis of relative gene expression data using real-time quantitative PCR and the 2− ΔΔCT method, Methods 25 (4) (2001) 402–408.
[30] I. Vermes, et al., A novel assay for apoptosis flow cytometric detection of phosphatidylserine expression on early apoptotic cells using fluorescein labelled annexin V, J. Immunol. Methods 184 (1) (1995) 39–51.
[31] M.E. Saeed, et al., Disruption of lipid raft microdomains, regulation of cd38, tp53, and myc signaling, and induction of apoptosis by lomitapide in multiple myeloma cells, Cancer Genom. Proteom. 19 (5) (2022) 540–555.

[32] N.N. Hooten, M.K. Evans, Techniques to induce and quantify cellular senescence, J. Vis. Exp. 123 (2017).
[33] B.M. Gyori, et al., OpenComet: an automated tool for comet assay image analysis, Redox Biol. 2 (2014) 457–465.
[34] P. Ortiz-Montero, A. Londoño-Vallejo, J.-P. Vernot, Senescence-associated IL-6 and IL-8 cytokines induce a self-and cross-reinforced senescence/inflammatory milieu strengthening tumorigenic capabilities in the MCF-7 breast cancer cell line, Cell Commun. Signal. 15 (2017) 1–18.
[35] C.A. Schmitt, B. Wang, M. Demaria, Senescence and cancer—role and therapeutic opportunities, Nat. Rev. Clin. Oncol. 19 (10) (2022) 619–636.
[36] N.R. Jette, et al., ATM-deficient cancers provide new opportunities for precision oncology, Cancers 12 (3) (2020) 687.
[37] S. Matsuoka, et al., ATM and ATR substrate analysis reveals extensive protein networks responsive to DNA damage, Science 316 (5828) (2007) 1160–1166.
[38] D. Menolfi, S. Zha, ATM, ATR and DNA-PKcs kinases—the lessons from the mouse models: inhibition≠ deletion, Cell Biosci. 10 (1) (2020) 8.
[39] S. Putti, et al., ATM kinase dead: from ataxia telangiectasia syndrome to cancer, Cancers 13 (21) (2021) 5498.
[40] V. Stagni, et al., ATM kinase-dependent regulation of autophagy: a key player in senescence? Front. Cell Dev. Biol. 8 (2021) 599048.
[41] M. Choi, T. Kipps, R. Kurzrock, ATM mutations in cancer: therapeutic implications, Mol. Cancer Therapeut. 15 (8) (2016) 1781–1791.
[42] K. Yamamoto, et al., Kinase-dead ATM protein is highly oncogenic and can be preferentially targeted by Topo-isomerase I inhibitors, eLife 5 (2016) e14709.
[43] Y. Zhou, et al., ATM deficiency confers specific therapeutic vulnerabilities in bladder cancer, Sci. Adv. 9 (47) (2023) eadg2263.
[44] E. Stefàno, et al., An overview of altered pathways associated with sensitivity to platinum-based chemotherapy in neuroendocrine tumors: strengths and prospects, Int. J. Mol. Sci. 25 (16) (2024) 8568.
[45] T. Boulikas, M. Vougiouka, Cisplatin and platinum drugs at the molecular level, Oncol. Rep. 10 (6) (2003) 1663–1682.
[46] D.J. Stewart, Mechanisms of resistance to cisplatin and carboplatin, Crit. Rev. Oncol.-Hematol. 63 (1) (2007) 12–31.
[47] L. Wang, L. Lankhorst, R. Bernards, Exploiting senescence for the treatment of cancer, Nat. Rev. Cancer 22 (6) (2022) 340–355.
[48] K.M. Aird, R. Zhang, ATM in senescence, Oncotarget 6 (17) (2015) 14729.
[49] J. Campisi, F. d'Adda di Fagagna, Cellular senescence: when bad things happen to good cells, Nat. Rev. Mol. Cell Biol. 8 (9) (2007) 729–740.
[50] H.T. Kang, et al., Chemical screening identifies ATM as a target for alleviating senescence, Nat. Chem. Biol. 13 (6) (2017) 616–623.
[51] J. Zhao, et al., ATM is a key driver of NF-κB-dependent DNA-damage-induced senescence, stem cell dysfunction and aging, Aging (Albany NY) 12 (6) (2020) 4688.
[52] J.M. Van Deursen, The role of senescent cells in ageing, Nature 509 (7501) (2014) 439–446.
[53] M. Eppard, J.F. Passos, S. Victorelli, Telomeres, cellular senescence, and aging: past and future, Biogerontology 25 (2) (2024) 329–339.
[54] M. Reimann, S. Lee, C.A. Schmitt, Cellular senescence: neither irreversible nor reversible, J. Exp. Med. 221 (4) (2024) e20232136.
[55] M.U. Kuk, et al., Alleviation of senescence via ATM inhibition in accelerated aging models, Mol. Cells 42 (3) (2019) 210–217.
[56] J.-H. Lee, Oxidative stress and the multifaceted roles of ATM in maintaining cellular redox homeostasis, Redox Biol. 75 (2024) 103269.
[57] S.K. Niture, R. Khatri, A.K. Jaiswal, Regulation of Nrf2—an update, Free Radic. Biol. Med. 66 (2014) 36–44.
[58] W. Li, A.N. Kong, Molecular mechanisms of Nrf2-mediated antioxidant response, Mol. Carcinog.: Publ. Cooperat. University of Texas MD Anderson Cancer Center 48 (2) (2009) 91–104.
[59] H.S. Khalil, Y. Deeni, NRF2 inhibition causes repression of ATM and ATR expression leading to aberrant DNA Damage Response, BioDiscovery 15 (2015) e8964.

5. Conclusion

The main factor underlying cisplatin resistance is increasingly accumulation of mutations and altered expression levels. In consider of cancer heterogenous nature, identification right target to overcome cancer resistance requires in- dept bioinformatics analyses. The identification of precise targets and the factors underlying altered signalling pathways will be crucial for developing strategies to cancer treatment. In these studies, we also aim to select the right target by avoiding conflicting results and further conducting the pathway analyses.

PARP3 was identified as a key factor in cisplatin resistance through integrative survival and mutation analyses. *PARP3* overexpression is correlated with poor survival. *PARP3* inhibition makes breast cancer cells sensitive to cisplatin by downregulating PDGF and GPCRs-signaling pathways. According to our findings, agents targeting PARP3 may enhance chemotherapy efficacy by modulating proliferation and survival-related pathways.

In conclusion, our findings emphasize the multiple roles of *MSH6* within MMR system. *MSH6* modulates the balance between pro-survival and pro-death autophagy as well as maintains genomic stability. The *MSH6* inhibition makes cancer cells vulnerable to platinum-based drugs, resulting in drug sensitivity. The role of MSH6 is primarily linked to the disruption of autophagy and alternative cell death pathways activation, including apoptosis and ferroptosis. Particularly, the findings highlight the modulatory role of MSH6-associated pro-survival and pro-death autophagy processes. Notably, the altered signalling activation in MSH6-deficient cells — characterized by increased activity in the NRF2, mTOR, and PI3K/Akt pathways — contributes to enhanced drug efficacy and decreased cellular proliferation, even at lower cisplatin doses. MSH6 may be considered as a therapeutic target for the development of new drug agent. The development of drug agents targeting MSH6 may optimize cisplatin-based regimens in a more personalized oncology framework.

ATM was identified as another possible biomarker responsible for cisplatin resistance in lung cancer. According to obtained data, ATM inhibition enhances the cytotoxicity of cisplatin by increasing ROS levels and changing activation of alternative cell death pathways, such as necroptosis, ferroptosis, and NRF2 signalling. The alteration of pathways associated with oxidative stress contribute to the induction of senescence. Also, the obtained findings reveal the critical role of ATM in mediating oxidative stress-induced senescence related cellular responses. Moreover, transcriptomic data provided as a supporting result for this hypothesis.

6. References

1. Yeh, A.C. and S. Ramaswamy, *Mechanisms of cancer cell dormancy—another hallmark of cancer?* Cancer research, 2015. **75**(23): p. 5014-5022.
2. Friedl, W. and C. Herfarth, *Long-term prognosis of breast cancer—retrospective examination of 973 patients.* Langenbecks Archiv für Chirurgie, 1992. **377**: p. 168-173.
3. Leman, J. and R. Mac Kie, *Late (> 10 years) recurrence of melanoma: the Scottish experience.* British Journal of Dermatology, 2003. **148**(2): p. 372-373.
4. Carbone, A., *Cancer classification at the crossroads.* Cancers, 2020. **12**(4): p. 980.
5. Jardim, M.J., et al., *Reduced ATR or Chk1 expression leads to chromosome instability and chemosensitization of mismatch repair–deficient colorectal cancer cells.* Molecular biology of the cell, 2009. **20**(17): p. 3801-3809.
6. Krokan, H.E., et al., *Base excision repair of DNA in mammalian cells.* FEBS letters, 2000. **476**(1-2): p. 73-77.
7. Sancar, A., et al., *Molecular mechanisms of mammalian DNA repair and the DNA damage checkpoints.* Annual review of biochemistry, 2004. **73**(1): p. 39-85.
8. Hanahan, D. and R.A. Weinberg, *The hallmarks of cancer.* cell, 2000. **100**(1): p. 57-70.
9. Hanahan, D. and R.A. Weinberg, *Hallmarks of cancer: the next generation.* cell, 2011. **144**(5): p. 646-674.
10. A. Baudino, T., *Targeted cancer therapy: the next generation of cancer treatment.* Current drug discovery technologies, 2015. **12**(1): p. 3-20.
11. Debela, D.T., et al., *New approaches and procedures for cancer treatment: Current perspectives.* SAGE open medicine, 2021. **9**: p. 20503121211034366.
12. Kaur, R., A. Bhardwaj, and S. Gupta, *Cancer treatment therapies: traditional to modern approaches to combat cancers.* Molecular biology reports, 2023. **50**(11): p. 9663-9676.
13. Chu, D.-T., et al., *Recent progress of stem cell therapy in cancer treatment: molecular mechanisms and potential applications.* Cells, 2020. **9**(3): p. 563.
14. Ross, G., *Induction of cell death by radiotherapy.* Endocrine-related cancer, 1999. **6**(1): p. 41-44.
15. Abraham, J. and J. Staffurth, *Hormonal therapy for cancer.* Medicine, 2011. **39**(12): p. 723-727.
16. Wirth, T. and S. Ylä-Herttuala, *Gene therapy used in cancer treatment.* Biomedicines, 2014. **2**(2): p. 149-162.
17. Tilsed, C.M., et al., *Cancer chemotherapy: insights into cellular and tumor microenvironmental mechanisms of action.* Frontiers in oncology, 2022. **12**: p. 960317.
18. Behranvand, N., et al., *Chemotherapy: a double-edged sword in cancer treatment.* Cancer immunology, immunotherapy, 2022. **71**(3): p. 507-526.
19. DeVita Jr, V.T. and E. Chu, *A history of cancer chemotherapy.* Cancer research, 2008. **68**(21): p. 8643-8653.
20. Oun, R., Y.E. Moussa, and N.J. Wheate, *The side effects of platinum-based chemotherapy drugs: a review for chemists.* Dalton transactions, 2018. **47**(19): p. 6645-6653.
21. Peters, G.J., *Novel developments in the use of antimetabolites.* Nucleosides, Nucleotides and Nucleic Acids, 2014. **33**(4-6): p. 358-374.
22. Ralhan, R. and J. Kaur, *Alkylating agents and cancer therapy.* Expert Opinion on Therapeutic Patents, 2007. **17**(9): p. 1061-1075.
23. Warwick, G., *The mechanism of action of alkylating agents.* Cancer research, 1963. **23**(8_Part_1): p. 1315-1333.
24. Chan, K., C.G. Koh, and H. Li, *Mitosis-targeted anti-cancer therapies: where they stand.* Cell death & disease, 2012. **3**(10): p. e411-e411.
25. Naaz, F., et al., *Anti-tubulin agents of natural origin: Targeting taxol, vinca, and colchicine binding domains.* European journal of medicinal chemistry, 2019. **171**: p. 310-331.

26. Jiang, N., et al., *Advances in mitotic inhibitors for cancer treatment.* Mini Reviews in Medicinal Chemistry, 2006. **6**(8): p. 885-895.
27. Hortobagyi, G., *Anthracyclines in the treatment of cancer: an overview.* Drugs, 1997. **54**(Suppl 4): p. 1-7.
28. Weiss, R.B. *The anthracyclines: will we ever find a better doxorubicin?* in *Seminars in oncology*. 1992.
29. McGowan, J.V., et al., *Anthracycline chemotherapy and cardiotoxicity.* Cardiovascular drugs and therapy, 2017. **31**: p. 63-75.
30. Singal, P.K. and N. Iliskovic, *Doxorubicin-induced cardiomyopathy.* New England Journal of Medicine, 1998. **339**(13): p. 900-905.
31. Persson, I., *Estrogens in the causation of breast, endometrial and ovarian cancers—evidence and hypotheses from epidemiological findings.* The Journal of steroid biochemistry and molecular biology, 2000. **74**(5): p. 357-364.
32. Key, T.J., *Hormones and cancer in humans.* Mutation Research/Fundamental and Molecular Mechanisms of Mutagenesis, 1995. **333**(1-2): p. 59-67.
33. Padma, V.V., *An overview of targeted cancer therapy.* BioMedicine, 2015. **5**: p. 1-6.
34. Zhong, L., et al., *Small molecules in targeted cancer therapy: advances, challenges, and future perspectives.* Signal transduction and targeted therapy, 2021. **6**(1): p. 201.
35. Hoelder, S., P.A. Clarke, and P. Workman, *Discovery of small molecule cancer drugs: successes, challenges and opportunities.* Molecular oncology, 2012. **6**(2): p. 155-176.
36. Behl, A., et al., *Monoclonal antibodies in breast cancer: A critical appraisal.* Critical reviews in Oncology/hematology, 2023. **183**: p. 103915.
37. Masoud, V. and G. Pagès, *Targeted therapies in breast cancer: New challenges to fight against resistance.* World journal of clinical oncology, 2017. **8**(2): p. 120.
38. Harries, M. and I. Smith, *The development and clinical use of trastuzumab (Herceptin).* Endocrine-related cancer, 2002. **9**(2): p. 75-85.
39. Johnson, P. and M. Glennie, *Rituximab: mechanisms and applications.* British journal of cancer, 2001. **85**(11): p. 1619-1623.
40. Saxena, M., et al., *Therapeutic cancer vaccines.* Nature Reviews Cancer, 2021. **21**(6): p. 360-378.
41. Belete, T.M., *The current status of gene therapy for the treatment of cancer.* Biologics: Targets and Therapy, 2021: p. 67-77.
42. Colella, P., G. Ronzitti, and F. Mingozzi, *Emerging issues in AAV-mediated in vivo gene therapy.* Molecular therapy Methods & clinical development, 2018. **8**: p. 87-104.
43. Merten, O.-W., et al., *Large-scale manufacture and characterization of a lentiviral vector produced for clinical ex vivo gene therapy application.* Human gene therapy, 2011. **22**(3): p. 343-356.
44. Cox, D.B.T., R.J. Platt, and F. Zhang, *Therapeutic genome editing: prospects and challenges.* Nature medicine, 2015. **21**(2): p. 121-131.
45. Pickar-Oliver, A. and C.A. Gersbach, *The next generation of CRISPR–Cas technologies and applications.* Nature reviews Molecular cell biology, 2019. **20**(8): p. 490-507.
46. Zhan, T., et al. *CRISPR/Cas9 for cancer research and therapy*. in *Seminars in cancer biology*. 2019. Elsevier.
47. Chen, M., et al., *CRISPR-Cas9 for cancer therapy: Opportunities and challenges.* Cancer letters, 2019. **447**: p. 48-55.
48. Brown, A., S. Kumar, and P.B. Tchounwou, *Cisplatin-based chemotherapy of human cancers.* Journal of cancer science & therapy, 2019. **11**(4): p. 97.
49. Mantri, Y., S.J. Lippard, and M.-H. Baik, *Bifunctional binding of cisplatin to DNA: why does cisplatin form 1, 2-intrastrand cross-links with AG but not with GA?* Journal of the American Chemical Society, 2007. **129**(16): p. 5023-5030.

50. Rezaei, S., et al., *Investigation on the Effect of Fluorescence Quenching of Calf Thymus DNA by Piperine: Caspase Activation in the Human Breast Cancer Cell Line Studies.* DNA and Cell Biology, 2024. **43**(1): p. 26-38.
51. Tchounwou, P.B., et al., *Advances in our understanding of the molecular mechanisms of action of cisplatin in cancer therapy.* Journal of experimental pharmacology, 2021: p. 303-328.
52. Dasari, S. and P.B. Tchounwou, *Cisplatin in cancer therapy: molecular mechanisms of action.* European journal of pharmacology, 2014. **740**: p. 364-378.
53. Romani, A.M., *Cisplatin in cancer treatment.* Biochemical pharmacology, 2022. **206**: p. 115323.
54. Kartalou, M. and J.M. Essigmann, *Mechanisms of resistance to cisplatin.* Mutation Research/Fundamental and Molecular Mechanisms of Mutagenesis, 2001. **478**(1-2): p. 23-43.
55. Akiyama, S., et al., *Resistance to cisplatin.* Anti-cancer drug design, 1999. **14**(2): p. 143-151.
56. Kaina, B., et al., *MGMT: key node in the battle against genotoxicity, carcinogenicity and apoptosis induced by alkylating agents.* DNA repair, 2007. **6**(8): p. 1079-1099.
57. Christmann, M., et al., *Mechanisms of human DNA repair: an update.* Toxicology, 2003. **193**(1-2): p. 3-34.
58. Xu, M., et al., *MGMT DNA repair gene promoter/enhancer haplotypes alter transcription factor binding and gene expression.* Cellular Oncology, 2016. **39**: p. 435-447.
59. Pegg, A.E., *Repair of O6-alkylguanine by alkyltransferases.* Mutation Research/Reviews in Mutation Research, 2000. **462**(2-3): p. 83-100.
60. Kostka, T., et al., *Repair of O 6-carboxymethylguanine adducts by O 6-methylguanine-DNA methyltransferase in human colon epithelial cells.* Carcinogenesis, 2021. **42**(8): p. 1110-1118.
61. Mishina, Y., E.M. Duguid, and C. He, *Direct reversal of DNA alkylation damage.* Chemical reviews, 2006. **106**(2): p. 215-232.
62. Sedgwick, B., *Repairing DNA-methylation damage.* Nature reviews Molecular cell biology, 2004. **5**(2): p. 148-157.
63. Dianov, G. and T. Lindahl, *Reconstitution of the DNA base excision—repair pathway.* Current biology, 1994. **4**(12): p. 1069-1076.
64. Camacho, I.S.C.E., *Effects of UV radiation exposure on DNA and DNA repair enzymes*. 2012, Faculdade de Ciências e Tecnologia.
65. Hegde, M.L., T.K. Hazra, and S. Mitra, *Early steps in the DNA base excision/single-strand interruption repair pathway in mammalian cells.* Cell research, 2008. **18**(1): p. 27-47.
66. Hanssen-Bauer, A., et al., *X-ray repair cross complementing protein 1 in base excision repair.* International journal of molecular sciences, 2012. **13**(12): p. 17210-17229.
67. Nilsen, H. and H.E. Krokan, *Base excision repair in a network of defence and tolerance.* Carcinogenesis, 2001. **22**(7): p. 987-998.
68. Levine, A.J., *p53, the cellular gatekeeper for growth and division.* cell, 1997. **88**(3): p. 323-331.
69. Jansson, K., et al., *Evolutionary loss of 8-oxo-G repair components among eukaryotes.* Genome integrity, 2010. **1**(1): p. 1-10.
70. Krokan, H.E., R. Standal, and G. Slupphaug, *DNA glycosylases in the base excision repair of DNA.* Biochemical Journal, 1997. **325**(1): p. 1-16.
71. Schärer, O.D. and J. Jiricny, *Recent progress in the biology, chemistry and structural biology of DNA glycosylases.* Bioessays, 2001. **23**(3): p. 270-281.
72. Hang, B., *Base excision repair*, in *DNA Repair, Genetic Instability, and Cancer*. 2007, World Scientific. p. 23-64.
73. Jackson, S.P. and J. Bartek, *The DNA-damage response in human biology and disease.* Nature, 2009. **461**(7267): p. 1071-1078.
74. Mullins, E.A., et al., *Emerging roles of DNA glycosylases and the base excision repair pathway.* Trends in biochemical sciences, 2019. **44**(9): p. 765-781.

75. Wallace, S.S., D.L. Murphy, and J.B. Sweasy, *Base excision repair and cancer.* Cancer letters, 2012. **327**(1-2): p. 73-89.
76. Fortini, P., et al., *The base excision repair: mechanisms and its relevance for cancer susceptibility.* Biochimie, 2003. **85**(11): p. 1053-1071.
77. Chatterjee, N. and G.C. Walker, *Mechanisms of DNA damage, repair, and mutagenesis.* Environmental and molecular mutagenesis, 2017. **58**(5): p. 235-263.
78. Zharkov, D., *Base excision DNA repair.* Cellular and molecular life sciences, 2008. **65**(10): p. 1544-1565.
79. Lindahl, T., *An N-glycosidase from Escherichia coli that releases free uracil from DNA containing deaminated cytosine residues.* Proceedings of the National Academy of Sciences, 1974. **71**(9): p. 3649-3653.
80. Jacobs, A.L. and P. Schär, *DNA glycosylases: in DNA repair and beyond.* Chromosoma, 2012. **121**(1): p. 1-20.
81. Lindahl, T., *Repair of intrinsic DNA lesions.* Mutation Research/Reviews in Genetic Toxicology, 1990. **238**(3): p. 305-311.
82. Wyatt, M.D., et al., *3-methyladenine DNA glycosylases: structure, function, and biological importance.* Bioessays, 1999. **21**(8): p. 668-676.
83. Fortini, P., et al., *The type of DNA glycosylase determines the base excision repair pathway in mammalian cells.* Journal of Biological Chemistry, 1999. **274**(21): p. 15230-15236.
84. Fromme, J.C., A. Banerjee, and G.L. Verdine, *DNA glycosylase recognition and catalysis.* Current opinion in structural biology, 2004. **14**(1): p. 43-49.
85. Brooks, S.C., et al., *Recent advances in the structural mechanisms of DNA glycosylases.* Biochimica et Biophysica Acta (BBA)-Proteins and Proteomics, 2013. **1834**(1): p. 247-271.
86. Nilsen, H., et al., *Uracil-DNA glycosylase (UNG)-deficient mice reveal a primary role of the enzyme during DNA replication.* Molecular cell, 2000. **5**(6): p. 1059-1065.
87. Otterlei, M., et al., *Post-replicative base excision repair in replication foci.* The EMBO journal, 1999. **18**(13): p. 3834-3844.
88. Raja, S. and B. Van Houten, *The multiple cellular roles of SMUG1 in genome maintenance and cancer.* International Journal of Molecular Sciences, 2021. **22**(4): p. 1981.
89. Cortázar, D., et al., *The enigmatic thymine DNA glycosylase.* DNA repair, 2007. **6**(4): p. 489-504.
90. Wu, P., et al., *Mismatch repair in methylated DNA: Structure and activity of the mismatch-specific thymine glycosylase domain of methyl-CpG-binding protein MBD4.* Journal of Biological Chemistry, 2003. **278**(7): p. 5285-5291.
91. Au, K., et al., *Escherichia coli mutY gene product is required for specific AG----CG mismatch correction.* Proceedings of the National Academy of Sciences, 1988. **85**(23): p. 9163-9166.
92. Klungland, A. and S. Bjelland, *Oxidative damage to purines in DNA: role of mammalian Ogg1.* DNA repair, 2007. **6**(4): p. 481-488.
93. Janik, J., et al., *8-Oxoguanine incision activity is impaired in lung tissues of NSCLC patients with the polymorphism of OGG1 and XRCC1 genes.* Mutation Research/Fundamental and Molecular Mechanisms of Mutagenesis, 2011. **709**: p. 21-31.
94. Stanczyk, M., et al., *The association of polymorphisms in DNA base excision repair genes XRCC1, OGG1 and MUTYH with the risk of childhood acute lymphoblastic leukemia.* Molecular biology reports, 2011. **38**(1): p. 445-451.
95. Krokan, H.E. and M. Bjørås, *Base excision repair.* Cold Spring Harbor perspectives in biology, 2013. **5**(4): p. a012583.
96. Wilson III, D.M. and D. Barsky, *The major human abasic endonuclease: formation, consequences and repair of abasic lesions in DNA.* Mutation Research/DNA Repair, 2001. **485**(4): p. 283-307.
97. Dyrkheeva, N., S. Khodyreva, and O. Lavrik, *Multifunctional human apurinic/apyrimidinic endonuclease 1: Role of additional functions.* Molecular Biology, 2007. **41**(3): p. 402-416.

98. Mitra, S., et al., *Intracellular trafficking and regulation of mammalian AP-endonuclease 1 (APE1), an essential DNA repair protein.* DNA repair, 2007. **6**(4): p. 461-469.
99. Wallace, S.S., *Base excision repair: a critical player in many games.* DNA repair, 2014. **19**: p. 14-26.
100. Sattler, U., et al., *Long-patch DNA repair synthesis during base excision repair in mammalian cells.* EMBO reports, 2003. **4**(4): p. 363-367.
101. Sung, J.S. and B. Demple, *Roles of base excision repair subpathways in correcting oxidized abasic sites in DNA.* The FEBS journal, 2006. **273**(8): p. 1620-1629.
102. Balakrishnan, L., et al., *Long patch base excision repair proceeds via coordinated stimulation of the multienzyme DNA repair complex.* Journal of Biological Chemistry, 2009. **284**(22): p. 15158-15172.
103. Liu, Y., et al., *DNA polymerase β and flap endonuclease 1 enzymatic specificities sustain DNA synthesis for long patch base excision repair.* Journal of Biological Chemistry, 2005. **280**(5): p. 3665-3674.
104. Matsumoto, Y. and K. Kim, *Excision of deoxyribose phosphate residues by DNA polymerase β during DNA repair.* Science, 1995. **269**(5224): p. 699-702.
105. Dianov, G.L., et al., *Repair of abasic sites in DNA.* Mutation Research/Fundamental and Molecular Mechanisms of Mutagenesis, 2003. **531**(1-2): p. 157-163.
106. Tomkinson, A.E. and Z.B. Mackey, *Structure and function of mammalian DNA ligases.* Mutation Research/DNA Repair, 1998. **407**(1): p. 1-9.
107. Henneke, G., E. Friedrich-Heineken, and U. Hübscher, *Flap endonuclease 1: a novel tumour suppresser protein.* Trends in biochemical sciences, 2003. **28**(7): p. 384-390.
108. Bambara, R.A., R.S. Murante, and L.A. Henricksen, *Enzymes and reactions at the eukaryotic DNA replication fork.* Journal of Biological Chemistry, 1997. **272**(8): p. 4647-4650.
109. Matsumoto, Y., *Molecular mechanism of PCNA-dependent base excision repair.* Progress in nucleic acid research and molecular biology, 2001. **68**: p. 129-138.
110. Helt, C.E., et al., *9-1-1 complex involvement in DNA repair: evidence that DNA damage detection machinery participates in DNA repair.* Cell cycle, 2005. **4**(4): p. 529-532.
111. Gembka, A., et al., *The checkpoint clamp, Rad9-Rad1-Hus1 complex, preferentially stimulates the activity of apurinic/apyrimidinic endonuclease 1 and DNA polymerase β in long patch base excision repair.* Nucleic acids research, 2007. **35**(8): p. 2596-2608.
112. Prasad, R., et al., *Specific interaction of DNA polymerase β and DNA ligase I in a multiprotein base excision repair complex from bovine testis.* Journal of Biological Chemistry, 1996. **271**(27): p. 16000-16007.
113. Conde-Pérezprina, J.C., M.Á. León-Galván, and M. Konigsberg, *DNA mismatch repair system: repercussions in cellular homeostasis and relationship with aging.* Oxidative medicine and cellular longevity, 2012. **2012**.
114. Wang, J.Y. and W. Edelmann, *Mismatch repair proteins as sensors of alkylation DNA damage.* Cancer cell, 2006. **9**(6): p. 417-418.
115. Ramilo, C., et al., *Partial reconstitution of human DNA mismatch repair in vitro: characterization of the role of human replication protein A.* Molecular and cellular biology, 2002. **22**(7): p. 2037-2046.
116. Li, G.-M., *Mechanisms and functions of DNA mismatch repair.* Cell research, 2008. **18**(1): p. 85-98.
117. Ijsselsteijn, R., J.G. Jansen, and N. de Wind, *DNA mismatch repair-dependent DNA damage responses and cancer.* DNA repair, 2020. **93**: p. 102923.
118. Li, Z., A.H. Pearlman, and P. Hsieh, *DNA mismatch repair and the DNA damage response.* DNA repair, 2016. **38**: p. 94-101.
119. Kunkel, T.A. and D.A. Erie, *Eukaryotic mismatch repair in relation to DNA replication.* Annual review of genetics, 2015. **49**: p. 291.
120. Kunkel, T.A. and D.A. Erie, *DNA mismatch repair.* Annu. Rev. Biochem., 2005. **74**: p. 681-710.

121. Fink, D., S. Aebi, and S.B. Howell, *The role of DNA mismatch repair in drug resistance.* Clinical cancer research: an official journal of the American Association for Cancer Research, 1998. **4**(1): p. 1-6.
122. O'Brien, V. and R. Brown, *Signalling cell cycle arrest and cell death through the MMR System.* Carcinogenesis, 2006. **27**(4): p. 682-692.
123. Duckett, D.R., et al., *hMutSα-and hMutLα-dependent phosphorylation of p53 in response to DNA methylator damage.* Proceedings of the National Academy of Sciences, 1999. **96**(22): p. 12384-12388.
124. Ko, L.J. and C. Prives, *p53: puzzle and paradigm.* Genes & development, 1996. **10**(9): p. 1054-1072.
125. Jun, S.H., T.G. Kim, and C. Ban, *DNA mismatch repair system: Classical and fresh roles.* The FEBS journal, 2006. **273**(8): p. 1609-1619.
126. Fedier, A., et al., *Resistance to topoisomerase poisons due to loss of DNA mismatch repair.* International journal of cancer, 2001. **93**(4): p. 571-576.
127. Fishel, R., *Signaling mismatch repair in cancer.* Nature medicine, 1999. **5**(11): p. 1239-1241.
128. Reyes, G.X., et al., *New insights into the mechanism of DNA mismatch repair.* Chromosoma, 2015. **124**(4): p. 443-462.
129. Peltomäki, P., *DNA mismatch repair and cancer.* Mutation Research/Reviews in Mutation Research, 2001. **488**(1): p. 77-85.
130. Trautmann, K., et al., *Chromosomal instability in microsatellite-unstable and stable colon cancer.* Clinical Cancer Research, 2006. **12**(21): p. 6379-6385.
131. Nojadeh, J.N., S.B. Sharif, and E. Sakhinia, *Microsatellite instability in colorectal cancer.* EXCLI journal, 2018. **17**: p. 159.
132. Vilar, E. and S.B. Gruber, *Microsatellite instability in colorectal cancer—the stable evidence.* Nature reviews Clinical oncology, 2010. **7**(3): p. 153-162.
133. Geigl, J.B., et al., *Defining 'chromosomal instability'.* Trends in Genetics, 2008. **24**(2): p. 64-69.
134. Pino, M.S. and D.C. Chung, *The chromosomal instability pathway in colon cancer.* Gastroenterology, 2010. **138**(6): p. 2059-2072.
135. Chung, D.C. and A.K. Rustgi, *The hereditary nonpolyposis colorectal cancer syndrome: genetics and clinical implications.* Annals of internal medicine, 2003. **138**(7): p. 560-570.
136. Pećina-Šlaus, N., et al., *Mismatch repair pathway, genome stability and cancer.* Frontiers in molecular biosciences, 2020: p. 122.
137. Kolodner, R.D. and G.T. Marsischky, *Eukaryotic DNA mismatch repair.* Current opinion in genetics & development, 1999. **9**(1): p. 89-96.
138. Russo, M.T., et al., *The oxidized deoxynucleoside triphosphate pool is a significant contributor to genetic instability in mismatch repair-deficient cells.* Molecular and cellular biology, 2004. **24**(1): p. 465-474.
139. Modrich, P., *Mechanisms in eukaryotic mismatch repair.* Journal of Biological Chemistry, 2006. **281**(41): p. 30305-30309.
140. Sixma, T.K., *DNA mismatch repair: MutS structures bound to mismatches.* Current opinion in structural biology, 2001. **11**(1): p. 47-52.
141. Jiricny, J., *The multifaceted mismatch-repair system.* Nature reviews Molecular cell biology, 2006. **7**(5): p. 335-346.
142. Guo, S., et al., *Differential requirement for proliferating cell nuclear antigen in 5′ and 3′ nick-directed excision in human mismatch repair.* Journal of Biological Chemistry, 2004. **279**(17): p. 16912-16917.
143. Hsieh, P., *Molecular mechanisms of DNA mismatch repair.* Mutation Research/DNA Repair, 2001. **486**(2): p. 71-87.
144. Junop, M.S., et al., *Composite active site of an ABC ATPase: MutS uses ATP to verify mismatch recognition and authorize DNA repair.* Molecular cell, 2001. **7**(1): p. 1-12.
145. Lamers, M.H., H.H. Winterwerp, and T.K. Sixma, *The alternating ATPase domains of MutS control DNA mismatch repair.* The EMBO journal, 2003. **22**(3): p. 746-756.

146. Ortega, J., et al., *Mispair-bound human MutS–MutL complex triggers DNA incisions and activates mismatch repair.* Cell research, 2021. **31**(5): p. 542-553.
147. Fukui, K., *DNA mismatch repair in eukaryotes and bacteria.* Journal of nucleic acids, 2010. **2010**.
148. Pannafino, G. and E. Alani, *Coordinated and independent roles for MLH subunits in DNA repair.* Cells, 2021. **10**(4): p. 948.
149. Marti, T.M., C. Kunz, and O. Fleck, *DNA mismatch repair and mutation avoidance pathways.* Journal of cellular physiology, 2002. **191**(1): p. 28-41.
150. Putnam, C.D., *Strand discrimination in DNA mismatch repair.* DNA repair, 2021. **105**: p. 103161.
151. Umar, A., et al., *Requirement for PCNA in DNA mismatch repair at a step preceding DNA resynthesis.* Cell, 1996. **87**(1): p. 65-73.
152. Kelman, Z. and J. Hurwitz, *Protein–PCNA interactions: a DNA-scanning mechanism?* Trends in biochemical sciences, 1998. **23**(7): p. 236-238.
153. Flores-Rozas, H., D. Clark, and R.D. Kolodner, *Proliferating cell nuclear antigen and Msh2p-Msh6p interact to form an active mispair recognition complex.* Nature genetics, 2000. **26**(3): p. 375-378.
154. Sameer, A.S., S. Nissar, and K. Fatima, *Mismatch repair pathway.* European Journal of Cancer Prevention, 2014. **23**(4): p. 246-257.
155. Majka, J. and P.M. Burgers, *The PCNA-RFC families of DNA clamps and clamp loaders.* Progress in nucleic acid research and molecular biology, 2004. **78**: p. 227-260.
156. Kadyrov, F.A., et al., *Endonucleolytic function of MutLα in human mismatch repair.* cell, 2006. **126**(2): p. 297-308.
157. Genschel, J. and P. Modrich, *Mechanism of 5'-directed excision in human mismatch repair.* Molecular cell, 2003. **12**(5): p. 1077-1086.
158. Longley, M.J., A.J. Pierce, and P. Modrich, *DNA polymerase δ is required for human mismatch repair in vitro.* Journal of Biological Chemistry, 1997. **272**(16): p. 10917-10921.
159. Friedberg, E.C., *How nucleotide excision repair protects against cancer.* Nature Reviews Cancer, 2001. **1**(1): p. 22-33.
160. Fojo, T., *Cancer, DNA repair mechanisms, and resistance to chemotherapy*. 2001, Oxford University Press. p. 1434-1436.
161. de Laat, W.L., N.G. Jaspers, and J.H. Hoeijmakers, *Molecular mechanism of nucleotide excision repair.* Genes & development, 1999. **13**(7): p. 768-785.
162. Marteijn, J.A., et al., *Understanding nucleotide excision repair and its roles in cancer and ageing.* Nature reviews Molecular cell biology, 2014. **15**(7): p. 465-481.
163. Petruseva, I., A. Evdokimov, and O. Lavrik, *Molecular mechanism of global genome nucleotide excision repair.* Acta Naturae (англоязычная версия), 2014. **6**(1 (20)): p. 23-34.
164. Balajee, A.S. and V.A. Bohr, *Genomic heterogeneity of nucleotide excision repair.* Gene, 2000. **250**(1-2): p. 15-30.
165. Svejstrup, J.Q., *Rescue of arrested RNA polymerase II complexes.* Journal of Cell Science, 2003. **116**(3): p. 447-451.
166. Schärer, O.D., *Nucleotide excision repair in eukaryotes.* Cold Spring Harbor perspectives in biology, 2013. **5**(10): p. a012609.
167. Saijo, M., *The role of Cockayne syndrome group A (CSA) protein in transcription-coupled nucleotide excision repair.* Mechanisms of ageing and development, 2013. **134**(5-6): p. 196-201.
168. Fousteri, M. and L.H. Mullenders, *Transcription-coupled nucleotide excision repair in mammalian cells: molecular mechanisms and biological effects.* Cell research, 2008. **18**(1): p. 73-84.
169. Staresincic, L., et al., *Coordination of dual incision and repair synthesis in human nucleotide excision repair.* The EMBO journal, 2009. **28**(8): p. 1111-1120.

170. Hanawalt, P.C., *Controlling the efficiency of excision repair.* Mutation Research/DNA Repair, 2001. **485**(1): p. 3-13.
171. Tan, W.H., et al., *Cockayne syndrome: the developing phenotype.* American journal of medical genetics Part A, 2005. **135**(2): p. 214-216.
172. van Hoffen, A., et al., *Deficient repair of the transcribed strand of active genes in Cockayne's syndrome cells.* Nucleic acids research, 1993. **21**(25): p. 5890-5895.
173. Karikkineth, A.C., et al., *Cockayne syndrome: Clinical features, model systems and pathways.* Ageing research reviews, 2017. **33**: p. 3-17.
174. De Boer, J. and J.H. Hoeijmakers, *Nucleotide excision repair and human syndromes.* Carcinogenesis, 2000. **21**(3): p. 453-460.
175. Bergmann, E. and J.-M. Egly, *Trichothiodystrophy, a transcription syndrome.* TRENDS in Genetics, 2001. **17**(5): p. 279-286.
176. Gillet, L.C. and O.D. Schärer, *Molecular mechanisms of mammalian global genome nucleotide excision repair.* Chemical reviews, 2006. **106**(2): p. 253-276.
177. Price, V.H., et al., *Trichothiodystrophy: sulfur-deficient brittle hair as a marker for a neuroectodermal symptom complex.* Archives of Dermatology, 1980. **116**(12): p. 1375-1384.
178. Knoch, J., et al., *Rare hereditary diseases with defects in DNA-repair.* European Journal of Dermatology, 2012. **22**(4): p. 443-455.
179. Kainov, D.E., et al., *Structural basis for group A trichothiodystrophy.* Nature structural & molecular biology, 2008. **15**(9): p. 980-984.
180. Stefanini, M., et al., *Trichothiodystrophy: from basic mechanisms to clinical implications.* DNA repair, 2010. **9**(1): p. 2-10.
181. Zurita, M. and C. Merino, *The transcriptional complexity of the TFIIH complex.* TRENDS in Genetics, 2003. **19**(10): p. 578-584.
182. Mydlikova, Z., J. Gursky, and M. Pirsel, *Transcription factor IIH-the protein complex with multiple functions.* Neoplasma, 2010. **57**(4): p. 287-290.
183. Gibbons, B.J., et al., *Subunit architecture of general transcription factor TFIIH.* Proceedings of the National Academy of Sciences, 2012. **109**(6): p. 1949-1954.
184. Moriwaki, S.I. and K.H. Kraemer, *Xeroderma pigmentosum–bridging a gap between clinic and laboratory.* Photodermatology, Photoimmunology & Photomedicine: Review article, 2001. **17**(2): p. 47-54.
185. Kouatcheu, S., et al., *Thyroid nodules in xeroderma pigmentosum patients: a feature of premature aging.* Journal of Endocrinological Investigation, 2021. **44**(7): p. 1475-1482.
186. DiGiovanna, J.J. and K.H. Kraemer, *Shining a light on xeroderma pigmentosum.* Journal of investigative dermatology, 2012. **132**(3): p. 785-796.
187. Lambert, W.C., H.-R. Kuo, and M.W. Lambert, *Xeroderma pigmentosum.* Dermatologic clinics, 1995. **13**(1): p. 169-209.
188. Lehmann, A.R., D. McGibbon, and M. Stefanini, *Xeroderma pigmentosum.* Orphanet journal of rare diseases, 2011. **6**(1): p. 1-6.
189. Cleaver, J.E., *Cancer in xeroderma pigmentosum and related disorders of DNA repair.* Nature Reviews Cancer, 2005. **5**(7): p. 564-573.
190. Steurer, B. and J.A. Marteijn, *Traveling rocky roads: the consequences of transcription-blocking DNA lesions on RNA polymerase II.* Journal of molecular biology, 2017. **429**(21): p. 3146-3155.
191. Schwertman, P., et al., *UV-sensitive syndrome protein UVSSA recruits USP7 to regulate transcription-coupled repair.* Nature genetics, 2012. **44**(5): p. 598-602.
192. Zhang, X., et al., *Mutations in UVSSA cause UV-sensitive syndrome and destabilize ERCC6 in transcription-coupled DNA repair.* Nature genetics, 2012. **44**(5): p. 593-597.
193. Nakatsu, Y., et al., *XAB2, a novel tetratricopeptide repeat protein involved in transcription-coupled DNA repair and transcription.* Journal of Biological Chemistry, 2000. **275**(45): p. 34931-34937.

194. Fagbemi, A.F., B. Orelli, and O.D. Schärer, *Regulation of endonuclease activity in human nucleotide excision repair.* DNA repair, 2011. **10**(7): p. 722-729.
195. Sugasawa, K., et al., *Xeroderma pigmentosum group C protein complex is the initiator of global genome nucleotide excision repair.* Molecular cell, 1998. **2**(2): p. 223-232.
196. Mitchell, J.R., J.H. Hoeijmakers, and L.J. Niedernhofer, *Divide and conquer: nucleotide excision repair battles cancer and ageing.* Current opinion in cell biology, 2003. **15**(2): p. 232-240.
197. Emmert, S., *Xeroderma Pigmentosum, Cockayne Syndrome and Trichothiodystrophy.* Harper's Textbook of Pediatric Dermatology, 2011. **1**: p. 135.1-135.24.
198. Kusakabe, M., et al., *Mechanism and regulation of DNA damage recognition in nucleotide excision repair.* Genes and Environment, 2019. **41**(1): p. 1-6.
199. Sugasawa, K., et al., *A multistep damage recognition mechanism for global genomic nucleotide excision repair.* Genes & development, 2001. **15**(5): p. 507-521.
200. Evans, E., et al., *Mechanism of open complex and dual incision formation by human nucleotide excision repair factors.* The EMBO journal, 1997. **16**(21): p. 6559-6573.
201. Wold, M.S., *Replication protein A: a heterotrimeric, single-stranded DNA-binding protein required for eukaryotic DNA metabolism.* Annual review of biochemistry, 1997. **66**(1): p. 61-92.
202. Guzder, S.N., et al., *Requirement of yeast Rad1–Rad10 nuclease for the removal of 3′-blocked termini from DNA strand breaks induced by reactive oxygen species.* Genes & development, 2004. **18**(18): p. 2283-2291.
203. Krejci, L., et al., *Homologous recombination and its regulation.* Nucleic acids research, 2012. **40**(13): p. 5795-5818.
204. Davis, A.J. and D.J. Chen, *DNA double strand break repair via non-homologous end-joining.* Translational cancer research, 2013. **2**(3): p. 130.
205. Featherstone, C. and S.P. Jackson, *DNA double-strand break repair.* Current Biology, 1999. **9**(20): p. R759-R761.
206. Pardo, B., B. Gómez-González, and A. Aguilera, *DNA repair in mammalian cells.* Cellular and Molecular Life Sciences, 2009. **66**(6): p. 1039-1056.
207. Jackson, S., *Detecting, signalling and repairing DNA double-strand breaks.* Biochemical Society Transactions, 2001. **29**(6): p. 655-661.
208. Karran, P., *DNA double strand break repair in mammalian cells.* Current opinion in genetics & development, 2000. **10**(2): p. 144-150.
209. Hefferin, M.L. and A.E. Tomkinson, *Mechanism of DNA double-strand break repair by non-homologous end joining.* DNA repair, 2005. **4**(6): p. 639-648.
210. Burma, S., B.P. Chen, and D.J. Chen, *Role of non-homologous end joining (NHEJ) in maintaining genomic integrity.* DNA repair, 2006. **5**(9-10): p. 1042-1048.
211. Weterings, E. and D.C. Van Gent, *The mechanism of non-homologous end-joining: a synopsis of synapsis.* DNA repair, 2004. **3**(11): p. 1425-1435.
212. Weterings, E. and D.J. Chen, *The endless tale of non-homologous end-joining.* Cell research, 2008. **18**(1): p. 114-124.
213. Doherty, A.J. and S.P. Jackson, *DNA repair: how Ku makes ends meet.* Current Biology, 2001. **11**(22): p. R920-R924.
214. Barnes, D.E., *Non-homologous end joining as a mechanism of DNA repair.* Current biology, 2001. **11**(12): p. R455-R457.
215. Pastwa, E. and J. Błasiak, *Non-homologous DNA end joining.* Acta Biochimica Polonica, 2003. **50**(4): p. 891-908.
216. San Filippo, J., P. Sung, and H. Klein, *Mechanism of eukaryotic homologous recombination.* Annu. Rev. Biochem., 2008. **77**: p. 229-257.
217. Sun, Y., et al., *Structural basis of homologous recombination.* Cellular and Molecular Life Sciences, 2020. **77**(1): p. 3-18.

218. Lee, J. and T. Paull, *Activation and regulation of ATM kinase activity in response to DNA double-strand breaks.* Oncogene, 2007. **26**(56): p. 7741-7748.
219. Ranjha, L., S.M. Howard, and P. Cejka, *Main steps in DNA double-strand break repair: an introduction to homologous recombination and related processes.* Chromosoma, 2018. **127**(2): p. 187-214.
220. Zhao, W., et al., *Promotion of BRCA2-dependent homologous recombination by DSS1 via RPA targeting and DNA mimicry.* Molecular cell, 2015. **59**(2): p. 176-187.
221. Orelli, B.J. and D.K. Bishop, *BRCA2 and homologous recombination.* Breast Cancer Research, 2001. **3**(5): p. 1-5.
222. Hinz, J.M., *Role of homologous recombination in DNA interstrand crosslink repair.* Environmental and molecular mutagenesis, 2010. **51**(6): p. 582-603.
223. Richardson, C., *RAD51, genomic stability, and tumorigenesis.* Cancer letters, 2005. **218**(2): p. 127-139.
224. Mortensen, U.H., M. Lisby, and R. Rothstein, *Rad52.* Current Biology, 2009. **19**(16): p. R676-R677.
225. Lavrik, O.I., et al., *Photoaffinity labeling of mouse fibroblast enzymes by a base excision repair intermediate: Evidence for the role of poly (ADP-ribose) polymerase-1 in DNA repair.* Journal of Biological Chemistry, 2001. **276**(27): p. 25541-25548.
226. Boehler, C., et al., *Poly (ADP-ribose) polymerase 3 (PARP3), a newcomer in cellular response to DNA damage and mitotic progression.* Proceedings of the National Academy of Sciences, 2011. **108**(7): p. 2783-2788.
227. Merchut-Maya, J.M., J. Bartek, and A. Maya-Mendoza, *Regulation of replication fork speed: Mechanisms and impact on genomic stability.* DNA repair, 2019. **81**: p. 102654.
228. Beck, C., et al., *Poly (ADP-ribose) polymerases in double-strand break repair: focus on PARP1, PARP2 and PARP3.* Experimental cell research, 2014. **329**(1): p. 18-25.
229. Swindall, A.F., J.A. Stanley, and E.S. Yang, *PARP-1: friend or foe of DNA damage and repair in tumorigenesis?* Cancers, 2013. **5**(3): p. 943-958.
230. Johansson, M., *A human poly (ADP-ribose) polymerase gene family (ADPRTL): cDNA cloning of two novel poly (ADP-ribose) polymerase homologues.* Genomics, 1999. **57**(3): p. 442-445.
231. Langelier, M.-F., A.A. Riccio, and J.M. Pascal, *PARP-2 and PARP-3 are selectively activated by 5' phosphorylated DNA breaks through an allosteric regulatory mechanism shared with PARP-1.* Nucleic acids research, 2014. **42**(12): p. 7762-7775.
232. Lehtiö, L., et al., *Structural basis for inhibitor specificity in human poly (ADP-ribose) polymerase-3.* Journal of medicinal chemistry, 2009. **52**(9): p. 3108-3111.
233. Rulten, S.L., et al., *PARP-3 and APLF function together to accelerate nonhomologous end-joining.* Molecular cell, 2011. **41**(1): p. 33-45.
234. Belousova, E., A. Ishchenko, and O. Lavrik, *Dna is a new target of Parp3.* Scientific reports, 2018. **8**(1): p. 1-12.
235. Ko, H.L. and E.C. Ren, *Functional aspects of PARP1 in DNA repair and transcription.* Biomolecules, 2012. **2**(4): p. 524-548.
236. Rodriguez-Vargas, J.M., L. Nguekeu-Zebaze, and F. Dantzer, *PARP3 comes to light as a prime target in cancer therapy.* Cell Cycle, 2019. **18**(12): p. 1295-1301.
237. Karicheva, O., et al., *PARP3 controls TGFβ and ROS driven epithelial-to-mesenchymal transition and stemness by stimulating a TG2-Snail-E-cadherin axis.* Oncotarget, 2016. **7**(39): p. 64109.
238. Beck, C., et al., *PARP3, a new therapeutic target to alter Rictor/mTORC2 signaling and tumor progression in BRCA1-associated cancers.* Cell Death & Differentiation, 2019. **26**(9): p. 1615-1630.
239. Augustin, A., et al., *PARP-3 localizes preferentially to the daughter centriole and interferes with the G1/S cell cycle progression.* Journal of cell science, 2003. **116**(8): p. 1551-1562.
240. Quan, J.-J., J.-N. Song, and J.-Q. Qu, *PARP3 interacts with FoxM1 to confer glioblastoma cell radioresistance.* Tumor Biology, 2015. **36**: p. 8617-8624.

241. Barak, F., et al., *The rate of the predominant Jewish mutations in the BRCA1, BRCA2, MSH2 and MSH6 genes in unselected Jewish endometrial cancer patients.* Gynecologic oncology, 2010. **119**(3): p. 511-515.
242. Terui, H., et al., *Molecular and clinical characteristics of MSH6 germline variants detected in colorectal cancer patients.* Oncology Reports, 2013. **30**(6): p. 2909-2916.
243. Liu, H.C., et al., *Inhibitory effect of MSH6 gene silencing in combination with cisplatin on cell proliferation of human osteosarcoma cell line MG63.* Journal of Cellular Physiology, 2019. **234**(6): p. 9358-9369.
244. Edelmann, W., et al., *Mutation in the mismatch repair gene Msh6 causes cancer susceptibility.* Cell, 1997. **91**(4): p. 467-477.
245. Fink, D., et al., *The role of DNA mismatch repair in platinum drug resistance.* Cancer research, 1996. **56**(21): p. 4881-4886.
246. Yang, G., et al., *Dominant effects of an Msh6 missense mutation on DNA repair and cancer susceptibility.* Cancer cell, 2004. **6**(2): p. 139-150.
247. Weber, A.M. and A.J. Ryan, *ATM and ATR as therapeutic targets in cancer.* Pharmacology & therapeutics, 2015. **149**: p. 124-138.
248. Shiloh, Y. and Y. Ziv, *The ATM protein kinase: regulating the cellular response to genotoxic stress, and more.* Nature reviews Molecular cell biology, 2013. **14**(4): p. 197-210.
249. Van Gent, D.C., J.H. Hoeijmakers, and R. Kanaar, *Chromosomal stability and the DNA double-stranded break connection.* Nature reviews genetics, 2001. **2**(3): p. 196-206.
250. Ditch, S. and T.T. Paull, *The ATM protein kinase and cellular redox signaling: beyond the DNA damage response.* Trends in biochemical sciences, 2012. **37**(1): p. 15-22.
251. Savitsky, K., et al., *A single ataxia telangiectasia gene with a product similar to PI-3 kinase.* Science, 1995. **268**(5218): p. 1749-1753.
252. Newton, R., et al., *Plasma and salivary pharmacokinetics of caffeine in man.* European journal of clinical pharmacology, 1981. **21**: p. 45-52.
253. Batey, M.A., et al., *Preclinical evaluation of a novel ATM inhibitor, KU59403, in vitro and in vivo in p53 functional and dysfunctional models of human cancer.* Molecular cancer therapeutics, 2013. **12**(6): p. 959-967.
254. Shen, M., et al., *Inhibition of ATM reverses EMT and decreases metastatic potential of cisplatin-resistant lung cancer cells through JAK/STAT3/PD-L1 pathway.* Journal of Experimental & Clinical Cancer Research, 2019. **38**: p. 1-14.

Ayşegül Varol

Personal Info.

Date of birth: 04.06.1990
Place of birth: Ankara/Turkey
Nationality: Turkish

Contact

Email: aysegvarol@gmail.com
Tel.: +49- 178-424-55-23
Address: Lucy-Hillebrand-Straβe 4
55128, Mainz
LinkedIn: https://www.linkedin.com/in/aysegul-varol 323340322

Profile

- Passionate about cancer and cancer drug research
- ~10 years of teaching and research experience in pharmacy, biochemistry, biotechnology, and pharmacology
- Published 7 peer-reviewed articles, 4 of which were first authored
- Enthusiastic and passionate about developing new skills.

Education

01.09.2009 – 19.06.2013

- **Anadolu University– Faculty of Science – Department of Biology Bachelor's Degree (GPA: 3.17 / 4.00)**
- **Advisor:** Prof. Ayşe Tansu Koparal

09.08.2010 03.09.2010

- **Eskişehir Osmangazi University – Medical School Department of Microbiology – internship**

06.02.2015 – 06.07.2017

- **Anadolu University – Graduate School of Science – Department of Biotechnology – Master of Science Degree (GPA: 3.20 / 4.00)**
- **Advisor:** Prof. Ayşe Tansu Koparal

16.12.2019 – 2025 expect

- **PhD candidate in Pharmacy**

Johannes Gutenberg University Mainz (Mainz, Germay)

- **Advisor:** Prof. Dr. Thomas Efferth

Practical Techniques

- Bionformatic-Survival analyses-Kaplan Meir
- 2D cell culture
- Wound Healing
- PCR&Western Blotting
- Flow Cytometry
- Microarray Assay
- Ingenuity Pathway Analysis-Chipster
- In silicon drug screening
- Fluorescence microscopy
- Microscale thermophoresis

Research Experience

2014 - 2017 ▪ "The investigation of suitability of the new type phthalocyanine complexes on photodynamic cancer therapy (PDT) with in vitro methods", The Commission of Scientific Research Projects of Anadolu University, Researcher, **(**Project no: 1106F116**)**

2015 - 2017 ▪ "Investigation of Biological Activities of the Novel Acyl-Hydrazone Schiff Base and Their Transition Metal Complexes by Using in vitro Tests", The Commission of Scientific Research Projects of Anadolu University, Researcher, (Project no: 1604S168)

2015 - 2017 ▪ "Investigation of the angiogenesis-targeted treatment potentials of the secondary metabolites isolated from lichens on tumor development and invasion", The Commission of Scientific Research Projects of Anadolu University, Researcher, (Project no: 1502F068)

2015 - 2017 ▪ "Investigation of the pazoponib activity on the in vitro psoriasis model", TUBITAK project, Researcher, (Project no: 1705S303)

2019 - 2025 ▪ "Identification and Functional Characterization of Potential Biomarkers in Cisplatin Resistance Through Bioinformatic Analyses" Johannes Gutenberg University Mainz (Mainz, Germay), Researcher.

IT

MS Office

GraphPad PRISM, SPSS, origin,

Photoshop, Image J

Languages

Turkish (mother tongue)

English (fluent)

German (A2.2)

Behavior

- Problem-solving skills
- Team-oriented / Team player
- Detail-oriented
- Good communication skills
- Responsible
- Hardworking

Fellowship & Award

2017-2020	▪ YÖK 100/2000 Ph.D scholarship
2017-~	▪ MEB scholarship

Teaching experience

Pharmacological Biology III, Johannes Gutenberg-Universität Mainz, 2020-2024

- Responsible for Qaulity control;Identification of *Panax ginseng* by PCR
- Flavanoide
- Tannin experiment